2009-12-18

A Multi-Model Approach to Predicting Pathogen Indicator Bacteria Loading in TMDL Analyses.

Donna-May G. Sakura-Lemessy
University of Miami, d.lemessy@umiami.edu

UNIVERSITY OF MIAMI

A MULTI- MODEL APPROACH TO PREDICTING PATHOGEN INDICATOR BACTERIA LOADING IN TMDL ANALYSES

By

Donna-May G. Sakura-Lemessy

A DISSERTATION

Submitted to the Faculty
of the University of Miami
in partial fulfillment of the requirements for
the degree of Doctor of Philosophy

Coral Gables, Florida

December 2009

UNIVERSITY OF MIAMI

A dissertation submitted in partial fulfillment of
the requirements for the degree of
Doctor of Philosophy

A MULTI-MODEL APPROACH TO PREDICTING PATHOGEN INDICATOR BACTERIA LOADING IN TMDL ANALYSES

Donna-May G. Sakura-Lemessy

Approved:

David A. Chin, Ph.D. Professor of Civil, Architectural and Environmental Engineering	Terri A. Scandura, Ph.D. Dean of the Graduate School
Antonio Nanni, Ph.D. Professor of Civil, Architectural and Environmental Engineering	James D. Englehardt, Ph.D. Professor of Civil, Architectural and Environmental Engineering

Fernando Miralles-Wilhelm, Ph.D.
Associate Professor of Civil and Environmental Engineering,
Florida International University

SAKURA-LEMESSY, DONNA-MAY G. (Ph.D., Civil Engineering)
(December 2009)

A Multi-Model Approach to Predicting Pathogen Indicator Bacteria Loading in TMDL Analyses

Abstract of a doctoral dissertation at the University of Miami

Dissertation supervised by Dr. David A. Chin
No. of pages in text (148)

This dissertation utilizes data from four sub-watersheds in the Little River Experimental Watershed, GA to develop models to improve forecast predictions related to the management of surface-water pollution due to non-point source runoff. Non-point source pollution is the primary cause of US surface-water quality impairment and a main transport mechanism for pathogens and other pollutants into receiving surface water bodies (US EPA 2008). In response to pollution reduction and watershed remediation mandates under the Federal Clean Water Act (1972)—particularly the Total Maximum Daily Load (TMDL) program—the role of water quality modeling in effectively rehabilitating impaired waters has taken on greater importance. Consequently, the significance of this study is that it is the first of its kind to incorporate a multi-model approach to address limitations in using single water quality models. In this regard, it builds on water quality engineering research by presenting methods to estimate contaminant concentrations and reduce uncertainty in overall model predictions in impaired water-bodies.

Methodologically, the key point of departure in this dissertation is centered on the fact that water quality modeling is the cornerstone of TMDL analyses but the associated

prediction uncertainty affects their adequacy in providing reliable contaminant loadings estimates in an impaired water body. As such, utilizing hydrological and water-quality process equations embedded in the two most widely used watershed-scale models, the Soil and Water Assessment Tool (SWAT) and Hydrological Simulation Program-Fortran (HSPF), and observed data from the sub-watersheds mentioned above, the dissertation addresses this limitation by combining results from the two competing models to reduce uncertainty and enhance accuracy of predictions.

The study was conducted in two phases. First, HSPF and SWAT—two extensively-used, scientifically-rigorous, US EPA-approved watershed-scale codes—were used to build models of the four study catchments. The models were individually calibrated and shown (based on Nash-Sutcliffe Efficiency (NSE) ratios) to produce reliable simulations of the hydrologic and water quality conditions in the watershed. The second phase of the analysis involved using a multi-model approach to combine model forecasts. Model combination, introduced by Bates and Granger in 1969, has emerged as a viable analytical technique (Claesken and Hjort, 2008; Ajami et al., 2006) and widely-used across disciplines to improve model-forecasting results (Kim et al., 2006; Shamseldin et al., 1997; Granger, 2001; Clemens, 1989; Thompson, 1976; Newbold and Granger, 1974; Dickinson, 1973).

After calibration, the model predictions were combined for each catchment using three different methods: the Weighted Average Method (WAM), the Nash-Sutcliffe Efficiency Maximization Method (NSE-max) and an Artificial Neural Network Method (ANN). Comparison of the results of the multi-model formulation with original individual model results showed improved estimates with all three combination methods.

The improvement in model accuracy (based on NSE ratios) varied from modest to significant in both hydrologic and water quality variables. These improvements were attributed to a reduction in model structural uncertainty resulting from the ability to capture aspects of some of the more complex watershed interactions from exogenous information provided by the contributing models. It should be noted here, however, that as model availability increases, if additional models (beyond those utilized here) are used with this approach, care should be taken to ensure the credibility of each individual model for simulating the watershed scale processes under review.

Limitations of this study include possible bias introduced by the use of deterministic models to estimate probabilistic contaminant distributions, limitations in available data, and the use of a seven-year study period that did not account for possible impacts of shorter periods of extreme hydrologic conditions on the individual model performances and model combination weightings. Recommendations for future research include (a) improving watershed-scale codes to better describe the probability distribution functions characteristic of contaminant distributions and data collection on wildlife species and populations; and investigating the fate and transport processes of pathogenic indicator bacteria deposited in forested areas and the impact of extreme hydrologic conditions on model performance and weighting.

Overall, the findings from this dissertation suggest that water quality modeling incorporating a multi-model approach has the potential to significantly improve predictions compared to the predictions obtained when only one model is used. Clearly, the findings reported here have significant implications in improving TMDL analyses and remediation plans by presenting an approach that exploits the strengths of two of the most

complete and well-accepted watershed-scale water quality models in the United States. Moreover, the findings of this dissertation auger well for the future of TMDL management in that it provides a more robust and cost effective basis for policy makers to decide on effective management strategies that incorporate acceptable risk, allowable loading and land use.

For my parents,

my beloved big brother Adolphus who departed this life ten months ago and

my daughter Adia, the light of my life.

ACKNOWLEDGEMENTS

As I reflect on the journey leading up to this important milestone, I cannot say enough about the support I received from all my friends, family and colleagues. To you all, I am eternally grateful. Dr. David Chin, who has grown to be more than just my dissertation chair, but someone whose mentorship, wisdom and guidance is irreplaceable - I say a special "Thank you." To Dr. Fernando Miralles-Wilhelm, Dr. Antonio Nanni and Dr. James Englehardt, I would like to express sincerely how invaluable your contributions were both personally and professionally. To Dr. David Bosch (USDA-ARS), Dr. George Vellidis and Dr. Paige Gay (University of Georgia, Tifton Campus), your generosity in giving me access to your data and other resources from the Little River Experimental Watershed is immeasurable. Thanks Paige, for being so accessible and forthcoming in giving of your time, expertise and words of advice particularly during some of my most difficult and frustrating moments.

To my immediate family, I have reserved a special place in my heart for all your prayers and encouragements. Each of you, from my mom Olga, my late dad Whitfield, and my late brother Adolphus, and my surviving siblings Daphne, Robbie, Vianda, Ingrid, Neil and Cleve is deserving of my utmost love and gratitude – at last, I can make up for all the missed family gatherings. Of course, this moment would not be possible without the support of my husband, Ian, and my daughter, Adia, who stood by me during all the travails of this huge undertaking. Thank you Adia for bring such a trooper—I promise to make up for all the times I couldn't play CandyLand or have more than one sip of pretend tea at your tea parties, and to make that gingerbread house this Christmas.

I'll also like to thank the faculty and staff at the College of Engineering's CAE Department for all their help during my tenure and last, I'll like to say a heartfelt thank you to the Bill and Melinda Gates Foundation for their generous financial support during my graduate training.

TABLE OF CONTENTS

UNITS OF MEASURE

cfu / 100 ml	colony forming units per 100 milliliter
cfu cm^2 h^{-1}	colony forming units per square centimeter per hour
cfu g^{-1}	colony forming units per gram
cfu mL^{-1}	colony forming units per milliliter
cm h^{-1}	centimeter per hour
cm	centimeter
cm^{-1}	per centimeter
d^{-1}	per day
FC d^{-1}	fecal coliform per day
FC ha^{-1} d^{-1}	fecal coliform per hectare per day
FC ha^{-1} mL^{-1}	fecal coliform per hectare per milliliter
FC ha^{-1}	fecal coliform per hectare
h^{-1}	per hour
kg ha^{-1} d^{-1}	kilogram per hectare per day

LIST OF FIGURES

LIST OF TABLES

CHAPTER 1: INTRODUCTION

1.0 Overview

The impact of non-point source pollution on surface-water bodies is one of the more serious contemporary environmental challenges facing US policymakers (Natural Resources Defense Council 1999a, Goonetilleke et al. 2005, Mein and Goyen 1988). In fact, over the last decade or so, non-point source pollution surpassed all other sources to become the leading cause of water quality impairment to US surface-water bodies (US EPA 2008). However, while the role of non-point source pollution as a medium of transport for pollutants (such as pathogens) into receiving waters is well established, the link between terrestrial loading and the impacts on receiving water bodies is not well understood (Goonetilleke et al. 2005, Parker et al. 2000).

Considerable research and water quality assessments have been conducted by the United States Environmental Protection Agency (US EPA) on the impact of non point source pollutants on receiving water bodies (US EPA 2006). The thrust of the EPA's effort has been to establish standards and regulations that ensure states identify, develop remediation plans, and implement programs to address impaired surface water bodies within their boundaries. The legislative authority to make recommendations and develop mandates for impaired water bodies is stipulated in Section § 303 (d) of the Federal Clean Water Act (1972). Specifically, the statute mandates that each state, territory and tribe designate uses for every natural surface water body within its jurisdiction and establish water quality criteria to protect them (US EPA 1991).

Surface water bodies identified and assigned a designated use by a state (or other governing body) must undergo a water quality assessment (Copeland 2006). Any water body that fails to meet the designated criteria—even after the application of pollution controls—is classified as impaired and placed on a local (state) and the National Section 303(d) List (Copeland 2005). Listed water bodies undergo a use attainability analysis (UAA) to determine the maximum pollutant loads consistent with attaining the associated water quality criteria (Chin 2006). These loads, more commonly referred to as total maximum daily loads or TMDLs, are used to determine the quantity of a specified pollutant a water body can assimilate without violating the qualitative water quality standards based on its designated use (Roffolo 1999).

When the application of technology-based pollution controls fail to bring a surface water body into compliance with required water quality standards, a TMDL must be proposed and implemented for the impaired water body. Common pollutants requiring the implementation of TMDLs include pathogens, nutrients, heavy metals, dissolved oxygen, temperature, organics and pesticides. According to the US EPA (40 CFR 130.2), a TMDL should indicate the sum of the allowable loads of a single pollutant from all contributing point and non-point sources and must include a margin of safety (US EPA 2002).

TMDLs are usually estimated using either or both of the following US EPA-approved methods: load duration curves and/or water quality models. In most small watersheds where flow is the primary mechanism in pollutant loading, duration curves are usually adequate to quantify contaminant loading on the receiving water body (US EPA 2007). Larger, more complex watersheds, on the other hand, frequently require a

more thorough analysis to determine causal relationships between contaminant loading and concentration in the receiving water body. This analysis typically entails the use of a watershed-scale fate and contaminant transport model.

Watershed-scale fate and transport models are widely used in TMDL analyses to quantify the complex relationships between the loading of a contaminant and its spatial and temporal distribution within a receiving water body (Chin 2009). A major shortcoming of these models, however, is the inherent predictive uncertainty associated with all simulation-based methods. This uncertainty stems from three major sources and is usually attributable to: (a) uncertain parameter values (parameter uncertainty), (b) the use of over-simplified and/or inadequate model equations or invalid assumptions (structural uncertainty), or (3) errors in the measured data (data uncertainty). In fact, one of the fundamental problems associated with watershed modeling is the limitation in the minimum predictive uncertainty that can be achieved based on the uncertainty stemming from errors or limitations in the structure of a given model (Chin, Sakura-Lemessy, Bosch and Gay 2009).

Although no systematic methods currently exist to reduce a model's structural uncertainty, combining the predictions of multiple models has emerged as a viable analytical technique to improve model-forecasting results (Claesken and Hjort 2008, Ajami et al. 2006). Since its inception, model combination has been used widely across disciplines (Bates and Granger, 1969; Granger, 2001; Clemens, 1989; Thompson, 1976; Newbold and Granger, 1974; Dickinson, 1973); however, it has never before been applied to predicting the fate and transport of pollutants in a watershed. Consequently, this dissertation addresses this gap in four ways. It builds on existing water quality

engineering research by using a multi-model approach to: (1) estimate the concentration of a contaminant in a receiving water body, (2) predict and quantify the dominant fate and transport processes in a watershed (3) determine which process equations better represent the watershed, and (4) quantify the reduction in predictive uncertainty obtainable by combining process equations in available codes in the analysis of a watershed.

1.1 Background of the problem

As early as 1996, the US EPA recognized non-point source pollution as the leading cause of surface-water quality impairment in the US (EPA 2000). One of the major implications of this is that it serves as a direct conduit for pathogenic organisms—presently the principal cause of water quality impairments—into receiving waterways (Zeckoski et al 2005). According to the US EPA, there are currently well over a hundred thousand miles of pathogen-impaired stream segments on the National 303 (d) list (US EPA 2009) and the affected states, territories and tribes are legally required to establish priority rankings and develop TMDLs for each.

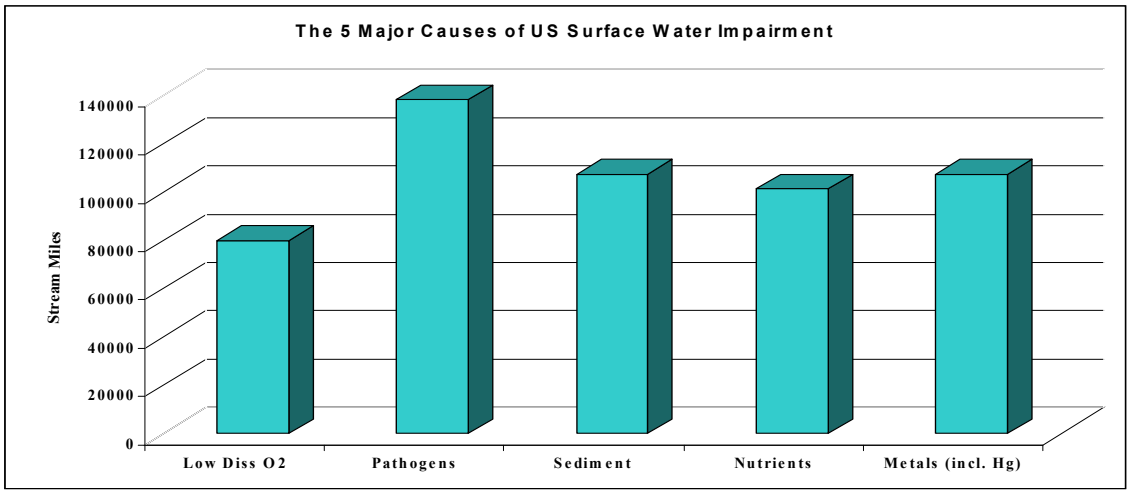

Figure 1: Five leading causes of US surface-water pollution (US EPA 2009)

TMDLs specify the maximum contaminant loading on a water body that is consistent with the water body not being impaired. They are designed to remediate impaired water bodies and estimated using a two-step process (Chin 2006). The first step involves a linkage analysis in which a water body is analyzed to determine the relationship between the contaminant loading on a water body and the concentration of the contaminant in the water body. The second step involves the disaggregation of terrestrial sources of the contaminant loading entering the water body (Chin 2006). Terrestrial sources are disaggregated according to the following relationship:

$$\boldsymbol{TMDL = \Sigma WLA + \Sigma LA + MOS} \quad (1)$$

where ΣWLA is the water load allocation associated with point sources, ΣLA the load allocation associated with non-point sources (including background concentrations) and MOS the required margin of safety as stipulated in section § 303 (d) of the Federal Clean Water Act (1972). The MOS is designed to account for any scientific uncertainty between the estimated and actual load allocations (EPA 1997). It can be expressed either implicitly as a portion of the load allocations or explicitly as a percentage (usually 10%) of the TMDL.

Waste load allocations (WLA) are typically associated with discharges from domestic wastewater treatment plants and municipal separate storm sewer systems (MS4s). However, while loadings from wastewater treatment plants can be reliably estimated from the US EPA's National Pollutant Discharge Elimination System (NPDES) permit allocations and mandatory monitoring reports, the process is not as clear-cut for

MS4s. This is attributable to the fact that though MS4s discharge through conduits such as drains, pipes, canals or ditches and classified as point sources, they actually originate from diffuse non-point sources in a watershed (Phillips 1988). Load allocations (LA) or loads from non-point sources, by contrast, are much harder to quantify than WLA. In fact, non-point source loads are particularly difficult to estimate without some understanding of the quantitative relationships between the terrestrial mass loading and the resulting concentration of a pollutant in the receiving water body.

In simple watersheds, TMDLs are most commonly determined using load duration curves. Load duration curves can be very effective in estimating pollutant loads when flow is the primary mechanism in pollutant loading and all other processes are relatively insignificant to the total loading to a water body (US EPA 2007). Whenever flow is only one of the components affecting the total loading on the water body, as in most complex watersheds, a terrestrial analysis is required to predict the relevant fate and transport processes of the pollutant and determine a strategy for any required loading reductions. Terrestrial analyses usually require the use of a watershed-scale fate and contaminant transport model.

When terrestrial fate and transport models are used, the uncertainties associated with relating load allocation on water bodies with land use activities in surrounding uplands can be significant (Chin 2009). This can result from uncertainty in: (1) model structure, (2) input parameters, and/or (3) input data. Uncertainty in model structure stems from the use of incorrect, inadequate or over-simplified process equations; invalid or unfulfilled assumptions; or the inadequate scaling of point to watershed processes. Parameter uncertainty is primarily due to errors in model input parameters (such as soil

profiles, land uses, stream geometry etc.) or imputing general values over an entire watershed with characteristics that vary in time and space. Data uncertainty, for both calibration and input data, results from limitations and/or errors in measured values (Chin 2009, Arabi et al. 2007, Shirmohammadi et al. 2006).

Conventional fate and transport models provide scientifically rigorous tools for quantifying relationships and estimating non-point source loading in impacted watersheds (Goonetilleke et al. 2005, Sartor and Boyd 1972, Parker et al 2000, Lopes et al 1995, Hall and Anderson 1986). Although these models have been instrumental in advancing our understanding of these relationships, significant gaps remain in our knowledge of the processes involved and the true impacts of terrestrial mass contaminant fluxes on the loading on receiving water bodies (Goonetilleke et al. 2005). The limited understanding of these processes manifest as—sometimes marked—differences between the predictions calculated by the model and the values observed in the watershed. The resultant generally weak correlation between model predictions and observed concentrations that plague water quality models stem from the significant predictive uncertainty introduced by unfulfilled/invalid structural assumptions or the oversimplification and resulting inadequate representation of the fate and transport process in the watershed (Shamseldin, O'Conner and Liang 1997).

Uncertainty related to model structure is extremely difficult to overcome. This is primarily because a model's efficiency is a direct measure of how well its incorporated algorithms simulate relevant processes. Currently, there is no systematic way to reduce a model's structural uncertainty without changing the actual model code. Therefore, short of reformulating the incorporated process equations, the only other option is to replace

the original model with another with process equations that better represent the processes within the watershed (Chin et al. 2009). While the latter option may frequently produce better individual results, no model—thus far—has been identified as ideal or shown to produce better results under all circumstances (Shamseldin et al. 1997, World Meteorological Organization 1975, 1992). While a bit dated, this observation is still relevant and supported by the proliferation of new models and the continuous revision of existing models in the current literature.

In sum, in spite of the insights gained from current analytical methods, watershed analysis continues to suffer from poor understanding of cause and effect relationships. This results in a gap in our ability to link watershed mechanics with the processes that control the terrestrial loading and transport of non-point source pollutants to a receiving water-body. This incomplete understanding of the dynamics in a watershed leads to uncertainty in model predictions, which is the basis of the environmental health assessments and evaluations currently utilized to determine strategies and management actions for the remediation of impaired waters.

At present, all fifty states and several US territories have impaired surface water-bodies that are officially included on the National Section 303(d) list, the majority of which are due to pathogen contamination (EPA 2008). Listed water bodies require the development of a TMDL, and more than half of all the pathogen-impaired water bodies will require the use of a watershed-scale fate and transport models to unravel the complex relationships between land use, pollutant loading and pollutant concentration in the receiving water bodies. Water quality models are known to produce inaccurate results (Chin 2009) but still constitute the foundation of management strategy decision-making.

Since the implementation of these management plans can have significant social and financial impacts, an efficient method to improve model predictions that does not require new model development and its attendant economic burden is not only necessary- it is also urgent.

1.2 Purpose and Significance

The purpose of this study is to use a multi-model approach to: (a) predict and quantify their dominant fate and transport processes of pathogenic indicator bacteria at the watershed scale; (b) determine the process equations that best represent the watershed; and (c) quantify the reduction in predictive uncertainty attainable by combining predictions from two watershed-scale terrestrial fate and transport models.

The significance of the study lies in its potential for advancing knowledge on TMDL development in several aspects. First, it has the ability to predict and quantify the dominant pathogenic indicator bacteria fate and transport processes which can present an effective means for relating required reductions in pathogenic indicator bacteria loading to impaired waters to reductions in terrestrial mass loadings. Second, the study identifies, quantifies and compares relevant fate and transport processes and process algorithms. This can assist in the determination of the process equations/watershed codes that best describe the processes in the watershed, which will not only improve model selection methods, but facilitate model development in watersheds with similar characteristics. Thirdly, the study has the ability to improve water quality model predictions by presenting an approach to reduce structural model uncertainty. Because this approach utilizes the predictions from two comprehensive water quality models to estimate bacteria

concentration, the overall model uncertainty has the potential to be less that if either individual model was used.

Although only pathogenic indicator bacteria are addressed in this study, the methodological approach presented here has greater applications and can be extended to include many other water quality contaminants. Overall, this study considerably improves watershed and water quality management by providing an adequate basis for policy makers to make decisions regarding acceptable risk, allowable loading, and terrestrial land use that is compatible with unimpaired receiving waters.

CHAPTER 2: LITERATURE REVIEW

2.1 Surface water pollution

Though identified as a potential problem for centuries, water pollution and its attendant problems were relatively ignored in the United States until well into the 20th century. In fact, it was not until the Cuyahoga River in Cleveland, Ohio spontaneously ignited in 1969 that US water quality issues came to a head (NOAA 2005, EPA 2003). This crisis led to the establishment of several federal and state agencies (for example, the US EPA) and the evolution and enforcement of several federal mandates, including the Clean Water Act (1972), which oversees surface water quality protection in the US. Under the authority of the Clean Water Act (1972), the US EPA regulates the concentration and frequency of all pollutants discharged directly into receiving surface water bodies in the US (EPA 2006).

Strict control on direct or point source discharges into surface water bodies—a direct result of the Clean Water Act—helped to substantially reduce US surface water pollution. Concomitantly, this reduction helped illuminate the far subtler but no less insidious problem posed by the discharge of diffuse or non-point source pollutants into receiving waterways. By 1996, US EPA identified non-point source pollution as the leading cause of surface-water quality impairment in the US (EPA 1996). According to the US EPA, the primary sources of non-point source pollution to surface water bodies in the US are agricultural sources, municipal sources and urban runoff (1996).

Non point source pollution is now directly responsible for the impairment of water in thousands of surface water bodies throughout the US (US EPA 2008). While, in

fairness to the US EPA, it should be noted that this legislation was addressed in section § 303(d) of the Federal Clean Water Act (1972), it was none-the-less virtually ignored for well over 15 years. The apathy was abruptly ended by a spate of civil laws suits, fuelled by public concern about the deleterious impact of non-point source pollution on receiving water bodies, which propelled the US EPA to step up efforts to enforce the legislative mandates as stated in Section § 303(d) of the CWA (Ruffolo 1999).

The final mandates implementing Section §303(d) of the Clean Water Act (1972) were published on July 13th 2000 (Birkeland 2001). The thrust of the latest regulations is less on restricting "end of pipe" discharges and more on instituting pollution abatement measures to improve and control the quality of US surface waters. They place a ceiling on the quantity of pollutants entering a water body and now require states to allocate maximum pollutant loads (TMDL) to keep the total concentration under applicable water quality standards based on specified designated uses (Birkeland 2001).

Although the US EPA has been very successful in drastically reducing water pollution due to point sources, attempts to regulate non point source pollution is not as straightforward and presents a new and quite different set of challenges. One of the primary challenges associated with controlling non point source pollution is that this current threat to water quality can only be ameliorated by addressing previously unregulated non point sources. Because of the direct relationship between non point source pollution and the land uses in a contributing watershed (McFarland and Hauck 1999, Wang et al. 1997), the pollution can invariably only be controlled by managing these land uses. However, the EPA (neither at the state or federal level) has no

jurisdiction over land management practices in the US (Birkeland 2001), so the only alternative is to attempt to regulate these sources indirectly which can prove a major challenge for regulatory bodies.

The Clean Water Act

Growing public awareness and concern for controlling water pollution, led to the enactment of the Federal Water Pollution Control Act in 1948 (for reviews see Copeland 1999). Since its enactment, the statute has undergone several substantive amendments, the most significant of which was in 1972, after which it became commonly known as the Clean Water Act (EPA 2003, Copeland 1999). The Clean Water Act (CWA) is the cornerstone of surface-water quality protection in the United States. As constituted today, the act consists of two major parts: Title II provisions, which authorize federal funding and Title IV, which outlines the regulatory requirements (Copeland 1999). The Clean Water Act (1972) establishes the framework for regulating the discharge of pollutants into the nation's waterways. It utilizes a combination of regulatory and non-regulatory tools to provide financing for municipal wastewater facilities, guidelines for reducing the direct discharge of pollutants (point source pollution) and regulations for managing stormwater runoff (non-point source pollution) into the nation's surface waterways (EPA 2003).

The Clean Water Act utilizes two overlapping approaches to the regulation of water quality: (a) regulating point source pollution and (b) establishing water quality standards for all contaminants in surface water bodies (Roffolo 1999). Section §303(d) of the act, requires each state to prepare a list of impaired water bodies—that is, all

bodies of water not meeting applicable water quality standards—and establish Total Maximum Daily Loads (TMDLs) for each pollutant identified for each impaired water body on the list. However, this requirement was virtually ignored for several years after the federal mandate, and most of the focus placed on regulating point source pollution, which both decreased pollution levels and increased the visibility of the impacts on surface water quality specifically attributable to diffuse or non-point pollution.

As the impact of non point source pollution on surface water bodies became one of the most dominant factors in maintaining surface water quality, a wave of environmental lawsuits ensued. Of particular importance is *Scott vs. City of Hammond (1984)*, when in a landmark decision the Seventh Circuit Court ruled that the EPA had to develop Total Maximum Daily Loads (TMDLs) if the states failed to do so (for reviews see Ruffolo 1999). This decision now known as the "*theory of constructive submission*" began a series of similar lawsuits all culminating with the courts forcing the EPA to issue lists of impaired water bodies and establish TMDLs if the states had failed to do so (1999). Ultimately, in response to the pressure from both the courts and the public, Congress amended the Clean Water Act in 1987 to include section §319 *the non point source program* requiring states to prepare and submit a non point source assessment report for approval by the EPA (1999). This requirement was subsequently revised and the EPA now also requires states to develop implementations plan for TMDLs in addition to their assessment plans.

2.2 Total Maximum Daily Loads

Total Maximum Daily Loads (TMDLs) are federally mandated standards that define the quantity of a particular pollutant that a given water-body can assimilate daily without exceeding the water quality standards for the designated uses of a water body (Roffolo, 1999). TMDLs were designed by the EPA as a systemic approach to establishing objective, quantitative standards for water quality in surface water bodies. They are specific to individual pollutants and designed to control pollutant loadings and improve the quality of receiving waters (for reviews see Roffolo, 1999). According to the federal mandate, a TMDL should be "*established at a level necessary to implement the applicable water quality standards with seasonal variations and a margin of safety which takes into account any lack of knowledge concerning the relationship between effluent limitations and water quality"* (US Code: Title 33 §1313 (d) (1) (C)).

The regulations set forth by the US EPA (40 CFR 130.2) stipulate that a TMDL should indicate the sum of the individual waste load allocations for point sources, load allocations for non-point sources and load allocations for natural background concentrations. Where a waste load allocation is "*the portion of receiving water's loading capacity that is allocated to one of its existing or future point sources*" and a load allocation *"the potion of a receiving water's loading capacity that is attributed either to one existing or future nonpaying sources of pollution or to natural background sources*" (US EPA 2002).

According to the US EPA (40 CFR 130.2), a TMDL should indicate the sum of the allowable loads of a single pollutant from all contributing point and non-point sources and must include a margin of safety (US EPA, 2002). They are estimated using a two-

step process (Chin, 2006), involving (a) a linkage analysis used to determine the relationship between the terrestrial mass contaminant loading and the concentration of the contaminant in a water body; and (b) the disaggregation of terrestrial sources of contaminant loading entering the water body (Chin, 2006).

TMDLs are calculated as the sum of the waste load allocation (WLA) which is comprised of all the point sources, the load allocation (LA) which accounts for all the nonpoint sources and includes the natural background concentrations and a margin of safety (MOS) which accounts for scientific uncertainty between estimated and actual load allocations (see equation 1). The margin of safety is usually expressed either implicitly as a portion of the load allocations or explicitly as a percentage (usually 10%) of the TMDL (US EPA, 1997).

Waste load allocations (WLA) are typically associated with discharges from domestic wastewater treatment plants, which can be reasonably estimated from National Pollutant Discharge Elimination System (NPDES) permit allocations and mandatory monitoring reports and municipal separate storm sewer systems (MS4s). TMDLs are usually determined by either or both of the most commonly used US EPA-approved methods: the load duration curve method or a terrestrial fate and transport model. The load duration curve method is typically used in watersheds where it is not necessary to track the contributions from individual sources and detailed terrestrial fate and contaminant transport models are used in more complex and typically larger watersheds when detailed terrestrial analysis may be necessary to adequately assign load allocations (US EPA, 2007).

2.3 Pathogenic indicator bacteria: Water quality impairment and TMDLs

Microorganisms are ubiquitous in the environment and while many are beneficial, a small percentage of them are pathogenic. Extensive or prolonged contact or the ingestion of pathogenic organisms can lead to illness or even death in humans (US EPA 2001). In 2001, the US EPA cited pathogenic microorganisms as the leading cause of water quality impairment in the United States and listed as the number one contributor to non point source pollution (US EPA, 2001). In addition, the general consensus, based on extensive research conducted by the US EPA (1983) under the Nationwide Urban Runoff Program (NURP), and several others including Geldreich (1965), Field et al. (1975), Olivieri et al. (1977) and Ellis and Wang (1995), is that contact with water impaired by pathogen contamination poses a significant health concern (see Table 1).

Risks posed to humans through exposure to pathogen-impaired waters are typically assessed using theoretical evaluations (Pitt et al. 2008). However, because there are usually numerous different types of pathogenic microorganisms present in relatively small numbers (when compared with other organisms) in polluted waters, attempts to analyze and monitor pathogens can be difficult, expensive and prone to errors. Consequently, researchers normally choose to monitor a strain of more numeruos nonpathogenic bacteria that can be directly associated with pathogens transmitted by fecal contamination, but are far easier to sample and analyze (US EPA 2001). These are referred to as "pathogen indicator bacteria" and used to develop the water quality criteria necessary to sustain the designated uses of surface water bodies.

The adequate selection of pathogen indicator bacteria to support water quality criteria has been both contentious and difficult. Based on recommended guidelines (US

EPA 2001, Thomann and Mueller 1987), in order for an organism to adequately function as an indicator of fecal contamination, it should:

- be easily detectable using simple laboratory analysis
- be generally not present in unpolluted waters

Pathogen	Type	Disease	Effects
Adenovirus (types 40 and 41)	Virus	Respiratory disease, gastroenteritis	Various effects
Astrovirus	Virus	Gastroenteritis	Vomiting, diarrhea
Balantidium coli	Protozoa	Blantidiasis	Diarrhea, dysentery
Calicivirus e.g. Norwalk-like, Sapporo-like viruses)	Virus	Gastroenteritis	Vomiting, diarrhea
Cryptosporidium	Protozoa	Cryptosporidium	Diarrhea, death in susceptible populations
Entamoeba histolytica	Protozoa	Amebiasis (amoebic dysentery	Prolonged diarrhea with bleeding, abscesses of the liver and small intestine
Enterovirus (e.g. polio, echo, encephalitis, conjunctivitis, Coxsackie viruses	Virus	Gastroenteritis, heart anomolies, meningitis	Various effects
Eschericheria coli (0157:H7)	Bacteria	Gastroenteritis	Vomiting, diarrhea
Giardia lamblia	Protozoa	Giardiasis	Mild to severe diarrhea, nausea, indigestion
Hepatitis A	Virus	Infectious hepatitis	Jaundice, fever
Reovirus	Virus	Gastroenteritis	Vomiting, diarrhea
Rotavirus	Virus	Gastroenteritis	Vomiting, diarrhea
Salmonella	Bacteria	Salmonellosis	Diarrhea, dehydration
Salmonella typhi	Bacteria	Typhoid Fever	High fever, diarrhea, ulceration of small intestine
Shigella	Bacteria	Shigellosis	Bacillary dysentery
Vibrio cholerae	Bacteria	Cholera	Extremely heavy diarrhea, dehydration
Yersinia enterolitica	Bacteria	Yersinosis	Diarrhea

Pathogens of Table 1: concern to water quality (EPA 2007)

- appear in concentrations that can be correlated with the extent of contamination;
- have a die-off rate that does not exceed that of the pathogen of concern.

Some of the most commonly used indicators include coliform bacteria (total, fecal and *E. Coli*) and fecal streptococci (US EPA 2001). However, studies have proven that the use of fecal coliform as an indicator may be problematic because fecal coliform not only replicate in the tropical and subtropical environments, they have different rates of inactivation based on the geography and climate in a region (US EPA 2007).

Other suggestions include those by Davies-Colley et al (1994) who looked at using the *enterococcus* group because the die-off is slower than fecal coliform and Howel et al. (1995) proposed using the ratio between fecal coliform / fecal streptococci counts to determine the origin of bacterial pollution. Neither of these suggestions have been fully accepted as alternatives because *enterococci* are not human specific and relationships between the fecal coliform and streptococci are difficult to generalize because different species of fecal streptococci have different die-off rates (Novotony and Olem 1994; APHA, 1995).

The Clean Water Act requires the implementation of ambient water quality criteria, established by US EPA in 1986, and monitoring indicators of fecal contamination to determine the level of pathogen contamination and assess risks to human health associated with exposure. These water quality standards were based on epidemiological studies which examined the resulting concentration of fecal indicator bacteria in a receiving water body that was impacted by human sewage from point sources (US EPA 2007). Since then, more recent research has shown this approach to be limited in that it failed to consider the impacts of geography, climate, ecology and other

contributing sources of fecal coliform on the overall pollutant concentration in the receiving water body (US EPA 2007). Suggestions for improving the methodology include the use of a "tiered" approach, which will begin conservatively (using the traditional fecal indicators) and progress to more specific indicators that account for source specificity and contaminant loading (US EPA 2007).

The results of studies conducted on pathogen indicators, for example Cabelli at al (1982), Wade et al (2003) and Wiedenmann et al. (2006), have indicated that of the traditional pathogen indicators used, only *Escherichia coli* has been found to consistently relate human health outcomes to exposure for freshwater. *Escherichia coli*, however, is inactivated far more readily that *enterococci* in saltwater and therefore not as well correlated (US EPA 2007). To date, there is still no single approach that can accurately identify the sources of fecal pollution but the lists of alternative fecal indicators for the new-tiered approach include:

(a) *Escherichia coli*,

(b) *enterococci* (*E. faecium*)

(c) *Clostridium perfringens* (in tropical environments where *Escherischia coli* and *enterococci* are also naturally present in soil and sediments),

(d) *Bactericides* of which some isolates may be definitely associated with human feces; and

(e) *Bacteriophages* which are not only hardy, but can be detected using standardized internationally acceptable methods e.g. US EPA, European Council (EU) and the International Organization for Standardization (ISO) (US EPA 2007).

Pathogen indicator bacteria TMDLs

By law, each impaired water body documented in the Clean Water Act's Section § 303(d) list requires the development of a TMDL. A glance at the US EPA's National Section § 303(d) List confirms that the majority (14.2%) of reported water quality impairments are due to pathogens. Based on this, thousands of the TMDLs currently legally required will have to be developed for pathogenic indicator bacteria.

TMDL analysis generally requires determining the contaminant loading on an impaired water body. Loading is typically determined either by load reduction equations where allocated loads are estimated from a flow duration curve (estimated from flow measurements) or by a detailed fate and contaminant transport model (usually HSPF or SWAT). TMDLs are developed from a thorough assessment of the impairment of the listed water body, which involves assessment of the regulatory water quality criteria and measurements of contaminant concentrations.

Regulatory water quality criteria for pathogenic indicator bacteria are generally expressed in statistical terms, usually as a geometric mean, a specified percentile and/or a maximum allowable value. The criteria are based on US EPA recommendations that require regulatory bacteria water quality standards be comprised of both an individual maximum pollutant concentration (usually taken as the 95-percentile concentration value) and a maximum acceptable geometric mean concentration. These measurements must be based on a minimum of five equally-spaced sampling results obtained during a 30 day monitoring period. The individual sample maximum or percentile value must not exceed a specified upper confidence limit determined by the designated use and frequency of contact with the water body, which is not to exceed 95 % (US EPA, 1986). In light of

this, the water quality criteria for pathogens in most states include a target geometric mean and specified percentile value (between 75 and 95 %) in a 30-day sampling period.

Current typical (percentile) regulatory water quality standards for pathogen impairment are that concentrations of fecal coliform bacteria not exceed 400/100 ml more than 10% over a given time (US EPA 2001). However, if the binomial test for delisting impaired water bodies is used, a higher percentile may be more appropriate (Lin et al., 2000; Smith et al., 1997; Shabman and Smith, 2003). Regulatory guidelines in the state of Georgia, assert that if a water body exceeds a water quality threshold (200/100 ml in May through October or 1000/100 ml from November to April) more than 25% of the time then it is classified as impaired (Georgia Department of Natural Resources 2003a; 2003b). Whenever the contaminant concentrations in a water body violate any of the statistical water quality standards mentioned above, the water body is deemed to be impaired and a TMDL must be developed to remediate it.

CHAPTER 3: STUDY AREA

3.0 Site Selection

The area selected for this study is the Little River Experimental Watershed, located in the Suwannee River Basin in south-central Georgia. This site was selected for several reasons, but specifically because (a) it has a lengthy and comprehensive hydrologic and water quality data record; and (b) as a research watershed it provides a microcosmic framework for evaluating and studying watershed processes at a level of detail that can facilitate the development and testing of methodologies (Dedrick, 2004; USDA-ARS, 2008).

3.1 Little River Experimental Watershed

The Little River Experimental Watershed (LREW) lies in the Tifton Upland sub-province of the US Southern Coastal Plain physiographic region. The center of watershed is located at approximately 31.61° N Latitude and 83.66° W Longitude, and it is one of twelve benchmark watersheds in the USDA's Conservation Effects Assessment Project - Watershed Assessment Studies (Sullivan et al. 2007, USDA-ARS 2008). The LREW is 334 km^2 in area and straddles three counties in south-central Georgia: Tift, Turner and Worth. It is instrumented to measure both rainfall and stream flow, and consists of a primary watershed and seven nested sub-watersheds ranging from 3 km^2 to 115 km^2 in size (Bosch et al., 2007).

The LREW is a heavily vegetated, slow moving stream system located in an area characterized by broad floodplains, river terraces and mild slopes. The upland slopes are

predominantly between 2 % and 5%, though some may range from around 5% to as much as 15% in some of the valleys (Bosch et al., 2007). The major soil series in the watershed is loamy sand with an underlying limestone layer (part of the geologic formation of the Floridan aquifer), and the watershed sits on a seasonally dependent shallow aquifer that drains into the stream network (USDA-ARS 2008; Bosch et al., 2007).

The stream slopes range from 0.1% to 0.4% (Bosch and Sheridan, 2007) and the depth of the surficial alluvium ranges from 2 m in the headwater streams to about 6 m at the lower end of the watershed (Shirmohammadi et al., 1986). The hydrology is characterized by high infiltration rates (~5 cm/hr), low surface runoff and high groundwater inflow to streams, which is normal for regions in the southern Coastal plains.

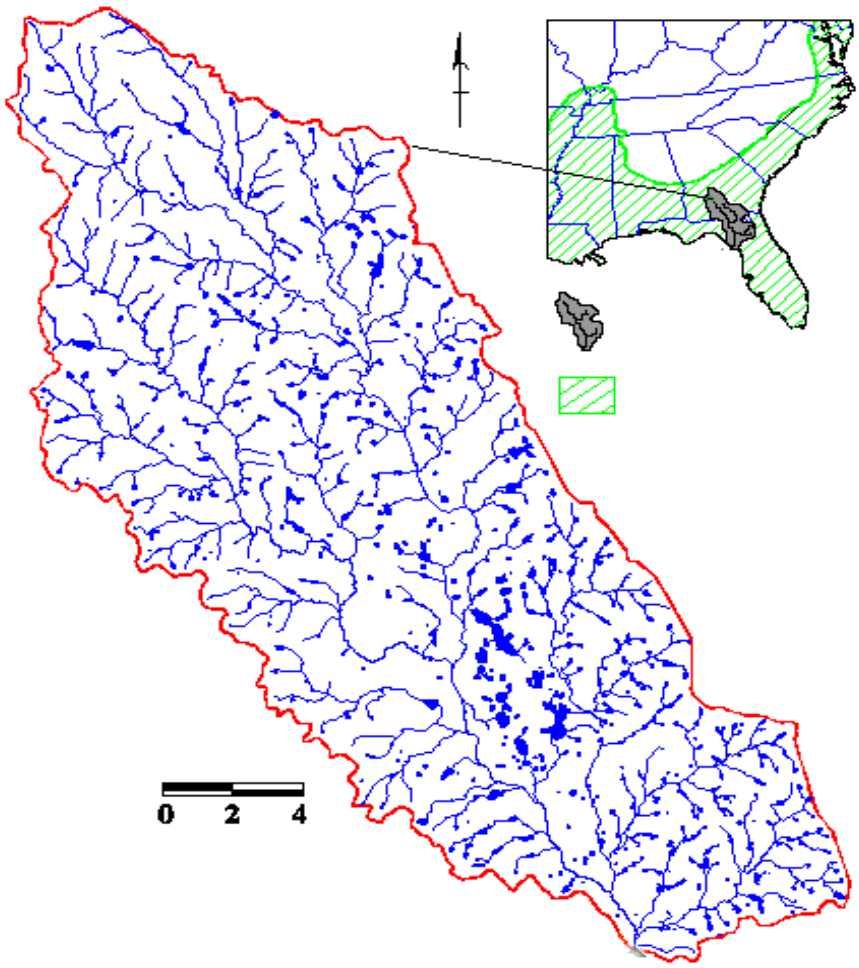

Figure 2: The Little River Experimental Watershed, South-Central Georgia

3.2 Instrumentation

The LREW is outfitted with an extensive network of instruments that includes 46 rain gages, 8 stream gages, and 3 ground-water stage sites (Sullivan 2006, Bosch and Sullivan 2007). The rain gages are set up to continuously record data, and spaced roughly 2.4 km apart (upper portion) and 4.8 km apart (lower portion) throughout the watershed (Bosch et al., 2007). Most of the gages consist of Texas Electronics® TE525 tipping buckets with operational specifications of 0.254 mm (minimum measurement

precision), ± 0.5 mm/hr (accuracy), and a recording interval of 5 minutes. Readings from the individual rain gages in the watershed are combined by the USDA-ARS South East Watershed Research Laboratory (SEWRL) and used to generate average daily quantities for each sub-basin. An explanation of the weighting procedure is detailed in Bosch et al (2000).

Stream flow is measured by horizontal weirs with V-notch center sections, which are installed at the pour points of each sub-basin (Bosch and Sheridan 2007). Horizontal broad-crested weirs were used to measure flow from Catchments I, J, K, and a horizontal sharp-crested weir was used at Catchment O. All weirs are rectangular with a 10:1 side slope V-notch center section in the weir cap. The dimensions for each of the weirs used in this study are as follows:

Catchment ID	Weir Length (m)	V-notch depth (cm)	25-yr max flow rate (m^3/s)
I	26.6	49.7	41.7
J	16.8	47.2	20.8
K	178	44.2	16.5
O	14.8	62.5	14.5

Table 2: ***Weirs in selected sub-catchments in the LREW (Bosch and Sheridan, 2007)***

Digital data loggers installed in the catchments also recorded surface water elevation at 5-minute intervals throughout the study period. Water elevation measurements (to the nearest 2 mm) were taken, both upstream and downstream from the weir, by a pressure transducer. Field measurements, in conjunction with laboratory

results and theoretical considerations, were used to develop rating curves for the flow measurements structures installed in the watershed (Bosch and Sheridan, 2007).

3.3 Sampling

Instruments installed at the flow sites in the LREW were set up to record flows and simultaneously collect composite samples for water quality analysis (Vellidis et al., 1999). In addition to the composite samples, a biweekly on-site analysis was also conducted in each sub-basin. The on-site analysis consisted of collecting a grab sample for fecal coliform/fecal streptococci analysis, and measuring in-situ parameters, including stream depth, pH, water temperature and dissolved oxygen concentration. The parameters were measured using a standard YSI 6820 Water Quality Multi-parameter Sonde probe (Vellidis et al., 1999) and the grab samples collected in 530 ml sterile plastic sampling bags, stored on ice, and analyzed within two hours of collection (APHA 1995).

Grab samples were analyzed for fecal coliform using the EC Medium test, which utilizes a membrane filtration technique and mFC media to identify fecal coliform colonies (APHA, 1995). According to guidelines published in the US EPA's Microbiology Manual Part III (1978), when incubated at 44.5°C, 93 % of blue colonies produced on this medium are verifiable as fecal coliform. A confirmatory test for fecal coliform was conducted on each sample in conjunction with the medium test. Precision and accuracy were documented using sample duplicates, laboratory blanks, and National Institute of Standards and Technology (NIST) traceable reference standards (Vellidis et al., 1999). None of the sample duplicates deviated by more than 25% from the calculated

mean, and over 75% deviated by 10% or less. No correction factors were applied to the data.

3.4 Land use

The principal land uses in the LREW are forest and agriculture, but they also include some wetlands and a small percentage of urban areas (see table 3 below).

Land Use	Percentage
Forest	44
Agriculture	
Cultivated	25
Pasture	15
Wetlands	13
Urban	3

Table 3: Land use distribution in Little River Experimental Watershed in 1998

The forested lands are primarily comprised of both planted and naturally regenerated pine trees (Sullivan 2006). The forested areas are largely very heavily populated with wildlife and some areas are commonly used as recreational hunting reserves (Bosch 2008). The most common wildlife species is deer, but the area also has relatively high populations of wild turkeys, geese, raccoons, beavers, muskrats, river otters and migratory ducks (DNR 2006). Most of the game animals inhabit the riparian areas along the stream banks increasing the potential for fecal matter to enter the stream during storm events. In spite of this, waterfowl (primarily geese and ducks) are still

generally considered to potentially be the greatest contributors of fecal coliform to the surrounding water-bodies (DNR 2006). Unfortunately, it was not possible to estimate their bacteria contribution to the study watershed because only population estimates for deer are currently available in the state of Georgia (DNR 2006, EPD 2006).

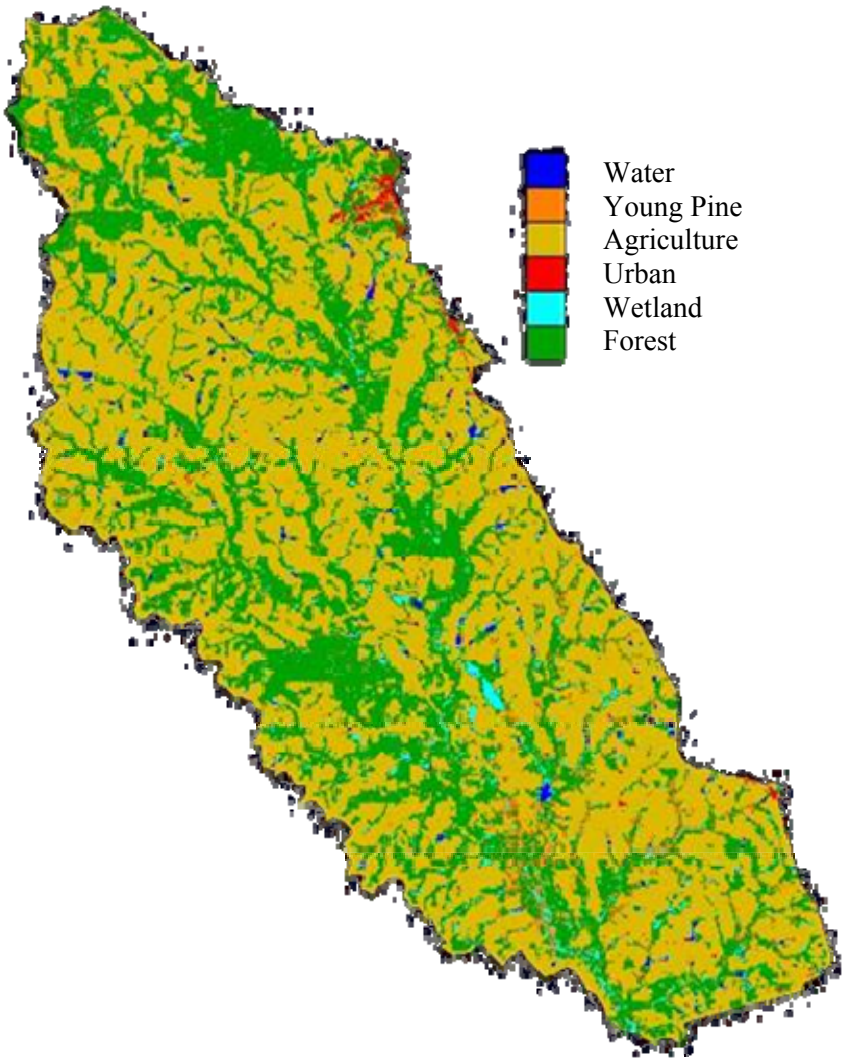

Figure 3: Land Use Distribution in LREW

Row crops and pasture dominate the agricultural land-uses in the LREW. Roughly, two-thirds of the agricultural area is devoted to row crops (mostly peanuts and cotton) and the remainder to pasture (USDA-ARS 2008). During the study period, there were approximately 7,700 head of beef cattle and 240 dairy cows in the watershed. The watershed also contains two broiler houses that grow approximately 440,000 chickens per year. In addition, there were about 1500 pigs in the watershed at the beginning of the study period; however, this number continually dwindled and was down to around 500 by the middle of 1998. The watershed also contains the University of Georgia's Tifton Campus Animal Science Farm, a research dairy housing 200 milking cows.

3.5 Sub-basins

The LREW (USGS HUC 03110204) is comprised of one primary and seven nested sub-basins. Four of the sub-basins in the watershed were selected for use in this study: Catchment I (ID 6840), Catchment J (ID 4850), Catchment K (ID 4860), and Catchment O (ID 6860). The drainage area of Catchment I is 50.0 km^2 and it is centered at 31°40′29″ N Latitude and 83° 41′ 26″ W Longitude, southwest of the city of Ashburn, in Turner County, Georgia. Catchment J is located west of the city of Ashburn, in Turner County, Georgia. The coordinates at its center point are 31°41′33″ N Latitude and 83° 42′ 08″ W Longitude and is 22.1 km^2 in area. Catchment K is also located west of the city of Ashburn, in Turner County, Georgia. It drains an area of 16.8 km^2, and the location of its center coordinates are 31°41′47″ N Latitude and 83° 41′ 51″ W Longitude. Catchment O is 15.9 km^2 and is located northwest of the city of Tifton in Tift County, Georgia. It is centered at 31°29′37″ N Latitude and 83° 34′ 03″ W Longitude.

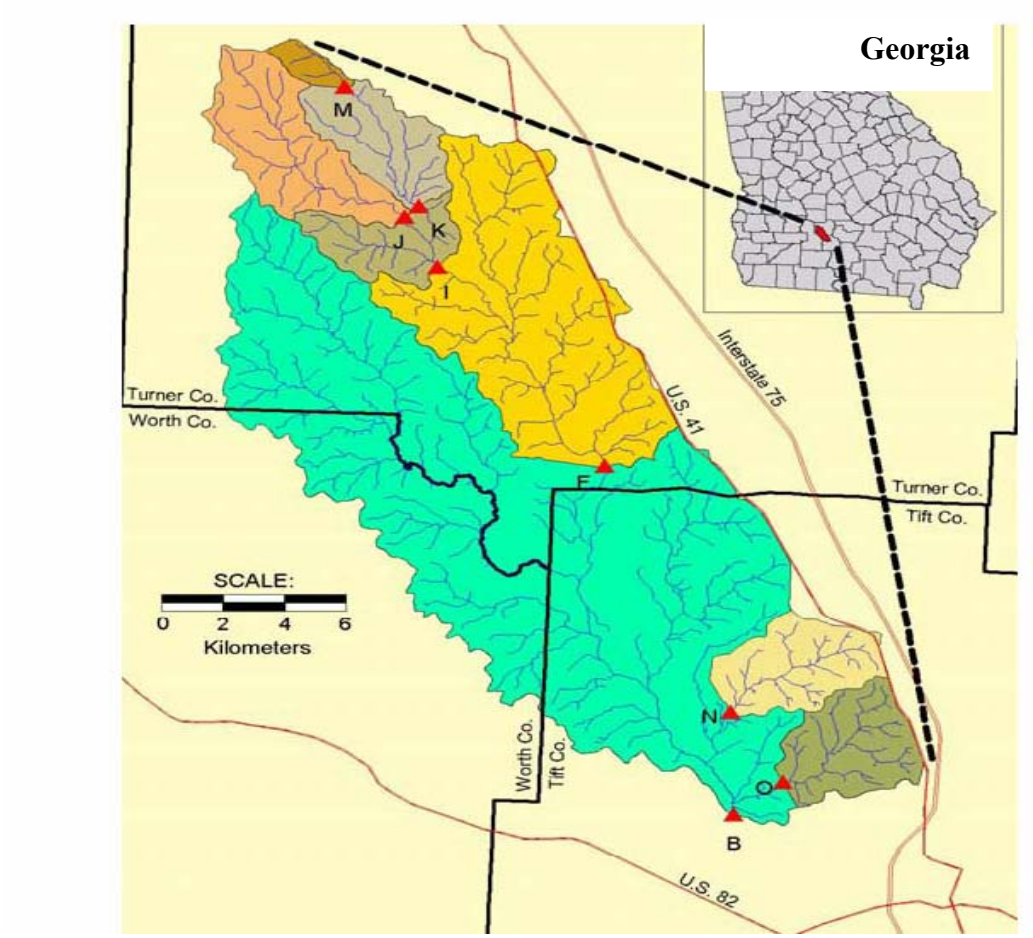

Figure 4: Sub-basins in the Little River Experimental Watershed (Bosch et al., 2007)

3.6 Data

The study period for this project was seven years, beginning in January 1996 and ending December 2002. Data collected in the experimental watershed during the study period include daily flow, maximum and minimum instantaneous discharge, precipitation, in situ parameters (pH, dissolved oxygen, conductivity), turbidity, and water quality parameters including fecal coliform and fecal streptococci. The hydrological constituents were collected daily and water-quality constituents roughly

every two weeks depending on daily average stream flows. All of the streams in the study area are ephemeral and typically go dry (no flow) during the summer from around the middle of May until early to mid September. In addition to this natural variability in stream flow, the study period includes a period of drought which began in 1998 and ended in 2000 (United States Geological Survey 2000). This is reflected in the dataset by some extended periods with very low or no flow.

Hourly rainfall for each catchment was calculated from the five-minute measurements at rain gages RG 34, RG 43, and RG 63 (see table 3). Meteorological data (solar radiation, wind speed, cloud cover, dew point, air temperature, potential evaporation) were collected at MET station 747810 located at the Valdosta Regional Airport, in Valdosta, Georgia. MET Station 747810 was selected because it was the closest station to the study area with a complete meteorological data record. Although it is located about 70 km from the LREW, this distance should not significantly affect the model results since meteorological parameters do not vary appreciably over such relatively small length scales, and overall are not as important as rainfall in simulating runoff in a catchment (Chin et al., 2009).

Catchment ID	Area (km^2)	Rain Gage No.	Center of Catchment (Lat/Long)	Location of rain gage (Lat/Long)
I	50.0	34	31° 40’ 29” (N) 83° 41’ 26” (W)	31° 41’ 30” (N) 83° 41’ 34” (W)
J	22.1	43	31° 41’ 33” (N) 83° 42’ 08” (W)	31° 43’ 33” (N) 83° 42’ 59” (W)
K	16.8	43	31° 41’ 47” (N) 83° 41’ 51” (W)	31° 43’ 33” (N) 83° 42’ 59” (W)
O	15.9	63	31° 29’ 37” (N) 83° 34’ 03” (W)	31° 31’ 17” (N) 83° 32’ 53” (W)

Table 4: Areas, coordinates and rain gages for Catchments I, J, K and O.

CHAPTER 4: THEORY

4.0 Theoretical Overview

The primary aim of this study was to utilize a multi-model approach to (a) predict the concentration of pathogen indicator bacteria in a receiving water body; (b) quantify the dominant bacteria fate and transport processes within the watershed; (c) determine the process equations that best represent the watershed; and (d) quantify the reduction in predictive uncertainty obtained by implementing a multi-model approach to water quality analysis. The study utilized two watershed-scale fate and transport codes: Hydrological Simulation Program-Fortran (Bicknell et al. 2001) and the Soil and Water Assessment Tool (Neitsch et al. 2005) in the analysis. These codes were selected because they are not only US-EPA approved, but they are also the most widely used codes in TMDL analysis. The individual models developed form these codes were used to predict the concentration of pathogen indicator bacteria (fecal coliform) in the watershed and their predictions were combined to reduce model uncertainty and improve the overall accuracy of the predictions.

The first step of the analysis involved the calibration of the individual models. Each model was calibrated first for hydrology and then for water quality. Both phases of the calibration process involved the use of a three-step approach that systematically adjusted the model's process parameters to replicate the measured stream flow values for the hydrology and concentration values for the water quality. The models were considered to be calibrated when the model predictions were in reasonable agreement with the measured data evaluated by the Nash-Sutcliffe Efficiency coefficient (NSE).

The NSE was selected because it is extensively used in hydrological studies and recommended for use in model evaluation by the American Society of Civil Engineers (ASCE) (1993).

The next step in the analysis involved combining the model predictions. Three different methods were used to combine the model predictions: (1) the weighted average method (WAM), (2) the Nash-Sutcliffe Efficiency Maximization method (NSE_max) and (3) using an artificial neural network (ANN). Both the WAM and the NSE_max method are linear combination methods; specifically, they utilize linear regression functional relationships to relate individual model output to an overall combined estimate. However, since many of relationships within watersheds are not linear, an ANN approach was included in the analysis to take advantage of its ability to exploit complicated non-linear relationships between the input variables.

4.1 Watershed-Scale Codes

EPA BASINS®

Better Assessment Science Integrating Point and Non-point Sources (BASINS®) Version 4.0, the most recent release of EPA's BASINS® software system was used to facilitate the implementation of HSPF. BASINS® is a multipurpose, environmental analytical system designed to perform watershed and water quality analyses. Originally released in 1996, BASINS® has since undergone revisions in 1998, 2002 and 2004, with the most substantive in April of 2007, when the software was reconstructed to include an open source GIS software architecture (US EPA 2007). The open source GIS not only

allows the model to run without the use of proprietary software, it utilizes standard GIS files including shapefiles, dbf and GeoTiff files.

BASINS© version 4.0 has all the functionality of the previous version (3.1) including a data extractor, projector, project builder, GIS interface and tools, a series of models and a custom database (available for download through a web data extraction tool) (US EPA 2007). However, while like the previous version (BASINS 3.1), the program contains linkages to many of the models including the Hydrological Simulation Program-Fortran (HSPF) (also used in this analysis); it does not link to either the Automated Geospatial Watershed Assessment Tool (AGWA) or Soil and Water Assessment Tool (SWAT) models. BASINS© version 4 was used to identify and extract the watershed characteristics for the four sub-watersheds used in this study. These characteristics included the drainage area, stream network, the length of the watershed, the slope, surface roughness, soil texture and structure, land use/land cover and soil moisture.

SWAT was run using the ArcSWAT® graphical user interface. The interface runs on the ESRI® ArcGIS platform which provides the GIS functionality required to extract the watershed characteristics, delineate the watershed and define the stream network to prepare the data to build the SWAT model.

Selection of models

The Hydrological Simulation Program -Fortran (HSPF) and the Soil and Water Assessment Tool (SWAT) are two watershed-scale loading and transport models recommended by the US EPA for TMDL research. In fact, until its most recent version

(version 4), both models were integrated into the framework of US EPA's BASINS® system. Current trends suggest that these models will more than likely continue to be extensively used in the future as analytical tools for the development and management of water resources (Van Liew et al., 2003).

Amongst the currently available models, HSPF has been identified as one of most complete models for predicting runoff and non-point source constituent loads in watersheds (Fontaine and Jacomoni, 1997; Whittemore and Beebe, 2000; Laroche et al., 1997; Van Liew et al., 2003). Comparatively speaking, SWAT, a relatively newer model, offers the user more flexibility than HSPF in the configuration of a watershed during analysis (Srinivasan and Arnold, 1994). In light of the aforementioned and their widespread use in TMDL analysis, both HSPF and SWAT were used in this study.

4.1.1 Hydrological Simulation Program Fortran

The Hydrological Simulation Program-Fortran (HSPF) codeis a watershed-scale physically based, lumped-parameter code that originated from Crawford and Linsley's Stanford Watershed Model (1966). HSPF continuously simulates hydrological and water quality processes on pervious and impervious surfaces, both in streams and in well-mixed impoundments (Bricknell et al. 2001). The model simulates hydrological processes using a water balance approach that incorporates a series of flows and storages in the upper, lower and groundwater zones. It initially divides the watershed into land and reservoirs/reaches, before subdividing the land segment into pervious and impervious

areas. Land segmentation allows the model to effectively simulate fate and transport processes unique to pervious and impervious areas (Hydrocomp Inc., 2008).

Hydrologic processes including infiltration, overland flow, interception and evapotranspiration are modeled using empirical equations, and the volume and rate of outflow from the reaches are simulated using the kinematic wave approximation (Bricknell et al. 2001). The model includes a water quality module, which uses a separate subroutine to simulate fate and transport processes both on land and in water. The constituent modeled in this study, fecal coliform, is simulated on land as a completely dissolved constituent using buildup/wash off relationships, and in water using first order decay equations (Im et al. 2004).

4.1.2 Soil and Water Assessment Tool

The Soil and Water Assessment Tool (SWAT) is a watershed-scale code developed by the USDA-ARS to simulate the relationship between land management practices, water quality, sediment, and agricultural yields in large complex watersheds over long periods (Neitsch et al. 2005). SWAT is a physically based, distributed parameter, continuous time code that utilizes a water-balance approach to simulate numerous different physical processes. The hydrology is simulated by dividing the hydrologic cycle into two separate phases: (i) a land phase that controls the quantity of water and contaminant loads (nutrients, sediments, pesticides etc) to the main channel and a (ii) water/routing phase that controls the movement of water and contaminants through the watershed channel network to outlets (Neitsch et al 2005).

In SWAT, the hydrology is modeled using the following equation:

$$SW_t = SW_0 + \sum_{i-1}^{t} \left(R_{day} - Q_{surf} - E_a - w_{seep} - Q_{gw} \right) \quad (2)$$

where SW_t is the final soil water content, SW_0 the initial soil water content on day i, t the time, R_{day} the amount of precipitation on day i, E_a the amount of precipitation, Q_{surf} surface runoff, w_{seep} amount of water entering the vadose zone from the soil profile on day i and Q_{gw} the amount of return flow on day i.

Bacteria are assumed to either interact with surface runoff (present on foliage or in the top 10 mm of soil), or become incorporated deeper into the soil (transport or tillage) and die-off. Bacteria on foliage and in top soil are simulated using a wash-off and a die-off/re-growth process. Wash-off is modeled as a function of the characteristics of the bacteria, timing and intensity of the rainfall and plant morphology. Die-off/re-growth is modeled using Chick's Law to simulate the quantity of bacteria loss through die-off and added through re-growth in the system.

4.1.3 Comparison of the codes

Though both HSPF and SWAT are physically based watershed-scale codes, they differ significantly in three fundamental respects: (1) the spatial disaggregation of the watershed, (2) the simulation time step, and (3) the process equations used to simulate the both hydrological and the fate and transport processes associated with bacteria.

Spatial disaggregation

The HSPF and SWAT algorithms both divide the watershed into sub-units during an analysis. However, while HSPF divides the watershed based on the type of land use and previous and impervious areas based on their hydrology, SWAT divides the watershed into a number of sub-catchments, before sub-dividing each sub-catchment into a number of smaller hydrologic response units (HRU) based on uniform land use and soil type (Neitsch et al 2000). The pervious and impervious areas and hydrologic response units form the unit of analysis for HSPF and SWAT respectively.

Temporal aggregation

Another fundamental—but no less important—difference between HSPF and SWAT is the simulation time-step. Of the two models, SWAT is more constrained in that it operates using a daily time-step. HSPF, conversely, can run simulations at time-steps ranging from a minute to a day, though one-hour intervals are the most common analytical unit utilized. In this study, HSPF was used with the time step of one hour and SWAT used with the time step of one-day.

4.2 Process Equations

The section that follows provides a comparative analysis of the process equations used by HSPF and SWAT in the hydrological and water quality analysis routines in each model.

4.2.1 Hydrology

Hydrologic processes in HSPF are modeled by a water balance approach that divides the watershed into land and streams, the land into pervious and impervious areas, and finally the pervious land area into a series of interconnected water storage zones. Flux is simulated between the zones (upper, lower and groundwater) and the flows (surface, interflow and groundwater) from the land area to a stream reach using equations containing parameters determined either by measurement or calibration.. Overland flow is modeled as turbulent flow and simulated using the Chezy-Manning equation and an empirical relationship that relates outflow depth to depression storage (Bicknell et al., 2001). The rate and volume of the outflow in each stream segment calculated using the kinematic wave approximation and a storage-routing technique is used to move water from one reach to the other during stream processes.

The model calculates actual evapotranspiration (ET) as a function the potential evapotranspiration (PET) and the amount of moisture available for ET on the land and in the soil. In addition, HSPF uses several lumped parameters to account for the effect of vegetation and tile flow in the watershed (Singh et al., 2008). For example, one lumped parameter not only controls ET from the lower storage zone, it also accounts for the effects of the vegetation type, density, developmental stage and root growth of the plants in the watershed. Water removal due to tiling is controlled by the lumped parameters that also control water storage in the upper and lower storage zones (Singh et al., 2008).

SWAT also uses a water balance approach to simulate hydrologic processes but this approach divides the watershed into separate storage zones representing the canopy,

soil and deep and shallow aquifers. SWAT employs a soil-water balance method that uses measured precipitation values to simulate a daily balance of the soil water content, surface runoff, evapotranspiration, percolation and return flow (Benaman et al 2005). The model simulates ground-water flow by routing a component of the shallow ground water to the stream reach and estimates surface water runoff using the SCS curve number approach (Arnold and Allen 1996). Interflow is simulated usng a kinematic storage model and the water is routed to the stream reach to simulate important in-stream hydrological and sediment transport mechanisms (Benaman et al 2005).

Other processes modeled in the soil layer include infiltration, evaporation, plant uptake, lateral flow and percolation (Singh et al. 2008). Sediment erosion is simulated using the modified universal soil loss equation (Williams and Berndt 1977) and actual evapotranspiration (ET) estimated as the sum of the evaporation and transpiration in the system. Evaporation is estimated using an exponential function that relates the soil depth and the available water and the transpiration is estimated as a linear function of the potential ET, leaf area index, rooting depth and soil water content (Singh et al. 2008). Unlike the lumped parameter method used by HSPF, SWAT models tile flow as a function of the tile depth, the time required to drain the soil to field capacity and the lag time.

4.2.2 Water Quality: Bacteria

Modeling the fate and transport of bacteria in a watershed involves simulating several complex natural processes including the release of bacteria into the environment,

how they are transported over land (with surface runoff and sediment) and in sub-surface flow, and their die-off and re-growth rate. Both watershed-scale codes used in this study contain modules that utilize built-in hydrologic codes for simulating the transport of bacteria, though the methods used by the two models are substantially different. The section that follows contains a review and comparison of the major differences between the bacteria fate and transport process equations in the two codes.

4.2.2.1 Loading

The bacteria loading rates to the watershed can typically be represented either as a constant or varying loading rate; however, while these rates can be varied daily in SWAT, they are only allowed to vary monthly in HSPF. Additionally, the two codes use different methods to specify loading rates to the watershed: as a direct loading rate (cfu $ha^{-1}h^{-1}$) in HSPF and as the product of the loading rate of the manure *(kg* $ha^{-1}d^{-1}$*)* and its associated bacteria content (cfu g^{-1}) in SWAT.

Bacteria deposited in a watershed is modeled as becoming dissolved in the available water in the upper soil layer and become entrained in the surface runoff. The quantity of bacteria (in solution) released into the surface runoff from the upper soil layer at each time step is estimated differently by each of the codes. HSPF uses an exponential relationship (equation 5) and SWAT a linear relationship (equation 6) to model the release of bacteria to the environment (Benham et al., 2006). The relationships can be expressed as follows:

$$\Delta M_r = M_s[1-\exp(-k_2\Delta Q)] \quad \text{(HSPF)} \quad (5)$$

$$\Delta M_r = M_s k_1 \Delta Q \quad \text{(SWAT)} \quad (6)$$

where ΔM_r is the amount of bacteria (in solution) released from the soil solution into the surface water, M_s the quantity of bacteria in the soil storage layer at the beginning of the time interval, ΔQ is the runoff within the time interval and k_1 is the release rate constant (SWAT) and k_2 the release rate constant (HSPF).

Unlike HSPF, SWAT also simulates wash-off of bacteria from foliage, which is modeled as a function of the characteristics of the bacteria, the timing and intensity of the rainfall and the morphology of the plant. The wash-off of bacteria from foliage is estimated using the equation below:

$$bact_{wsh} = fr_{wsh} \times bact_{fol} \quad (7)$$

where the quantity of bacteria washed off the plant ($bact_{wsh}$) is equal to the product of the wash-off fraction for the bacteria (fr_{wsh}) and the quantity of bacteria originally on the foliage ($bact_{fol}$) (Neitsch et al. 2005). A wash-off factor of 1 was used in this analysis

4.2.2.2 Partitioning

HSPF models deposited bacteria either as (a) fully dissolved in the upper layer of the soil water facilitating entrainment in surface runoff (b) associated (by a potency factor) with sediments in the overland flow (Chin 2006), or (c) suspended in the groundwater (Benham et al., 2006). In SWAT, only a portion of bacteria is modeled in

solution, and the model uses a partitioning coefficient and the linear isotherm given below (equation 8) to divide the bacteria load into a soluble/suspended phase and a sorbed phase:

$$S = k_p c \tag{8}$$

where S is the density of the sorbed bacteria (cfu g^{-1}), k_p the partitioning coefficient (mL g^{-1}) and c the concentration of the bacteria (in solution) in the top 10 mm of soil (cfu mL^{-1}). Another important difference in the simulation routines is that while both models simulate the direct entrainment of a portion of the bacteria solution in the upper soil water layer in the surface runoff, SWAT also allows a portion of the sorbed bacteria to be transported with the sediment entrained in the surface runoff.

4.2.2.3 Fate processes

HSPF simulates bacteria die-off on land by limiting the quantity of bacteria that accumulates on the land's surface. SWAT uses different first-order decay rates to simulate the die-off of bacteria on foliage, dissolved in the soil solution and adsorbed to soil particles (Mancini, 1978). Die-off in water, in both HSPF and SWAT is simulated using Chick's Law (first order decay) as follows:

$$N_t = N_0 \exp(-k_d t) \tag{9}$$

where N_t is the number of bacteria (*cfu*) at time t, N_0 the initial number of bacteria (*cfu*) and K_d the decay constant that varies with temperature.

Though in nature several factors contribute to die-off rates, temperature is the only variable that can be varied to adjust die-off rates in either code (Benham et al., 2006). If required, the die-off rate can be adjusted using the following equation:

$$\mu = \mu_{20}\theta^{T-20} \tag{10}$$

where μ_{20} is the die-off rate at 20°C, θ is the temperature correction parameter for the first-order decay and T is the temperature.

4.2.2.4 Transport processes

Bacteria transport to receiving water bodies is simulated as dissolved constituents in surface runoff. In both model formulations, a series of overland and groundwater process equations account for the dispersion of bacteria in the watershed. The mass flux is modeled as a purely advective process using the following equation:

$$q = vC \tag{11}$$

where q is the mass flux per unit area (cfu cm^{-2} h^{-1}), v is the velocity of the flow and C is the concentration of the bacteria (Benham et al., 2006). Besides mass flux, HSPF allows bacteria to be transported suspended in the groundwater by allowing the user to specify either a constant or a monthly variation of the concentration of bacteria in both the

interflow and the shallow ground water flow to the stream reach. SWAT, conversely, assumes complete die-off of all bacteria beyond the top 10 mm of soil (Neitsch et al. 2005). This reduces the bacteria concentrations in subsurface flows to zero, in spite of abundant evidence suggesting that bacteria can not only exist in the subsurface but can move very far along preferential pathways in saturated conditions (Benham et al., 2006; Ferguson et al., 2003; Tyrrell and Quinton, 2003; Jamieson et al., 2002).

4.3 Other processes

In addition to the difference discussed above, SWAT allows for the tracking of two different types of bacteria (persistent and less persistent) simultaneously. This feature facilitates the simulation of two different types of bacteria with different growth and die-off rates concurrently. It also allows the accounting of the presence and long-term impacts of persistent and often serious pathogen strains in conjunction with less hardy indicator bacteria (Neitsch et al. 2005). HSPF models a single type of bacteria only.

CHAPTER 5: METHODS

5.1 Data Preparation

The four catchments (I, J, K, and O) used in this study are nested sub-watersheds located in the LREW (USGS HUC 3110204 (see Figure 4) Time series of meteorological data collected at the Valdosta Regional Airport in Georgia were prepared and used in this analysis. Precipitation files were prepared from the 5-minute rain gage data collected in the study catchments. The average daily flow measurements were obtained from the USDA Southeast Watershed Research Laboratory (SWERL) database (ftp://www.tiftonars.org/) and observed fecal coliform measurements for each of the catchments were obtained from the National Environmentally Sound Production Agricultural Laboratory (NESPAL) at the University of Georgia, Tifton Campus, GA. The fecal coliform data consisted of forty-three instantaneous data points for Catchment I, fifty-five data points for Catchment J, fifty-three for Catchment K, and forty-eight for Catchment O.

US EPA's BASINS system was used to prepare data for the HSPF model. The watersheds were delineated and stream system defined based on the digital elevation model (DEM) and national hydrography dataset (NHD) which were included in BASINS system. After delineation of the catchments and definition of the stream network and catchment outlets in BASINS, HSPF was used to combine the data and meteorological information and build a model simulating the hydrology and water quality in each catchment. Based on the stream network definition, the channel geometry characteristics were estimated and related the stage and runoff in the relevant stream segment (US EPA

BASINS Technical Note 6). The SWAT model was built using the ArcSWAT version 2.0 interface which runs on the ArcGIS® platform. ArcGIS provides the GIS functionality required by the program to build models of the catchments. Digital elevation models were used to delineate the watersheds and define the stream network. The coverages were then overlain with soil and land use map layers and used to create HRUs the analytical unit used by SWAT.

The same data set created for each catchment was used to build both models with the exception of the digital elevation models (DEM). The DEM packaged with the BASINS system and used with HSPF was not readily transferable to ArcSWAT and was therefore replaced by a DEM obtained from the USGS (http://seamless.usgs.gov) and imported into the ArcSWAT model. The same precipitation and meteorological data sets were used to build both the HSPF and SWAT models and both models were calibrated using the same flow and measured fecal coliform concentration values.

5.2 Single-model calibration

The models were calibrated for both the hydrological and water quality components using a three-step approach introduced by Chin (2009). This calibration technique utilizes a response-surface approach to (i) identify the sensitive model parameters (ii) estimate the maximum conditional likelihood functions, and (iii) verify that the model errors are normally-distributed, random and homoscedastic (i.e. its standard deviation and variance are constant). The method, which uses a Box-Cox transformation to normalize the model error distribution, is explained in Chin (2009) and summarized below.

The calibration of hydrologic and water quality watershed models is based on a comparative analysis between model predications and observed values and Bayesian methods are among the more common methods used to estimate the probability distributions (Chin 2009). From a Bayesian perspective, it can be shown that the probability distribution of a predictand, y, can be estimated using the equation below:

$$p_1(y \mid x) = \int_{\Theta} p_2(y \mid \theta, x) p_3(\theta)\, d\theta \qquad (12)$$

where $p_1(y|x)$ is the conditional probability density of the predictand, y, for the given input (covariate) data set; $p_2(y|\theta,x)$ the conditional probability density of y for a given parameter set θ ; $p_3(\theta)$ the probability density of the parameter set; and Θ the support space of θ or set of all possible parameters (Chin 2009). Implementation of this equation, however, can be , where computationally infeasible, so it is usually approximated using the generalized likelihood uncertainty estimation (GLUE) approach (Beven and Binley 1999, Chin 2009).

Despite frequent use of the GLUE algorithm to approximate equation 12, there are several disadvantages associated with its use to estimate probability distributions. For example, it (a) calculates the model-predicted ($p_1(\hat{y} \mid x)$) and not the actual ($p_1(y \mid x)$) value of the predictand where $\hat{y}$ is defined as model-predicted value of y (Chin 2006) and (b) is typically used with "less formal" likelihood functions that are generally inconsistent with the probability distribution of the model errors (Mantovan and Todini 2006). In light of this, the probability distribution is more frequently approximated using the alternative equation listed below:

$$p'(y \mid x) = p_2(y \mid \theta^*, x) \tag{13}$$

where θ^* is the maximum-likelihood value of the parameter vector θ. This equation (equation 13) is particularly well suited for predicting y^* (the expected value of y) when using a calibrated deterministic model with maximum likelihood parameters θ^*, and the probability density of y is derived directly from the probability density of the model errors relative to y^* (Chin 2009).

To reduce uncertainty in the probability density of y obtained from the probability density of the model errors relative to the predicted value of y, the parameter likelihood function used to calibrate the model must be consistent with the probability density of the model errors (Chin 2009). This requires that the model errors be random and have a quantifiable, stationary probability distribution. Since this is highly improbable under normal circumstances, a transformation method is usually applied to force the model errors to become stationary and normally distributed. The response-surface technique (Chin 2009) used in this analysis employs the Box and Cox transformation method (1964) which can be represented as follows:

$$z_i = \begin{cases} \dfrac{y_i^{\lambda} - 1}{\lambda} & \lambda \neq 0 \\ \log y_i & \lambda = 0 \end{cases} \tag{14}$$

where y_i is the untransformed variable (measured value), z_i the transformed variable, i the data index and λ the transformation parameter.

For instance, if the model errors are assumed to be normally distributed in a transformed domain for a deterministic model $g_i(\theta)$, where θ is the parameter vector, then the likelihood function for the parameter vector of a given set of observations y, used to predict y_i (the measured concentration) can be expressed as follows (Chin 2009):

$$L(\theta \mid y, \lambda) = \frac{1}{\sigma^N} \exp\left[-\frac{1}{2\sigma^2} \sum_{i=1}^{N} \left[z_i - g_i^{(\lambda)}(\theta) \right]^2 y_i^{\lambda - 1} \right] \qquad (15)$$

where σ is the standard deviation of the model errors in the transformed space, $g_i^{(\lambda)}$ is the Box-Cox transformed output of the deterministic model and $y_i^{\lambda-1}$ is the Jacobian of the transformation. As constituted, equation 15 above incorporates the assumption that the model errors are random, homoscedastic and normally distributed in its determination of the likelihood value of the parameter vector θ.

Evaluating equation 15 can be extremely computationally intensive particularly when model parameters are correlated which is quite common when modeling natural phenomena such as watershed processes. To address this problem, sensitivity analyses are typically conducted to reduce the parameter set prior to estimating the likelihood parameter values. Sensitivity analyses identify the most influential process parameters in model predictions. The identified parameters are then used to reduce the significant computational requirements by confining the likelihood functions to the set of sensitive parameters. Though relatively effective, sensitivity analytic methods are limited by the

fact that they tend to utilize nominal range sensitivity in an effort to reduce the computational burden and to ignore any interactions between and nonlinearity in the parameters (Chin 2009, Lenhart et al 2002).

One suggested method for overcoming this shortcoming is the application a response-surface iterative scheme as proposed by Chin (2009) which identifies the sensitive parameters, their maximum likelihood functions and values and verifies that the model errors are normal, random and homoscedastic. The response-surface iterative scheme is performed sequentially, where all but one of the parameter values (θ_i), are held constant and its maximum conditional likelihood found iteratively. This parameter is then fixed at its maximum conditional likelihood value, and the process repeated for each parameter until the parameter set converges to produce the maximum conditional likelihood parameter set. Specifically, if parameter likelihood functions at n discrete values for a model with p parameters, $\theta_1 \ldots\ldots \theta_p$, are to be identified for a defined parameter space, the procedure can be carried out using the following steps:

Step 1: Initialize the parameter vector as $\theta^{(1,1)} = \left[\theta_1, \theta_2^{(0)}, \ldots, \theta_p^{(0)}\right]^T$, where $\theta^{(1,1)}$ represents the 1st iteration on the first parameter θ_1 and $\theta_i^{(0)}$ indicates that θ_i is held at its initial zero-iteration value. The conditional likelihood function for θ_i is calculated as follows:

$$L\left(\theta_1 \mid \theta_2^{(0)}, \ldots, \theta_p^{(0)}, y, \lambda\right) = \frac{1}{\sigma^N} \exp\left[-\frac{1}{2\sigma^2} \sum_{i=1}^{N} \left[z_i - g_i^{(\lambda)}\left(\theta^{(1,1)}\right)\right]^2 y_i^{\lambda-1}\right] \qquad (16)$$

The maximum likelihood value of θ_1 determined from the conditional likelihood function is denoted by $\theta_1^{(1,*)}$.

Step 2: Update the parameter vector to $\theta^{(1,2)} = \left[\theta_1^{(1,*)}, \theta_2, \theta_3^{(0)}, \ldots, \theta_p^{(0)}\right]^T$ and calculate the conditional likelihood function for θ_2 as follows:

$$L\left(\theta_2 \mid \theta^{(1,*)}, \theta_3^{(0)}, \ldots, \theta_p^{(0)}, y, \lambda\right) = \frac{1}{\sigma^N} \exp\left[-\frac{1}{2\sigma^2} \sum_{i=1}^{N} \left[z_i - g_i^{(\lambda)}\left(\theta^{(1,2)}\right)\right]^2 y_i^{\lambda-1}\right] \qquad (17)$$

The maximum likelihood value of θ_1 determined from the conditional likelihood function is denoted by $\theta_2^{(1,*)}$.

Step 3: Repeat step 2 for all the sensitive parameters to complete the first iteration. Iteration 1 ends with taking the parameter vector as $\theta^{(1,p)} = \left[\theta_1^{(1,*)}, \ldots, \theta_{p-1}^{(1,*)}, \theta_p\right]^T$ and calculating the conditional likelihood function for θ_p as follows:

$$L\left(\theta_p \mid \theta_1^{(1,*)}, \ldots, \theta_{p-1}^{(1,*)}, \theta_p, y, \lambda\right) = \frac{1}{\sigma^N} \exp\left[-\frac{1}{2\sigma^2} \sum_{i=1}^{N} \left[z_i - g_i^{(\lambda)}\left(\theta^{(1,p)}\right)\right]^2 y_i^{\lambda-1}\right] \qquad (18)$$

Step 4: Start the 2nd iteration by taking the parameter vector as $\theta^{(1,2)} = \left[\theta_1, \theta_2^{(1,*)}, \ldots, \theta_p^{(1,*)}\right]^T$ where $\theta^{(1,*)}$ indicates that θ_i is held constant at its 1st iteration maximum-likelihood value. The conditional likelihood function for θ_1 is then calculated as follows:

$$L\left(\theta_1 \mid \theta_2^{(1,*)},\ldots,\theta_p^{(1,*)},y,\lambda\right)=\frac{1}{\sigma^N}\exp\left[-\frac{1}{2\sigma^2}\sum_{i=1}^{N}\left[z_i-g_i^{(\lambda)}\left(\theta^{(1,2)}\right)\right]^2 y_i^{\lambda-1}\right] \qquad (19)$$

The maximum likelihood value of θ_1 determined from the conditional likelihood function is denoted by $\theta_1^{(2,*)}$.

Step 5: Repeat step 4 for each parameter to complete the 2nd iteration. Iteration 2 ends with taking the parameter vector as $\theta^{(2,p)}=\left[\theta_1^{(2,*)},\ldots,\theta_{p-1}^{(2,*)},\theta_p\right]^T$ and calculating the conditional likelihood function for θ_p as follows:

$$L\left(\theta_p \mid \theta_1^{(2,*)},\ldots,\theta_{p-1}^{(2,*)},\theta_p,y,\lambda\right)=\frac{1}{\sigma^N}\exp\left[-\frac{1}{2\sigma^2}\sum_{i=1}^{N}\left[z_i-g_i^{(\lambda)}\left(\theta^{(2,p)}\right)\right]^2 y_i^{\lambda-1}\right] \qquad (20)$$

Step 6: Repeat steps 4 and 5 until the conditional likelihood function converges to its asymptote. The jth iteration ends with the parameter vector given as $\theta^{(j,p)}=\left[\theta_1^{(j,*)},\ldots,\theta_{p-1}^{(j,*)},\theta_p\right]^T$ and the conditional likelihood function for θ_p is given by:

$$L\left(\theta_p \mid \theta_1^{(j,*)},\ldots,\theta_{p-1}^{(j,*)},\theta_p,y,\lambda\right)=\frac{1}{\sigma^N}\exp\left[-\frac{1}{2\sigma^2}\sum_{i=1}^{N}\left[z_i-g_i^{(\lambda)}\left(\theta^{(2,p)}\right)\right]^2 y_i^{\lambda-1}\right] \qquad (21)$$

The final iteration cycle provides the maximal conditional likelihood function of all the parameters, where the maximal conditional likelihood function for each parameter is

defined as the likelihood function trained on the maximum likelihood values of all the other parameters (Chin 2009). As such, equation 21 will provide the conditional maximum likelihood for a model with p parameters, $\theta_1 \ldots\ldots \theta_p$.

Comparatively, the approach described above is more efficient at estimating the conditional maximum likelihood parameter values than the commonly used Monte Carlo methods (Stow et al 2007). The primary reason for this is that the method proposed by Chin (2009) uses the maximal conditional likelihood functions rather than the entire likelihood functions to identify the sensitivity and maximum likelihood values of the model parameters. The reduction in the parameter set significantly reduces the computational burden required to investigate all possible parameter combinations needed to define the response surface. This method was utilized to calibrate both the hydrology and water quality components of the analysis and is summarized in figure 5 below.

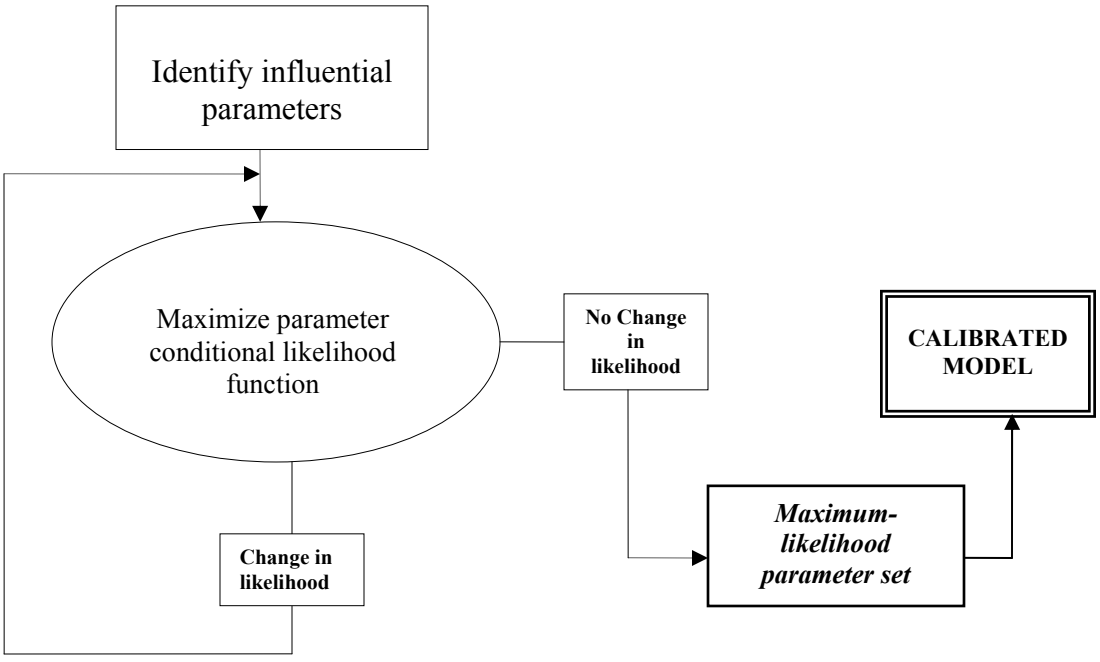

Figure 5: Flow chart of the calibration methodology

Each sub-basin was modeled using HSPF and SWAT and calibrated using the method described above. The calibrations were done for each of the four catchments (I, J, K and O) first for hydrological and subsequently for water quality parameters. Along with the maximum conditional likelihood values, quantitative comparisons between the predicted and observed daily flows (hydrology) and the measured and predicted concentrations for fecal coliform (water quality) were computed using the Nash-Sutcliffe Efficiency coefficient described by the equation below (Nash and Sutcliff, 1970):

$$NSE = 1 - \frac{\sum_{i=1}^{N} (y_i - m_i)^2}{\sum_{i=1}^{N} (m_i - \overline{m})^2} \qquad (22)$$

where y_i is the observed discharge and m_i the modeled discharge at time step i. Model performance ratings based on the distribution of NSE values are as follows (Moriasi et al. 2007):

0.75	<	NSE	<	1.00	Very Good
0.65	<	NSE	<	0.75	Good
0.50	<	NSE	<	0.65	Satisfactory
		NSE	≤	0.50	Unsatisfactory

5.2.1 Hydrology

The parameters identified as having a significant influence on hydrological processes in a watershed typically include the rate at which precipitation infiltrates into the soil, the water balance in upper and lower storage zones and the recession rates. The primary parameters that control these processes are listed and described below:

(1) HSPF

Infiltration rate (INFILT)

Infiltration is determined by changes in the moisture in the soil profile and can vary both spatially and temporally in the watershed. In HSPF, the parameter (INFILT) is used to account for this process. INFILT determines the allocation of water in the soil profile and controls the division of the available moisture from precipitation into surface runoff or more specifically - the quantity of water available for storage in a system. As a rule, the lower the values of INFILT – the greater the overland flow. INFILT is a function of soil characteristics in the area (for example, hydraulic conductivity and moisture content), closely related to SCS hydrologic soil groups and modeled using the Green-Ampt infiltration equation (1911).

Lower-zone nominal storage (LZSN)

The lower zone nominal storage capacity is a function of the precipitation patterns and the soil characteristics in a watershed. The lower zone nominal storage parameter (LZSN) is used to account for storage and based on the sum of the direct infiltration, percolation, lateral inflow and irrigation application that enters the storage zone. High LZSN values increase the quantity of water stored in the lower zone, which in turn, increases the potential for evapotranspiration. Low LZSN values increase the flow rates in the reach.

Ratio of soil infiltration (INFILD)

This parameter describes the ratio of the maximum infiltration and mean infiltration capacity over the land segment.

Fraction of groundwater lost to deep aquifer (DEEPFR)

The fraction of infiltrating water that is lost to the deep aquifer is represented by the parameter DEEPFR. Percolation and direct infiltration in the watershed that does not directly enter the lower storage zone will either flow into the active ground water or be lost to the deep aquifers (inactive groundwater). The parameter DEEPFR determines the distribution of this inflow to the active or inactive groundwater storage zones. The portion of the inflow not designated as inactive ground water will be routed and combined with the lateral and irrigation flow (if available) to make up the total inflow to active groundwater storage. DEEPFR also accounts for other losses that may not be measured by installed flow gages and reflected in the observed values used in the calibration of the model.

Active groundwater recession coefficient (AGWRC)

The active ground water recession coefficient is the ratio of the current groundwater discharge to that of the preceding 24 hours. The recession rate for a watershed is usually a complex function of several watershed conditions including climate, topography, soil and land-uses and it is typically estimated from the observed daily flow data using hydrograph separation techniques.

Interflow recession coefficient (IRC)

The interflow recession coefficient is the ratio of the present rate of interflow to the rate of the preceding 24 hours. It is used to determine the quantity and update the storage of the interflow. Interflow can significantly influence storm hydrographs particularly if there are shallow, less permeable soil layers present that may impede vertical percolation through the soil. Flow added to the interflow from surface flows or upslope external lateral flows are either retained in storage or routed as outflow from land segments. The IRC is assumed to have a linear relationship to storage and estimated as a function of a recession parameter, inflow, and storage.

Other potentially influential parameters include:

Exponent in the infiltration equation (INFEXP)

The exponent in the infiltration equation determines how much a deviation from the nominal lower zone storage affects the infiltration rate in the watershed.

Upper-zone nominal storage (UZSN)

The upper zone nominal storage is a function of the land surface characteristics, the topography and the quantity of lower zone nominal storage (LZSN) in a watershed. Because it is related to land surface characteristics, changes in land use including plant growth over a season and other agriculture processes can affect its value. As a general rule, the higher the value of UZSN in a area, the more water will be retained in the upper

zone and be available for evapotranspiration, which in turn decreases the quantity available for surface and direct overland flow.

Interflow inflow (INTFW)

The interflow inflow coefficient determines the quantity of water entering the ground from surface detention storage and converted to interflow. Because interflow can have a significant influence on storm hydrographs, changes to the interflow inflow coefficient can influence the shape of the hydrograph by delaying or accelerating the timing of the runoff. Increasing the INTFW affects the quantity of interflow, which decreases the direct overland flow and reduces the peak flows while maintaining the same runoff volume. As such, it can be used to raise or lower peaks to improve the agreement between the simulated and observed hydrographs.

Ground water recession flow (KVARY)

The groundwater recession flow parameter is used to describe the non-linear recession rate. This parameter is important when observed groundwater recession demonstrates seasonal variability such as faster recession during wet periods. KVARY controls the actions of groundwater recession flow, enabling it to be non-exponential in its decay with time.

Hydraulic routing weighting factor (KS)

The hydraulic weighting factor is used to estimate of the stream reach outflow. The outflow given at a time step is computed as the sum of the product of the weighting factor

at the beginning of the time-step and the product of the complement of the weighting factor at the end of the time-step.

(2) SWAT

Runoff curve number (CN2)

The CN2 is the initial runoff curve number for moisture condition II or average moisture conditions in the watershed. SWAT utilizes the USDA Soil Conservation Service runoff curve number method (SCS 1972) to estimate runoff under varying land uses and soil types. The curve number equation is as follows:

$$Q_{surf} = \frac{(R_{day} - 0.2S)^2}{(R_{day} + 0.8S)} \tag{23}$$

where

$$S = 2.54\left(\frac{1000}{CN} - 10\right) \tag{24}$$

and Q_{surf} the accumulated runoff, S the retention parameter, R_{day} the daily precipitation in the watershed and CN the SCS curve number. The curve number is a function of the soil permeability, the land uses/land cover and antecedent soil moisture condition in the watershed. Typical curve number II values (SCS Engineering Division 1986) are appropriate for 5% slopes and can be adjusted to reflect changes in land covers conditions including but not limited to plants, tillage and harvest/kill operations.

Groundwater revap (GW_REVAP)

The groundwater *revap* coefficient is used to control the amount of water that moves from the shallow aquifer to the root or overlying unsaturated zone. During dry periods, water from the capillary fringes that separate the saturated and unsaturated zone will evaporate and diffuse upwards into the overlying dry layer. Water removed from the saturated zone by capillary action is replaced by water from the underlying aquifer. GW_REVAP is a function of the overlying land use and only allowed to occur if the shallow aquifer exceeds a certain threshold. GW_REVAP is estimated as follows:

$w_{revap} = 0$ if $aq_{sh} \leq aq_{shthr,\,rvp}$

$w_{revap} = w_{revap,\,mx} - aq_{shthr,\,rvp}$ if $aq_{shthr,rvp} < aq_{sh} < (aq_{shthr,rvp} + w_{revap,mx})$

$w_{revap} = w_{revap,\,mx}$ if $aq_{sh} \geq (aq_{shthr,rvp} + w_{revap,mx})$

where $w_{revap,\,mx} = \beta_{rev} \times E_o$

and $aq_{shthr,rvp}$ is threshold level in the shallow aquifer for revap to occur, β_{rev} the revap coefficient, E_o the potential evapotranspiration for that day, aq_{sh} the amount of water stored in the shallow aquifer at the beginning of the day and w_{revap} the actual amount of water moving into the soil zone in response to the water deficiency.

Threshold aquifer water level depth for revap (REVAPMN)

In SWAT, the term *revap* is used to refer to the movement of water from the underlying shallow aquifer to the unsaturated layer above. *Revap* is a function of the water demand

for evaporation. It is closely related to the land use in an area and can be significant in watersheds with deep-root plants or saturated zones close to the surface. The threshold depth of water in the shallow aquifer for *revap* to occur is modeled by the parameter REVAPMN.

Threshold water level in shallow aquifer for base flow (GWQMN)

The threshold depth of water in the shallow aquifer required for return flow to occur to the stream (GWQMN) controls the amount of percolation to the deep aquifer and regulates the quantity of groundwater lost to the system. Groundwater flow to the stream reach is restricted if the depth of water in the shallow aquifer is less than the GQWMN threshold.

Aquifer percolation coefficient (RCHRG_DP)

The aquifer percolation coefficient determines the fraction of percolation from the root zone that recharges the deep aquifer. SWAT allows a portion of the total daily recharge to be routed to the deep aquifer. The quantity of water routed to the deep aquifer is estimated as the product of the aquifer percolation coefficient and the total amount of recharge entering both the shallow and deep aquifers.

Other potentially influential parameters include:

The base flow recession constant (ALPHA_BF)

The base flow recession constant or constant of proportionality is a direct index of the response in groundwater flow to changes in recharge (Smedema and Rycroft 1983).

Though this parameter can be calculated, it is best estimated by analyzing stream flows during periods of no recharge.

The ground water delay (GW_DELAY)

Water infiltrating or percolating through a soil profile will flow through the vadose zone and recharge the underlying shallow and deep aquifers. The lag between the time the water leaves the soil profile and when it enter the aquifers is measured by the ground water delay parameter in SWAT. Groundwater delay time is a function of the depth of the water table and the hydraulic properties of the geologic formation in the vadose and groundwater zones. The delay time cannot be measured directly and is usually estimated by simulating aquifer recharge while varying the delay time and comparing the simulations with observed values.

The effective hydraulic conductivity of the main channel (CH_K2)

The effective hydraulic conductivity of the main channel to used to relate the height of the groundwater level to the groundwater flow in the watershed.

Manning's *n* of the main channel (CH_N2)

Manning's coefficient *n* is based on land uses and to calculate the velocity and rate of flow in the stream reach at a given time step. Manning's equation for velocity and flow are given below:

$$v = \frac{R^{2/3} \times s^{1/2}}{n} \qquad (25)$$

$$q = \frac{A \times R^{2/3} \times s^{1/2}}{n} \quad (26)$$

where q is the rate of flow in the channel, v is the velocity, A is the cross-sectional area of flow, R is the hydraulic radius for a given depth and s is the slope and n the Manning's n for the channel.

5.2.2 Water Quality

The most influential parameters controlling the environmental fate and transport of bacteria in the watershed were identified as follows:

(1) HSPF

HSPF models bacteria as a water quality constituent and simulates the constituent as:

- a basic accumulation and depletion rate together with depletion with wash off, where the constituent outflow from the surface is a function of the water flow over the surface and the quantity of the constituent in storage; and/or
- associated with the inflow in the area.

Based on this, the most influential parameters associated with the bacteria fate and transport processes are:

<u>The rate of terrestrial accumulation of bacteria (ACQOP)</u>

The rate of terrestrial accumulation of bacteria determines the rate at which bacteria accumulate on the surface that can be washed off.

The storage limit of bacteria on the surface of the land (SQOLIM)

The storage limit of bacteria on the surface of the land indicates the maximum quantity of bacteria (highest concentration) that can be stored on the surface.

The rate of surface runoff that removes 90% of stored bacteria per hour (WSQOP)

The rate of surface runoff that removes 90% of stored bacteria per hour determines the rate of the surface runoff require to remove 90% of the stored bacteria from the available surface.

The interflow bacteria concentration (IOQC)

The interflow bacteria concentration determines the concentration of bacteria available in the interflow.

The point source mass flux (PSRC)

The point source mass flux determines the concentration per unit time from available point sources –or sources not associated with a land area in the watershed—that contribute to the stream reach.

First-order decay rate (FSTDEC)

The first-order decay rate, based on Chick's Law, determines the survival/die off rate of the bacteria in the system.

(2) SWAT

Bacteria application rate (CFRT_KG)

Land application of animal waste is one of the most common methods of disposing of animal manure. In SWAT, this process is accounted for by the bacteria application rate which indicates the amount of fertilizer or manure is applied to the watershed.

Bacteria soil partitioning coefficient (BACTKDQ)

The bacteria soil-partitioning coefficient is the ratio of the concentration of bacteria in the surface soil solution (top 10 mm of soil) to the concentration of bacteria in the surface runoff. Model assumptions in the simulation of the fate and transport processes of bacteria include the assumption that because of the low motility of bacteria, surface runoff will only interact with the top 10 mm of soil.

Bacteria percolation partitioning coefficient (BACTMX)

The bacteria percolation coefficient is the ratio of the concentration of bacteria in the surface soil solution (top 10 mm of soil) to the concentration of bacteria in the percolate.

The die-off factor for bacteria in water (WDPRCH)

The die off factor (survival rate) for bacteria in moving water (streams) per day at 20° C.

The die-off factor for bacteria in soil (WDPQ)

The die-off factor (survival rate) for bacteria in soil solution per day at 20° C.

The point source flux (BCNST)

The point source flux determines the concentration per unit time from available point sources –or sources not associated with a land area in the watershed—that contribute to the stream reach.

5.3 Multi-model formulation

The idea of combining the estimates from different model codes to improve forecasting was first introduced by Bates and Granger in 1969. Since then, an impressive body of work using forecasts combination has emerged in diverse fields ranging from economics and management science to statistics and meteorology (Granger, 2001; Clemens, 1989; Thompson, 1976; Newbold and Granger, 1975; Dickinson, 1973). In 1997, the method of combining forecasts was applied to the field of hydrology to improve rainfall-runoff models estimates (Kim et al., 2006; Shamseldin et al., 1997). The results of the study provided support for the notion that the method had the potential to improve hydrological forecasting estimates. Yet, in spite of the veritable abundance of studies conducted over the last forty years, this method has never been applied to water quality modeling or used to predict contaminant levels at a watershed scale. In this regard, this study is a significant improvement over existing watershed analytic methods, and more specifically, current TMDL analyses.

There are several reasons why a multi-model approach holds great promise for water quality/water resources engineering. First, the combination of model estimates facilitates the reduction in predictive uncertainty by including exogenous information from contributing models to improve overall predictions (Kim et al., 2006). Second, it

allows the exploitation of the strengths of several models simultaneously. Models are essentially abstractions or simplifications of complex natural phenomena and quite often use different algorithms to model the same process; accordingly, models may complement each other and in tandem better approximate true processes. Third, models usually include assumptions that not only vary from model to model but are not always met with data and other input information (Shamseldin et al 1997). This too, has the potential to substantially reduce overall model uncertainty.

In this study, model forecast results were combined using three different methods: (a) the weighted average method (WAM), (b) the Nash-Sutcliff Efficiency Maximization method (NSE-max) and (c) the artificial neural network method (ANN). The first two methods (WAM and NSE-max) are linear combination methods. However, although linear combination methods are relatively robust, they tend to produce unstable weights in the presence of multi-collinearity (Winkler, 1989). Unfortunately, an artifact of the majority of hydrological models is that the degree of multi-collinearity in a model is directly proportional to increases in its forecasting ability (Shamseldin et al., 1997). To account for this limitation in the linear combination models, a third method (ANN) which utilizes a nonlinear combination approach was included in the analysis.

5.3.1 Weighted Average Method (WAM)

The weighted average method (WAM) is the first of three methods used to combine model results in this study. WAM has been identified as an efficient method to combine the results of individual models particularly when the results of one model tend to be consistently more accurate than the other models used (Armstrong 1989). The

estimated outputs from the individual models are combined using the following equation (Granger and Ramanathan, 1984; Shamseldin et. al., 1997):

$$Q_i = \sum_{j=1}^{N} a_j \hat{Q}_{j,i} + e_i \qquad (27)$$

where Q_i is the observed discharge in the ith time step, a_j the weight assigned to the jth model, $\hat{Q}_{j,i}$ the estimated combined discharge and e_i the combination error term (Shamseldin et. al., 1997). Using matrix algebra notation, this equation is expressed as follows:

$$\mathbf{Q} = \mathbf{PA} + \mathbf{E} \qquad (28)$$

where the number of observations is denoted by k, and:

the output vector $\quad Q = (Q_1, Q_2, Q_3, \ldots\ldots, Q_{k-1}, Q_k)^T$

the weight vector $\quad A = (a_1, a_2, a_3, \ldots\ldots\ldots\ldots, a_{N-1}, a_N)^T$

the combination error vector $\quad E = (e_1, e_2, e_3, \ldots\ldots\ldots\ldots, e_{k-1}, e_k)^T$

and the input matrix $\quad P =$

$$\begin{bmatrix} \hat{Q}_{1,1} & \hat{Q}_{2,1} & \cdots & \cdots & \hat{Q}_{N-1,1} & \hat{Q}_{N,1} \\ \hat{Q}_{1,2} & \hat{Q}_{2,2} & \cdots & \cdots & \hat{Q}_{N-1,2} & \hat{Q}_{N,2} \\ \hat{Q}_{1,3} & \hat{Q}_{2,3} & \cdots & \cdots & \hat{Q}_{N-1,3} & \hat{Q}_{N,3} \\ \vdots & \vdots & \vdots & \vdots & \vdots & \vdots \\ \vdots & \vdots & \vdots & \vdots & \vdots & \vdots \\ \hat{Q}_{1,k-1} & \hat{Q}_{2,k-1} & \cdots & \cdots & \hat{Q}_{N-1,k-1} & \hat{Q}_{N,k-1} \\ \hat{Q}_{1,k} & \hat{Q}_{2,k} & \cdots & \cdots & \hat{Q}_{N-1,k} & \hat{Q}_{N,k} \end{bmatrix}$$

If equation 28 is conceptualized as a multiple linear regression model, then the weight vector (**A**) can be estimated using the ordinary least squares solution to the equation below (Draper and Smith, 1981):

$$\hat{A} = \left(P^T P\right)^{-1} P^T Q \tag{29}$$

To reduce bias, the weights in a WAM analysis are usually constrained to sum to unity (Dickinson, 1975). This is done to ensure that the mean output error of all the input models is zero, since if all the input models are unbiased, the combined output will also be unbiased (Granger and Ramanathan, 1984). The models are constrained using the following equation:

$$\sum_{i=1}^{N} a_i = 1 \tag{30}$$

and the original equation (equation 29) adjusted to reflect the constraints by estimating the weight vector using the method of constrained least squares as follows (Breun, 1985):

$$\hat{A}_{cls} = \left(P^T P\right)^{-1}\left(P^T Q + \tfrac{1}{2} b\lambda\right) \tag{31}$$

where $\hat{A}_{cls}$ is the weight vector estimated using the method of constrained least squares, b is the unit vector having the same dimension as the parameter vector A and λ is the

Lagrangian multiplier calculated as follows and the variables defined as above (Shamseldin et. al., 1997):

$$\lambda = 2\left(b^T\left(P^T P\right)^{-1} b\right)^{-1}\left(1 - b^T\left(P^T P\right)^{-1} P^T Q\right) \tag{32}$$

5.3.2 Nash-Sutcliff Efficiency Maximization Method

Chin et al. (2009) introduced the Nash-Sutcliff Efficiency maximization method (NSE-max) as an alternative method to combine prediction estimates in a multi-model analytic approach. The NSE-max equation is derived from the Nash-Sutcliffe Efficiency coefficient (Nash and Sutcliffe, 1970) which is extensively used in hydrologic studies to examine performance and assess the goodness of fit of a model. The Nash-Sutcliff Efficiency coefficient (NSE) is calculated as defined in equation 10:

$$NSE = 1 - \frac{\sum_{i=1}^{N}\left(y_i - m_i\right)^2}{\sum_{i=1}^{N}\left(m_i - \overline{m}\right)^2}$$

If the predictions from two models are considered and the weights are constrained to sum to unity, then a weighted model averaged prediction can be estimated using the following equation (Chin et al. 2009):

$$P_i = aI_{1_i} + (1-a)I_{2_i} \tag{33}$$

where P_i is the prediction at time step i; I_1 and I_2 the inputs, where I_{1i} the first model estimate and I_{2i} the second model estimate at time step i; and a a weighting factor between zero and one.

If the equation (equation 33) is then substituted into original NSE equation, the Nash-Sutcliffe efficiency coefficient can now be expressed as:

$$NSE = 1 - \frac{\sum_{i=1}^{N}\left[M_i - aI_{1_i} - (1-a)I_{2_i}\right]^2}{\sum_{i=1}^{N}\left(M_i - \overline{M}\right)^2} \tag{34}$$

where M_i is the measurement at time step i and $\overline{M}$ the average of the N measurements. The value of the weighting factor a that maximizes the NSE can then be calculated from the derivative of (equation 18) and shown to be:

$$\frac{dNSE}{da} = 0 \Rightarrow a = \frac{\sum_{i=1}^{N}\left(M_i - I_{1i}\right)\left(I_{1i} - I_{2i}\right)}{\sum_{i=1}^{N}\left(I_{1i} - I_{2i}\right)^2} \tag{35}$$

Taking the second derivative of the equation results in the equation below:

$$\frac{d^2 NSE}{da^2} = -\sum_{i=1}^{N} (I_{1_i} - I_{2_i})^2 < 0 \qquad (36)$$

which confirms that the weighting factor obtained using equation 35 will maximize the value of the NSE, and the resulting NSE will be greater than the original NSE values derived from either of the original individual models.

5.3.3 The Artificial Neural Network Method

The Artificial Neural Network (ANN) method is the third method used to combine model estimates in this study. Formally defined as a "complex structure used to solve complex data-analysis problems" (Priddy and Keller, 2005), neural networks are based on the simulation of the physiological properties of a biological nervous system. The notion of an artificial neural network as a computational model was first introduced by McCulloch and Pitts in 1943 (McCulloch and Pitts, 1943). The model drew significant scientific interest and most of its theoretical foundations were laid over the next two decades or so, including most notably, the development of the perceptron by Rosenblatt in 1958 (Rosenblatt, 1958).

However, mathematical proof of the perceptron's limitations, such as its inability to perform complex classifications (Minksy and Papert, 1969), led to waning interest in the model and it was abandoned by all but a handful or researchers, during the latter part of the 1960's and most of the 1970's (Priddy and Keller, 2005). During this time of limited research interest, the back-propagation technique was developed by Werbos

(1974), which when coupled with Hopfield's (1982) energy minimizing processes serve not only to revitalize but to revolutionize neural network research sparking mass interest and widespread use.

ANNs are presently widely used in several areas ranging from informatics (email/spam filtering, virus scanning, speech and optical character recognition) and business applications (financial/sales forecasting, credit card fraud detection, etc) to weather forecasting (meteorology) and engineering. Engineering applications employing this approach include but are not limited to the detection of explosives at airports, automatic target recognition, robotics and other artificial intelligence applications.

In 1993, Shi and Liu introduced the concept of using a neural network to combine model forecasts. The results of their study, which combined the results of three individual forecasting models, suggested that the combined model estimates were a significant improvement (based on the mean squared error) over the results obtained from the individual models (Shi and Liu, 1993). Since then, numerous studies using the neural network method to combine forecasts have surfaced (Donaldson and Kamstra, 1997; Fiordaliso, 1998; He and Xu, 2005), but none to date have applied the technique to watershed-scale water quality models. Therefore, this study constitutes the first attempt to use this method to improve contaminant concentration estimates in water quality analysis.

Neural Networks

From a physiological standpoint, a neural network is an interconnected group of highly specialized cells called neurons. In vertebrates, these interconnected neurons

cluster into large groups ultimately forming a control unit referred to as a brain. Within the brain, the neurons receive inputs from and send outputs to other neurons (Sheir et al 2009). Each neuron is comprised of three major parts: a cell body or soma that processes information, connecting fiber dendrites that receive electrochemical stimulation from other neurons and axons that communicate with neighboring neurons (Sheir et al 2009). The axons connect to the dendrite fibers through an electrochemical junction referred to as the synapse (Priddy and Keller, 2005). In highly developed animals, the brain has the ability to learn or adapt to a changing environment.

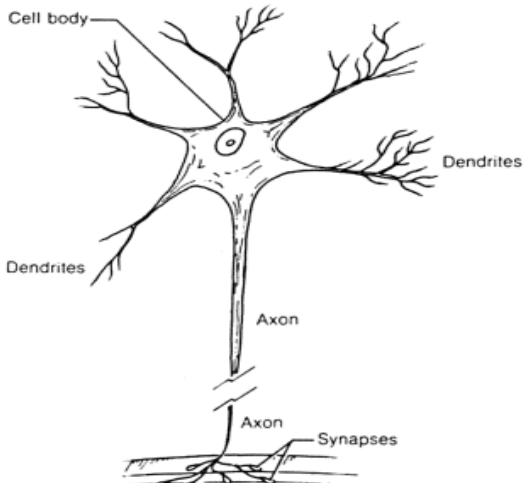

Figure 6: The structure of a neuron (Turchin, 1977).

Artificial neural networks attempt to mimic biological neural networks by using mathematical abstractions to simulate the interactions between the neurons in the brain. In the brain, neurons transmit signals to other neurons by sending action potentials down the axon. When a signal is received, depending on its relevance, the synapse will either

increase or decrease the electrical potential. If the signal strength meets the neuron's required threshold, the neuron will fire (Sheir et al. 2009) and the action potential firing rate determined by the relevance or strength of the stimulus.

In an ANN, this relationship is modeled by the use of a transfer function that mimics the firing rate of the action potential transmitted by a neuron. Inputs to the model—like inputs to the brain— depend on the relevance of the signal (i.e. whether or not the neuron should fire) represented in an ANN by the assignment of weights to the inputs (Priddy and Keller 2005). A transfer function is then used to describe the behavior of the output neuron. Neurons, as a whole, are conceptually small "computing engines" that accept and process inputs and transmit outputs (Priddy and Keller 2005).

ANNs consist of a number of neurons or nodes, linked together by connection pathways with associated weights. A neuron typically can receive many inputs, but usually transmits only one output (Wnek and Boelin 2008). The neuron accepts and accumulates all inputs (using a summation function), transforms them to an output (using a transfer function) then transmits the output to neighboring neurons via a number of connection pathways (Priddy and Keller 2005). Each neuron transmits the full output value to each of the neighboring neurons.

Weighted estimates (x_1/w_1, x_1/w_2) are inputted into the model and summed ($\sum$) as follows:

$$h = \sum_k w_k, x_k \tag{37}$$

where h is the output to a neuron in the hidden layer, k the number of neurons, w the weight and x the input from each of the other neurons.

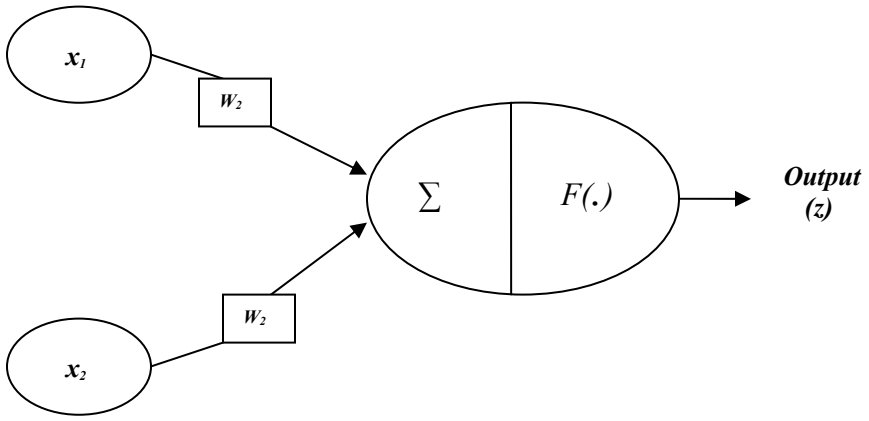

Figure 7: ***The structure of an artificial neural network*** (adapted from Priddy and Keller, 2005)

An appropriate transfer function (*F(.)*) is then used to produce an output (z) given by:

$$z = f\left(\sum_{i-1}^{N} w_i y_i + w_o\right) \tag{38}$$

where z is the neuron output, y_i the input vector , w_i the weight matrix, N the total number of inputs or neurons in preceding layer, w_o the neuron threshold or baseline value independent of the input, and f a non-linear function. The weights of the connection pathways, or weight matrix, are then estimated by calibrating or training to the model to adapt to its environment (Shamseldin et al., 1997).

Multi-layer feedforward networks

There are several variations of neural networks in existence today (Lippman, 1987) and one of the most commonly used network structures is the multi-layer feedforward network. The multi-layer feedforward network also referred to as a multi-layer perceptron is a universal approximator generally used to classify non-linear data models (Khan et al., 2007; Nielson, 1991; Shamseldin et al., 1997). The feedforward model consists of three layers of neurons:

- an inner layer that distributes inputs to the hidden layer
- hidden layer(s) that transforms the input values into a vector (numerical), and
- an outer layer that transforms the hidden values into a forecast

Though relatively simple in structure, a feedforward network is best described as an all-purpose model. In fact, its structure is so robust that a network that with one hidden layer can describe any continuous function and one containing two hidden layers any function (Hartman et. al., 1990). Based on this, the *multi-layer feedforward network* was selected for this analysis.

Transfer Functions

After selecting a model structure, the next and final step in constructing a neural network model is the selection of an appropriate transfer function. Transfer functions are comprised of an activation function that uses outputs to determine the total signal a neuron receives and an output function that determines the scalar output (Wnek and Bowlin 2008). Transfer functions add both non-linearity and stability to the structure of

an artificial neural network (Liptak 2006). Of the several functions available, the *sigmoid* or *logistic* function was selected for use in this analysis. The sigmoid function is one of the most commonly used functions in neural network modeling because it has the mathematical properties (such as monotonicity, continuity and differentiability) that are essential to enable networks with gradient descent to be correctly trained (Priddy and Keller, 2005). In this study, the following sigmoid function ($F(.)$) was applied to calculate the output to each neuron z:

$$z = f\left(\sum_{i-1}^{N} w_i y_i + w_o\right) \tag{39}$$

yielding an overall output equal to:

$$output = \frac{1}{1 + e^{-\left(\sum_i w_i y_i + w_0\right)}} \tag{40}$$

where i is the coefficient on inputs to the neuron, x_i is the input, w_i the weighting factor attached to the inputs and w_0 the bias to the neuron (Priddy and Keller, 2005).

The network is then calibrated or trained which can be likened to teaching the brain (network of neurons) to adapt. Training, a fundamentally an unconstrained optimization problem, was conducted in this analysis using the Broyden-Fletcher-Goldfarb-Shanno (BFGS) algorithm. The BFGS algorithm is based on the Hessian matrix update of Newton's method of optimization and is one of the most commonly used algorithms to solve unconstrained linear optimization problems in neural networks

(Wnek and Bowlin 2008). The architecture of the multi-layer feedforward network used in this study is given below:

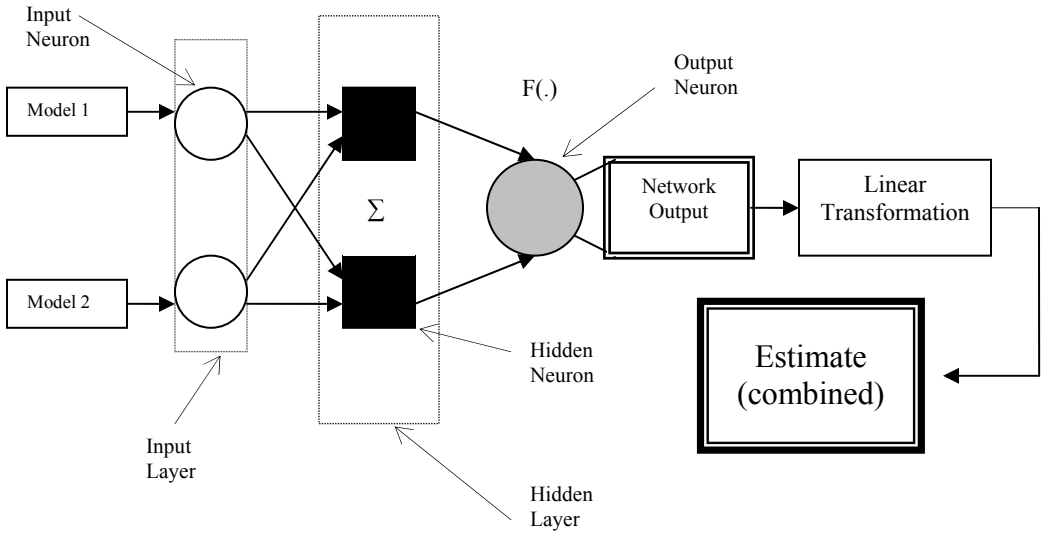

Figure 8: Architecture of the multi-model feedforward neural network (adapted from Priddy and Kelly, 2005)

CHAPTER 6: RESULTS

6.1 Single model approach

All four sub-basins were analyzed and models developed for the seven-year study period (January 1996 thru December 2002). The model results were evaluated the Nash-Sutcliffe Efficiency coefficient (NSE), to compare the results simulated by the models with the observed values from the sub-basins. The models were calibrated using the three-step approach described in the previous chapter and the maximum likelihood parameter sets obtained during the calibration process are listed below.

HSPF

The maximum likelihood parameter sets obtained for the hydrological and water quality components for each catchment are presented in Tables 5 - 8 as follows:

Table 5 HSPF: Maximum Likelihood Parameters - Catchment I

Parameters	*Value*	*Units*	*Description*
Hydrology			
AGWRC	0.98	d^{-1}	Basic groundwater recession rate
DEEPFR	0.10	--	Fraction of groundwater lost to the system
INFEXP	2.00	--	Exponent in the infiltration equation
INFILD	2.00	--	Ratio between maximum and mean infiltration
INFILT	0.51	cm h^{-1}	Infiltration capacity coefficient
INTFW	15.00	--	Interflow inflow parameter
IRC	0.35	d^{-1}	Interflow recession parameter
KS	0.50	--	Weighting factor for hydraulic routing
KVARY	1.27	cm^{-1}	Groundwater recession flow parameter
LZSN	6.35	cm	Lower zone nominal storage
UZSN	3.43	cm	Upper zone nominal storage
Water Quality			
ACQOP(A)	0.18	$\times 10^{8}$ FC ha^{-1} d^{-1}	FC accumulation rate (agriculture)
ACQOP(F)	2.60	$\times 10^{8}$ FC ha^{-1} d^{-1}	FC accumulation rate (forest)
FSTDEC	4.75	d^{-1}	First -order decay rate of FC in stream
IOQC	3.57	$\times 10^{6}$ cfu/100 mL	Interflow FC concentration
PSRC	2.81	$\times 10^{8}$ FC d^{-1}	Mass flux from direct source
SQOLIM	2.84	$\times 10^{11}$ FC ha^{-1}	Maximum surface storage of FC
WSQOP	0.51	cm h^{-1}	Rate of surface runoff that removes 90% of FC in 1 hour

Table 6 HSPF: Maximum Likelihood Parameters - Catchment J

Parameters	*Value*	*Units*	*Description*
Hydrology			
AGWRC	0.96	d^{-1}	Basic groundwater recession rate
DEEPFR	0.00	–	Fraction of groundwater lost to the system
INFEXP	2.00	–	Exponent in the infiltration equation
INFILD	2.00	–	Ratio between maximum and mean infiltration
INFILT	0.64	cm h^{-1}	Infiltration capacity index
INTFW	31.00	–	Interflow inflow parameter
IRC	0.30	d^{-1}	Interflow recession parameter
KS	0.44	–	Weighting factor for hydraulic routing
KVARY	2.03	cm^{-1}	Groundwater recession flow parameter
LZSN	5.33	cm	Lower zone nominal storage
UZSN	7.01	cm	Upper zone nominal storage
Water Quality			
ACQOP(A)	6.68	× 10^7 FC ha^{-1} d^{-1}	FC accumulation rate (agriculture)
ACQOP(F)	2.14	× 10^7 FC ha^{-1} d^{-1}	FC accumulation rate (forest)
FSTDEC	4.23	d^{-1}	First -order decay rate of FC in stream
IOQC	0.68	× 10^6 cfu/100 mL	Interflow FC concentration
PSRC	1.07	× 10^8 FC d^{-1}	Mass flux from direct source
SQOLIM	1.83	× 10^{11} FC ha^{-1}	Maximum surface storage of FC
WSQOP	0.54	cm h^{-1}	Rate of surface runoff that removes 90% of FC in 1 hour

Table 7 HSPF: Maximum Likelihood Parameters - Catchment K

Parameters	*Value*	*Units*	*Description*
Hydrology			
AGWRC	0.95	d^{-1}	Basic groundwater recession rate
DEEPFR	0.00	–	Fraction of groundwater lost to the system
INFEXP	2.00	–	Exponent in the infiltration equation
INFILD	2.00	–	Ratio between maximum and mean infiltration
INFILT	0.20	cm h^{-1}	Infiltration capacity index
INTFW	31.50	–	Interflow inflow parameter
IRC	0.45	d^{-1}	Interflow recession parameter
KS	0.50	–	Weighting factor for hydraulic routing
KVARY	0.25	cm^{-1}	Groundwater recession flow parameter
LZSN	6.60	cm	Lower zone nominal storage
UZSN	6.88	cm	Upper zone nominal storage
Water Quality			
ACQOP(A)	1.95	× 10^8 FC ha^{-1} d^{-1}	FC accumulation rate (agriculture)
ACQOP(F)	6.08	× 10^8 FC ha^{-1}/d^{-1}	FC accumulation rate (forest)
FSTDEC	5.25	d^{-1}	First -order decay rate of FC in stream
IOQC	0.98	× 10^6 cfu/100mL	Interflow FC concentration
PSRC	1.45	× 10^9 FC d^{-1}	Mass flux from direct source
SQOLIM	0.11	× 10^{11} FC ha^{-1}	Maximum surface storage of FC
WSQOP	1.08	cm h^{-1}	Rate of surface runoff that removes 90% of FC in 1 hour

Table 8 HSPF: Maximum Likelihood Parameters - Catchment O

Parameters	*Value*	*Units*	*Description*
Hydrology			
AGWRC	0.96	d^{-1}	Basic groundwater recession rate
DEEPFR	0.35	–	Fraction of groundwater lost to the system
INFEXP	2.00	–	Exponent in the infiltration equation
INFILD	2.00	–	Ratio between maximum and mean infiltration
INFILT	0.25	cm h^{-1}	Infiltration capacity index
INTFW	15.00	–	Interflow inflow parameter
IRC	0.45	d^{-1}	Interflow recession parameter
KS	0.50	–	Weighting factor for hydraulic routing
KVARY	0.00	cm^{-1}	Groundwater recession flow parameter
LZSN	6.35	cm	Lower zone nominal storage
UZSN	2.87	cm	Upper zone nominal storage
Water Quality			
ACQOP(A)	2.95	× 10^{8} FC ha^{-1} d^{-1}	FC accumulation rate (agriculture)
ACQOP(F)	3.50	× 10^{7} FC ha^{-1} d^{-1}	FC accumulation rate (forest)
FSTDEC	0.33	d^{-1}	First -order decay rate of FC in stream
IOQC	2.97	× 10^{4} cfu/100 mL	Interflow FC concentration
PSRC	1.61	× 10^{7} FC d^{-1}	Mass flux from direct source
SQOLIM	0.20	× 10^{11} FC ha^{-1}	Maximum surface storage of FC
WSQOP	7.87	cm h^{-1}	Rate of surface runoff that removes 90% of FC in 1 hour

SWAT

The maximum likelihood parameter sets obtained for hydrology and water quality for each catchment are presented in Tables 9 -12 as follows:

Table 9 SWAT: Maximum Likelihood Parameters - Catchment I

Parameters	*Value*	*Units*	*Description*
Hydrology			
ALPHA_BF	0.980	d^{-1}	Base flow recession constant
CH_K2	168.0	mm h^{-1}	Effective hydraulic conductivity
CH_N	0.032	–	Manning's n in main channel
CN2 (Ag)	35.0	–	Curve number for moisture condition II
CN2 (Fr)	51.0	–	Curve number for moisture condition II
GW_DELAY	2.0	d	Ground water delay time
GW_REVAP	0.039	d^{-1}	Ground water "revap" coefficient
GWQMN	0.00	mm	Threshold depth in shallow aquifer for return flow
RCHRG_DP	0.00		Deep aquifer percolation factor
REVAPMN	2.336	mm	Depth in shallow aquifer for percolation to deep aquifer
Water Quality			
BACTDQ	0.075	$m^3\ Mg^{-1}$	Bacteria soil partitioning coefficient
BACTMX	20.0	10 $m^3\ Mg^{-1}$	Bacteria percolation coefficient
BCNST	3.80	$\times 10^7$ cfu/100mL	Point-source concentration
CFRT_Kg(A)	50.0	kg $ha^{-1}\ d^{-1}$	Application rate at 10^5 cfu/g (agriculture)
CFRT_Kg(F)	80.0	kg $ha^{-1}\ d^{-1}$	Application rate at 10^5 cfu/g (forest)
WDPQ	0.503	d^{-1}	bacteria die-off coefficient in soils
WDPRCH	2.650	d^{-1}	Bacteria die-off coefficient in streams

Table 10 SWAT: Maximum Likelihood Parameters - Catchment J

Parameters	*Value*	*Units*	*Description*
Hydrology			
ALPHA_BF	0.900	d^{-1}	Base flow recession constant
CH_K2	128.0	mm h^{-1}	Effective hydraulic conductivity
CH_N	0.020	–	Manning's n in main channel
CN2 (Ag)	43.0	–	Curve number for moisture condition II
CN2 (Fr)	58.0	–	Curve number for moisture condition II
GW_DELAY	1.0	d	Ground water delay time
GW_REVAP	0.120	d^{-1}	Ground water "revap" coefficient
GWQMN	120.00	mm	Threshold depth in shallow aquifer for return flow
RCHRG_DP	0.00	–	Deep aquifer percolation factor
REVAPMN	1.450	mm	Depth in shallow aquifer for percolation to deep aquifer
Water Quality			
BACTDQ	0.430	m^3 Mg^{-1}	Bacteria soil partitioning coefficient
BACTMX	20.0	10 m^3 Mg^{-1}	Bacteria percolation coefficient
BCNST	3.25	$\times 10^8$ cfu/100mL	Point-source concentration
CFRT_Kg(A)	6.0	kg ha^{-1} d^{-1}	Application rate at 10^5 cfu/g (agriculture)
CFRT_Kg(F)	15.0	kg ha^{-1} d^{-1}	Application rate at 10^5 cfu/g (forest)
WDPQ	0.070	d^{-1}	bacteria die-off coefficient in soils
WDPRCH	4.000	d^{-1}	Bacteria die-off coefficient in streams

Table 11 SWAT: Maximum Likelihood Parameters - Catchment K

Parameters	*Value*	*Units*	*Description*
Hydrology			
ALPHA_BF	0.73	d^{-1}	Base flow recession constant
CH_K2	176.00	mm h^{-1}	Effective hydraulic conductivity
CH_N	0.71	–	Manning's n in main channel
CN2 (Ag)	38.00	–	Curve number for moisture condition II
CN2 (Fr)	50.00	–	Curve number for moisture condition II
GW_DELAY	1.00	d	Ground water delay time
GW_REVAP	0.21	d^{-1}	Ground water "revap" coefficient
GWQMN	140.00	mm	Threshold depth in shallow aquifer for return flow
RCHRG_DP	0.00	–	Deep aquifer percolation factor
REVAPMN	7.94	mm	Depth in shallow aquifer for percolation to deep aquifer
Water Quality			
BACTDQ	0.31	m^3 Mg^{-1}	Bacteria soil partitioning coefficient
BCNST	1.25	$\times 10^8$ cfu/100mL	Point-source concentration
CFRT_Kg(A)	12.00	kg ha^{-1} d^{-1}	Application rate at 10^5 cfu/g (agriculture)
CFRT_Kg(F)	28.00	kg ha^{-1} d^{-1}	Application rate at 10^5 cfu/g (forest)
WDPQ	0.10	d^{-1}	bacteria die-off coefficient in soils
WDPRCH	1.94	d^{-1}	Bacteria die-off coefficient in streams

Table 12 SWAT: Maximum Likelihood Parameters - Catchment O

Parameters	*Value*	*Units*	*Description*
Hydrology			
ALPHA_BF	0.900	d^{-1}	Base flow recession constant
CH_K2	146.0	mm h^{-1}	Effective hydraulic conductivity
CH_N	0.03	–	Manning's n in main channel
CN2 (Ag)	39.0	–	Curve number for moisture condition II
CN2 (Fr)	69.0	–	Curve number for moisture condition II
GW_DELAY	8.4	d	Ground water delay time
GW_REVAP	0.50	d^{-1}	Ground water "revap" coefficient
GWQMN	0.00	mm	Threshold depth in shallow aquifer for return flow
RCHRG_DP	0.31	–	Deep aquifer percolation factor
REVAPMN	0.63	mm	Depth in shallow aquifer for percolation to deep aquifer
Water Quality			
BACTDQ	0.080	$m^3\ Mg^{-1}$	Bacteria soil partitioning coefficient
BACTMX	2.70	10 $m^3\ Mg^{-1}$	Bacteria percolation coefficient
BCNST	9.90	$\times 10^7$ cfu/100mL	Point-source concentration
CFRT_Kg (A)	2.00	kg ha^{-1} d^{-1}	Application rate at 10^5 cfu/g (agriculture)
CFRT_Kg (F)	6.00	kg ha^{-1} d^{-1}	Application rate at 10^5 cfu/g (forest)
WDPQ	0.08	d^{-1}	bacteria die-off coefficient in soils
WDPRCH	3.50	d^{-1}	Bacteria die-off coefficient in streams

6.1.1 Hydrology

The maximum-likelihood parameter sets pertaining to the dominant hydrological process for HSPF and SWAT (section 6.1) were used to generate flow predictions for each of the catchments (I, J, K and O) in the study area. Model predictions were compared to observed flow for the seven-year calibration period using the Nash-Sutcliffe Efficiency (NSE) coefficient. The NSE values for the HSPF models indicated very good agreement (above 0.8) between the model predictions and observed monthly flows and good (0.63) to very good agreement (0.88) for daily flows in all four catchments. Comparison of the observed flows with flows simulated by SWAT also indicated very good correlation with observed monthly flows (all above 0.8) but only satisfactory (0.56) to good (0.73) values for the daily flows.

Table 13 HSPF: Single Model Performance (Hydrology)

Catchment	I	J	K	O
NSE (daily	.71	.70	.88	.63
NSE (monthly)	.82	.88	.90	.87

Table 14 SWAT: Single Model Performance (Hydrology)

Catchment	I	J	K	O
NSE (daily)	.56	.67	.73	.61
NSE (monthly)	.86	.84	.88	.87

A comparative analysis of the model results indicates that both models provided very good estimates of monthly flow and reasonable estimates of the daily flow in all four study catchments in the watershed. Quantitative comparison of the daily flow indicated fair to good agreement between the simulations and measured values as evidenced by NSE values ranging between 0.56 and 0.88. As has been observed and noted in previous studies conducted using HSPF and SWAT (Chin et al., 2009), model predictions of daily flow generated by HSPF were in better accord with observed daily values (higher NSE values) than the predictions generated by SWAT.

This pattern can be attributed to the smaller time steps (1-hour increments) used by HSPF which allows the model to resolve the catchment's response to storms with sub-daily durations better than the much longer time step (1-day increments) used by SWAT. The absolute volume error of each model was 12.7% (I), 6.2% (J), 5.4% (K) and 4.2% (O) for HSPF and 19% (I), 1.6% (J), 2.5% (K) and 9.5% (O) for SWAT for the seven-year calibration period (1996 – 2002). Collectively, these metrics indicate fair agreement between the prediction and measurements at the daily and good agreement at monthly time scales (Moraisi et al. 2007, Chin et al. 2009).

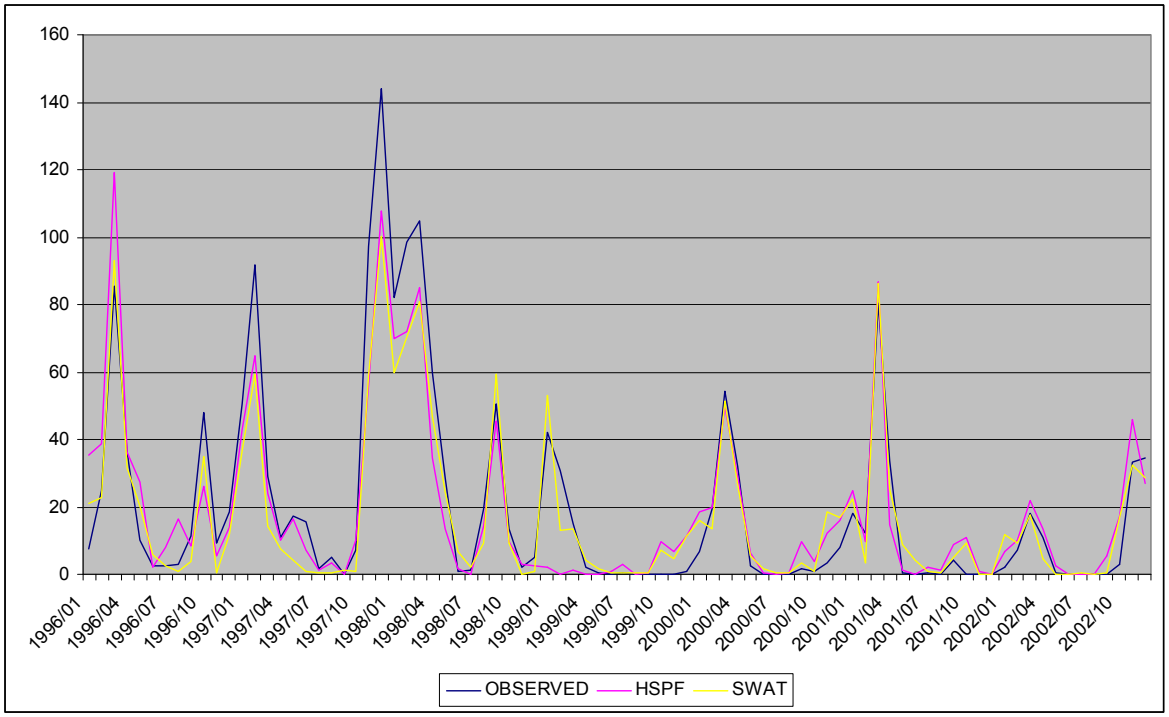

Figure 9 Hydrology: Monthly Flow Catchment I

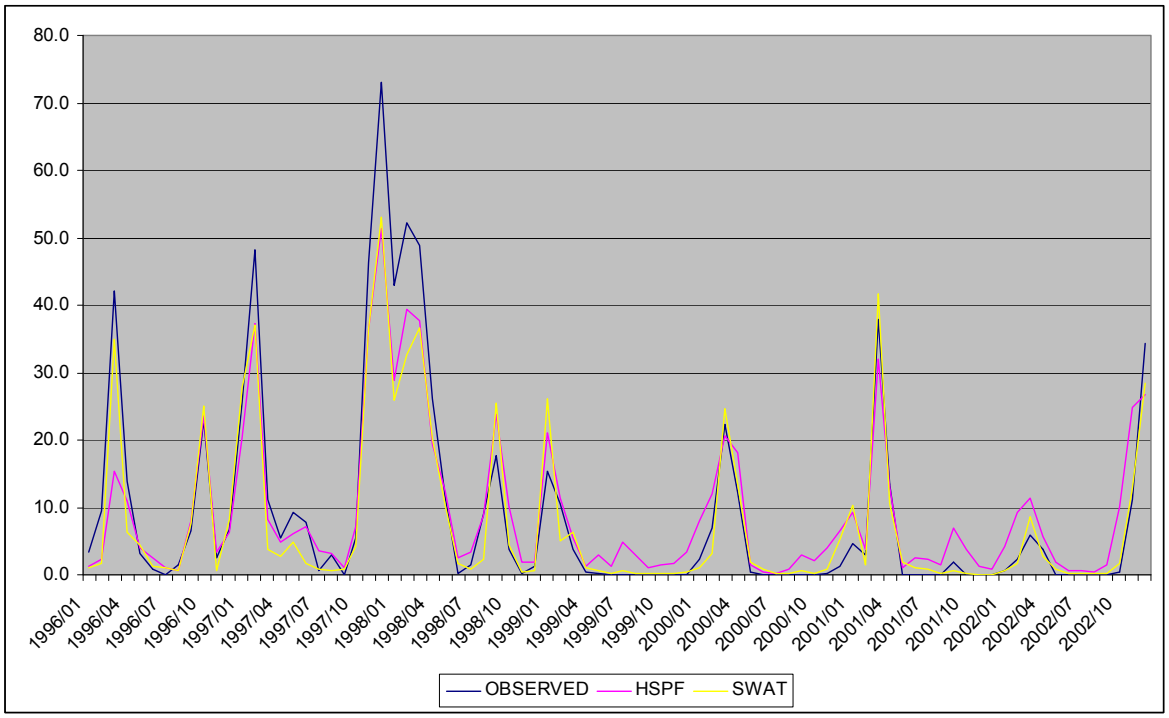

Figure 10 Hydrology: Monthly Flow Catchment J

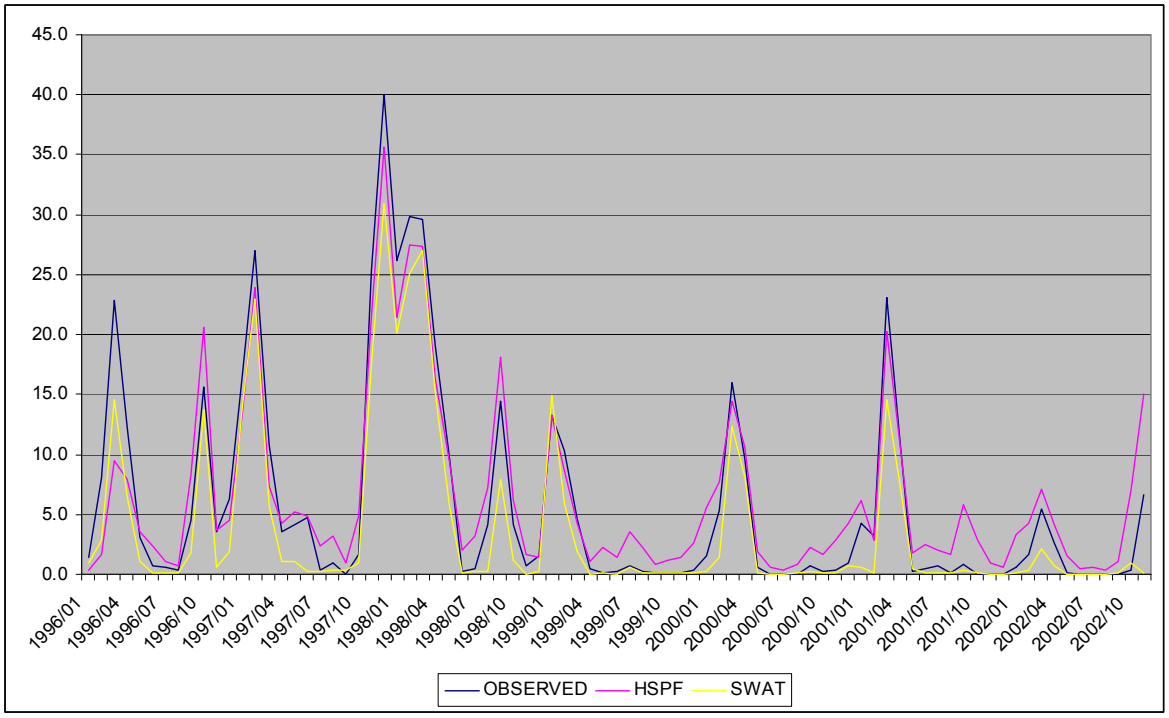

Figure 11: Hydrology: Monthly Flow Catchment K

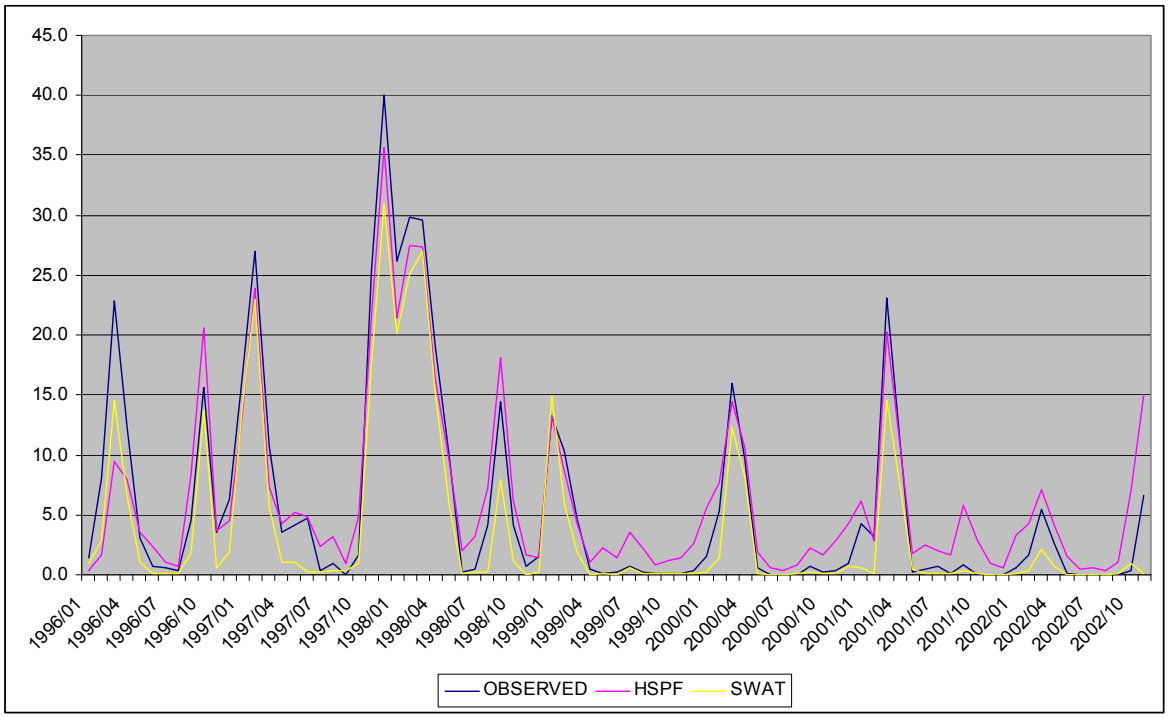

Figure 12: Hydrology: Monthly Flow Catchment O

6.1.2 Water Quality

As with the hydrological parameters, the maximum-likelihood parameters identified for the bacteria fate and transport processes (section 6.2) were used to predict fecal coliform concentrations in the four sub-watersheds. The NSE was used to evaluate how well the models predicted fecal coliform concentrations in the study area. The concentrations predicted by SWAT were in good agreement with the measured values (NSE all above 0.7); however, the estimates obtained by HSPF were comparatively very low (ranging from 0.24 to 0.45) indicating that the predictions generated by HSPF model were somewhat inconsistent with the fecal coliform concentrations of the observed values in the stream reaches.

Table 15 HSPF: Model Performance Water Quality (Bacteria)

Catchment	**I**	**J**	**K**	**O**
NSE	.44	.24	.33	.45

Table 16 SWAT: Model Performance Water Quality (Bacteria)

Catchment	**I**	**J**	**K**	**O**
NSE	.78	.77	.70	.76

A comparison of the results of the fecal coliform calibrations above show much better correlation with the predictions obtained from the SWAT model than with those

obtained from HSPF. Relatively low to fair agreement (NSE values ranging from 0.24 to 0.45) with HSPF predictions and good agreement (NSE values from 0.70 – 0.78) with SWAT predictions were obtained when the fecal coliform concentrations observed in the watershed were quantitatively compared to fecal coliform concentrations predicted by HSPF and SWAT respectively.

In general, quantitative comparisons between observed contaminant concentrations and model predictions are prone to error. First, observed contaminant concentration values are actually point estimates in time and space whereas modeled concentrations are spatially and temporally averaged (Shirmohammadi et al., 2006; Richards, 2001). Hence, the use of point estimates in a quantitative comparison has the potential to introduce significant estimator bias into the analysis (Chin et al., 2009; Shirmohammadi et al., 2006; Richards, 2001). These errors are generally caused by comparing an observed value (or instantaneous concentration measurement at a sampling point) to a model prediction (or averaged contaminant concentrations over a selected—usually daily—time-step). As a rule, daily-averaged values are incapable of capturing the variability in concentrations over an entire day and/or within a given stream reach (Chin et al. 2009).

Other explanations for the difference in accuracy (based on NSE values) obtained from the two models may lie in the methods used to separate overland flow and simulate the release and transport of bacteria. HSPF and SWAT process equations use distinctly different methods to separate overland flows into surface and sub-surface runoff components. For the study period, the average surface runoff volume for the four-catchments was about 1 % of the total flows in Catchment I and 2 % in all the other

catchments for HSPF and around 10 % for Catchment I and 17.9 % , 23 % and 14.6 %, and for Catchments J , K and O in SWAT.

The process equations used to simulate the release and transport bacteria also differ significantly in the two models. For example, SWAT partitions bacteria into phases and restricts transport to surface flows only; HSPF conversely, simulates transport in both surface and groundwater. Since the transport of the bacteria is dependant on flow, the proportion of flow allocated to surface and subsurface can drastically alter the final concentration estimates in the receiving stream. Relatively high total subsurface flow estimates of 99 % for Catchment I, 98 % for Catchment J, 98 % for Catchment K and 98 % for Catchment O were obtained by HSPF and 90 %, 82 %, 77 % and 85 % by SWAT for Catchments I, J, K and O respectively. Generally, high subsurface runoff volumes as observed in the simulations were not surprising because the hydrogeology of the study area is characterized by high infiltration rates and correspondingly low surface/high subsurface runoff (USDA-ARS 2008).

The differences in flow allocations noted above can directly influence the transport of bacteria and ultimate concentration in a groundwater-dominated system such the LREW. Given that HSPF allocated very small volumes to surface runoff, the relatively low to fair agreement between model predictions and observed values suggest that sub-surface flows may not be a dominant mechanism for bacteria transport in this study area. Overall, the comparatively superior NSE results obtained by the SWAT model may indicate that the fate and transport process equations for fecal coliform incorporated in SWAT are more representative of the watershed conditions in the LREW than the equations encoded in HSPF.

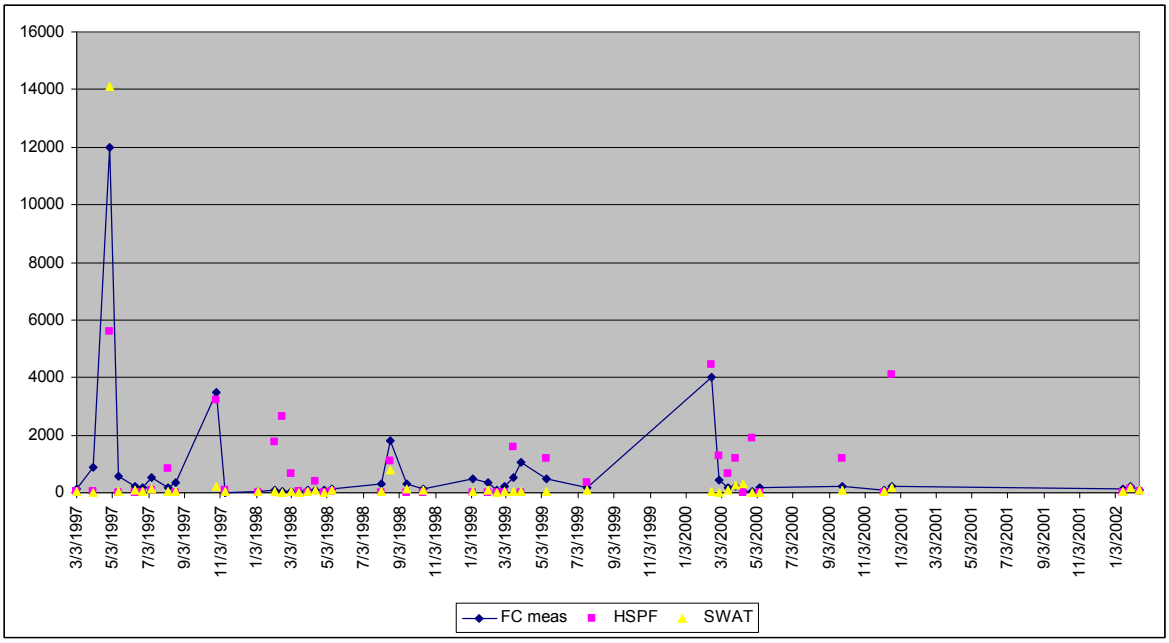

Figure 13: Water Quality: Fecal Coliform - Catchment I

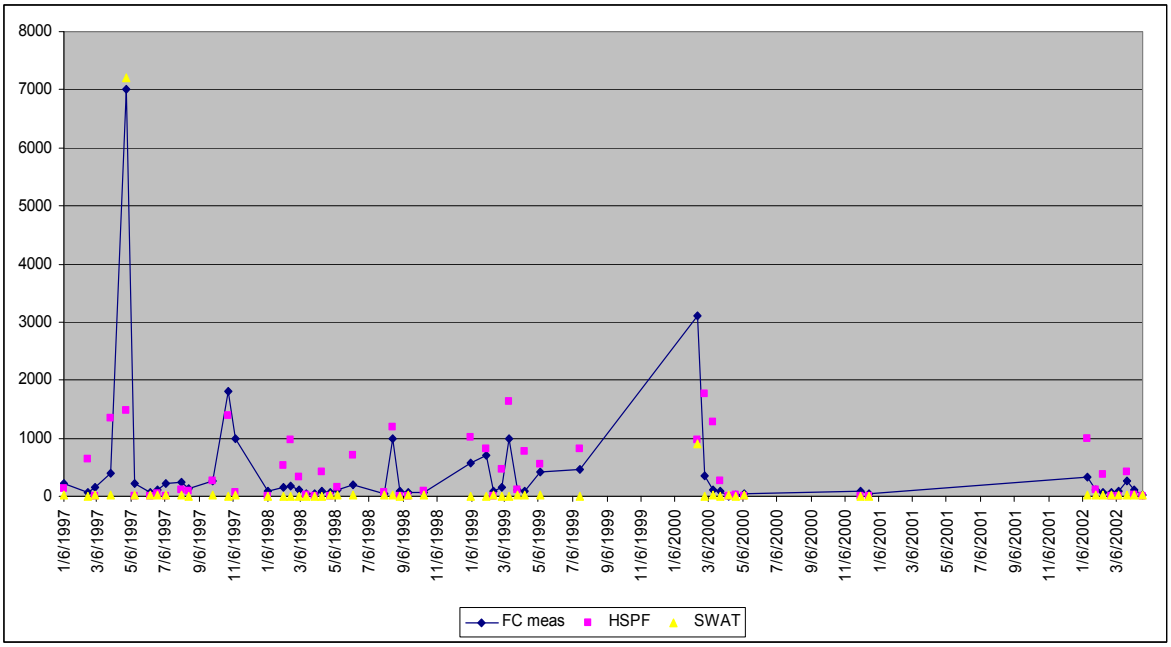

Figure 14: Water Quality: Fecal Coliform - Catchment J

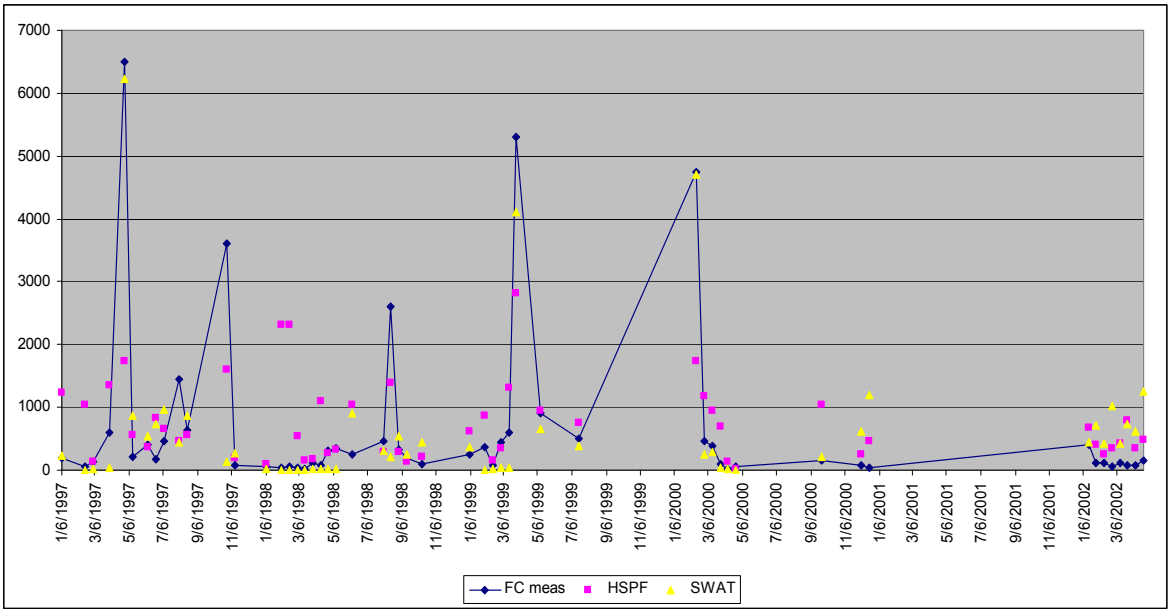

Figure 15: Water Quality: Fecal Coliform - Catchment K

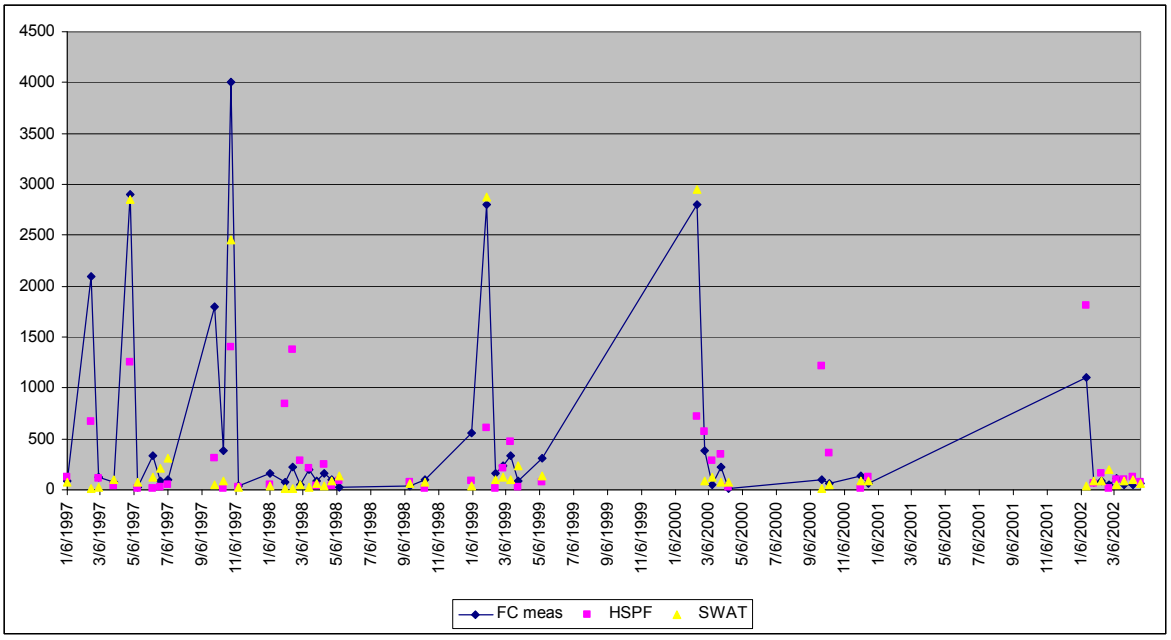

Figure 16: Water Quality: Fecal Coliform - Catchment O

6.1.2.1 Terrestrial Loading

The terrestrial loadings of fecal coliform obtained using the maximum - likelihood process parameters related to bacterial fate and transport derived from the HSPF and SWAT models were as follows:

Table 17: Terrestrial Loading (HSPF)

Catchment	I	J	K	O
Agriculture (cfu ha^{-1} d^{-1})	0.18×10^8	0.67×10^8	1.95×10^8	2.95×10^8
Forest (cfu ha^{-1} d^{-1})	2.65×10^8	0.21×10^8	6.08×10^8	0.35×10^8

Table 18: Terrestrial Loading (SWAT)

Catchment	I	J	K	O
Agriculture (cfu ha^{-1} d^{-1})	50.0×10^8	6.00×10^8	12.0×10^8	2.00×10^8
Forest (cfu ha^{-1} d^{-1})	80.0×10^8	15.0×10^8	28.0×10^8	6.00×10^8

Table 19: Direct Non-Point Source In-Stream Loading

Catchment	I	J	K	O
HSPF	2.81×10^8	1.07×10^8	14.5×10^8	0.16×10^8
SWAT	3.80×10^{10}	3.26×10^{10}	1.25×10^{10}	0.99×10^{10}

Terrestrial loadings estimated by HSPF were 0.2×10^8 to 2.3×10^8 cfu ha^{-1} d^{-1} (Catchment I), 0.21×10^8 to 0.67×10^8 cfu ha^{-1} d^{-1} (Catchment J), 1.95×10^8 to $6.08 \times$

10^8 cfu ha^{-1} d^{-1} (Catchment K) for agricultural and forest land uses, and 0.35×10^8 to 2.95×10^8 cfu ha^{-1} d^{-1} for forest and agricultural land uses in Catchment O. The terrestrial loading predicted by SWAT were 50×10^8 to 80×10^8 cfu ha^{-1} d^{-1} (Catchment I), 6.0×10^8 to 15.0×10^8 cfu ha^{-1} d^{-1} (Catchment J), 12.0×10^8 to 28.0×10^8 cfu ha^{-1} d^{-1} (Catchment K), and 2.0×10^8 to 6.0×10^8 cfu ha^{-1} d^{-1} (Catchment O) for agricultural and forest land uses in the four-catchment study area. These maximum-likelihood terrestrial loading estimates provide a reasonable level of confidence in narrowing the range of the existing bacteria loading to a magnitude of between 10^7 to 10^8 cfu ha^{-1} d^{-1} for Catchments I and J, 10^8 to 10^9 cfu ha^{-1} d^{-1} for Catchment K and 10^7 to 10^8 cfu ha^{-1} d^{-1} for Catchment O . Overall, the loading estimated for the four-catchment study area is between 10^7 to 10^9 cfu ha^{-1} d^{-1}.

The maximum-likelihood direct non-point source loadings estimated for the four-catchment study area were between 0.16×10^8 - 14.5×10^8 cfu d^{-1} for HSPF and between $0.99 \times 10^{10} - 3.8 \times 10^{10}$ cfu d^{-1} for SWAT (see table 19). These results indicate an overall direct loading of bacteria from in-stream sources in the study area in the range of 10^7 to 10^{10} cfu d^{-1}. The ranges for the individual sub-basins were between 0.2×10^9 and 38×10^9 cfu d^{-1}, 0.1×10^9 and 33×10^9 cfu d^{-1}, 1.5×10^9 and 13×10^9 cfu d^{-1}, and 0.02×10^9 and 10×10^9 cfu d^{-1} for Catchments I, J, K and O respectively.

Based on the catchment areas analyzed, the terrestrial loading for each catchment was estimated at 1.43×10^{12} cfu d^{-1} for Catchment I [area 50.9 km^2 (5091 ha)], 2.39×10^{11} cfu d^{-1} for Catchment J [area 22.3 km^2 (2230 ha)], 2.26×10^{12} cfu d^{-1} for Catchment K [area 15.6 km^2 (1558 ha)] and 2.65×10^{10} cfu d^{-1} for Catchment O [16.7 km^2 (1646 ha)]. In light of this, the average loading in the study area is estimated to fall

between 10^8 to 10^{12} cfu d^{-1} for Catchment I, 10^8 to 10^{11} cfu d^{-1} for Catchment J, 10^9 to 10^{12} cfu d^{-1} for Catchment K, 10^8 to 10^{10} cfu d^{-1} for Catchment O, with an overall average of between 10^8 and 10^{12} cfu d^{-1} for the study area.

Analysis of the terrestrial loading

The terrestrial loading of fecal coliform in a watershed is inextricably linked to the rainfall/runoff patterns and the land use/land cover in the area. An examination of the land uses in the four study catchments indicated approximately 51% agriculture and 49% forest in Catchment I, 50% agriculture and 50% forest in Catchment J, 46% agriculture and 54% forest in Catchment K and 84% agriculture, 12% forest and 4% water in Catchment O. For the purpose of this study, land use classifications were lumped into three basic categories: (a) agriculture (includes general agriculture and pasture), (b) forest (includes upland and riparian areas), and (c) water. There were no urban areas in any of the catchments used in this study.

Based on the results obtained, the largest contaminant loads were associated with Catchments I and K, and the highest percentage of loading to the receiving streams in the study area from direct non-point source loads. While this could be attributed to a number of reasons, the most likely explanation is the abundance of wildlife –population and species—inhabiting the watershed. Deer and other game animals are very prevalent in the riparian areas where fecal coliform deposited with their feces can readily enter streams via storm runoff (GA EPA 2006). Other wildlife species, primarily waterfowl with smaller populations of otters and beavers, are also known to inhabit these

catchments where they spend a considerable amount of time in the water frequently depositing their feces directly on its surface (GA EPA 2006).

Though the impact of water-dwelling animals on wildlife fecal coliform concentrations is well documented in the literature (GA EPD 2000; 2006), several states—including Georgia—collect statistics for deer populations only which are typically used to account for all wildlife fecal coliform contributions in watershed analyses (GA EPD 2000, GA EPD 2006). Deer density estimates for the study area were placed at between 30 and 45 animals per square mile (GA EPD, 2000) and Catchment K was identified as a recreational hunting preserve (personal comment D. Bosch, USDA-ARS April, 2008). Fecal coliform contributions from deer estimated at 5.0×10^8 cfu per animal per day were used to estimate wildlife contributions to the watershed in this analysis (ASAE, 1998; EPA BASINS fecal tool, 2001).

With the given wildlife populations, it is reasonable to expect high direct non-point source loadings of fecal coliform in these two catchments, most likely resulting from high fecal coliform concentrations in the riparian zones. Land use in Catchment K is predominantly forest and though only roughly half of Catchment I is classified as forest, this forested area is close to 15% larger than Catchment J and a little less than 40% larger than either Catchments K or O. The overall fecal coliform loading in the two catchments is estimated to be between 10^8 and 10^{12}. If the deer density in the area is taken in to consideration, there may have been between 300 and 450 deer living in the forested proportion of Catchment I and between 100 and 150 in Catchment K during the study period. Fecal coliform contributions from these deer—based on estimates given above— would be between 1.5×10^{11} and 3.0×10^{11} cfu day^{-1} and between 5.0×10^{10}

and 8.0×10^{10} cfu day^{-1} in Catchment I and K respectively. A comparison of these concentrations with the fecal coliform loadings estimated in this study indicates that these concentrations are well within the estimated range of between 10^8 and 10^{12} cfu d^{-1} for fecal coliform loads and therefore very reasonable for the respective watersheds.

Concentrations in Catchment J were a bit lower falling between 10^8 and 10^{11}. The area of Catchment J is 22.3 km^2 and the land use is evenly divided between forested lands and agriculture, as such, it would be logical to assume that wildlife contributions in this catchment would be much lower. Using the same deer density population estimates as above, deer in Catchment J should number between 130 and 195 and contribute an average of 6.5×10^{10} to 1.0×10^{11} cfu day^{-1}. This strongly supports the suggestion that the source of the majority of fecal coliform contributions to this watershed is also of wildlife origin.

Catchment O is the only sub-catchment in the study where the land use is dominated (84%) by agriculture. Catchment O lies in Tift County, GA and contains the University of Georgia's (UGA) Animal Research Farm, which encompasses 275 hectares and houses 200 dairy cows (Vellidis et al. 2008). Fecal coliform estimates for dairy cattle assume that the animals do not roam freely through the pastures and rarely have any contact with streams running through the area (GA EPD 2000). Dairy cows are regularly confined for a limited period every day (typically around four hours) for feeding and milking, and their manure usually collected, stored and distributed over crop and pasture lands to enrich and fertilize the soil (GA EPD, 2000).

Based on ASAE (1998) animal reference estimates of 1.01×10^{11} cfu/animal d^{-1}, for the dairy cows and deer estimates given above, fecal coliform contributions from the

dairy cows and wildlife are estimated to be around 7.44×10^9 cfu/acre/day for agriculture and 5.86×10^6 cfu/acre/day for forest. This represents a total fecal loading of approximately 2.53×10^{13} cfu/day. The numbers obtained are higher than those estimated for the watershed; however, the higher numbers are not entirely surprising and most likely explained by the die-off during overland transport to the stream reach that were not considered in the calculations.

The concentrations obtained using the maximum likelihood functions were consistent with the concentrations expected in the watershed. Modeled loadings and the estimates calculated based on animal species and density provides support for the loading estimates concentrations obtained. The lowest loadings were in Catchment O though it was the only catchment with a concentrated animal operation. This have have occurred because dairy cattle do not typically deposit their feces within the riparian area or on the riverbanks as common with wildlife, probable effects of storage/exposure (direct sunlight, heat, etc) on agriculture manure, and/or the bacteria fate during overland transport to the stream reach may have significantly impacted the survival rates of the bacteria.

6.2 Multi-Model approach

Two watershed-scale models, HSPF and SWAT, were used to simulate the hydrology and the fate and transport of bacteria in four sub-catchments in the LREW. The models were calibrated for the 7-year study period (1996 – 2002) using the three-step methodological approach described in Chapter 5. The outputs were then combined using three model combination methods: (a) the weighted average model (WAM), (b) Nash-

Sutcliff Efficiency Maximization method (NSE-max) and (c) an artificial neural network (ANN).

6.2.1 Weighted Average Method

For the Weighted Average Method (WAM), the weights for the models were constrained so that they summed to unity and estimated using the following equations (equations 31 and 32) restated below:

$$\hat{A}_{cls} = \left(P^T P\right)^{-1}\left(P^T Q + \tfrac{1}{2} b\lambda\right)$$

where the Langrangian multiplier λ is calculated as follows:

$$\lambda = 2\left(b^T\left(P^T P\right)^{-1} b\right)^{-1}\left(1 - b^T\left(P^T P\right)^{-1} P^T Q\right)$$

The results of this analysis are presented in Tables 20 and 21:

Table 20: Estimated Model Weights - Weighted Average Method

Catchment	Daily	Monthly	Water Quality
I	0.762	.236	0.339
J	.454	.256	0.204
K	.813	.534	0.191
O	.526	.497	0.153

Table 21: NSE Results - Method 1: Weighted Average Method

	I	J	K	O
NSE (daily)	.67	.70	.86	.62
NSE (monthly)	.85	.87	.88	.87
NSE (water quality	.68	.66	.63	.72

6.2.2 Nash-Sutcliffe Efficiency Maximization Method

Next, the model results were combined using the Nash-Sutcliffe Efficiency Maximization Method (NSE-max) described in Chapter 5. The combined model estimates were calculated using the equation below:

$$P_i = aHSPF_i + (1-a)SWAT_i \tag{41}$$

and the weighting factor, a, found by

$$a = \frac{\sum_{i=1}^{N}(M_i - SWAT_i)(HSPF_i - SWAT_i)}{\sum_{i=1}^{N}(SWAT_i - HSPF_i)^2} \tag{42}$$

The results of this analysis are shown below (see Table 22 and 23):

Table 22: Estimated Model Weights - NSE-Maximization Method

Catchment	Daily	Monthly	Water Quality
I	0.762	.236	0.339
J	.454	.256	0.204
K	.813	.534	0.191
O	.526	.497	0.153

Based on the weighted factors presented above, the prediction estimates for the sub-basins were found to be:

Table 23: NSE Results - Method 2: NSE-Maximization Method

	I	**J**	**K**	**O**
NSE (daily)	.67	.70	.86	.62
NSE (monthly)	.85	.87	.88	.87
NSE (water quality	.68	.66	.63	.72

6.2.3 Artificial Neural Network Method

Thirdly, the model results were combined using the Artificial Neural Network (ANN) method. A multi-layer forwardfeed network structure with one input layer, one hidden layer and one output layer was used in the analysis. The data were summed, a sigmoid transfer function was used to stabilize and add non-linearity to the structure, and

a squashing function added to the network which bounded the output in the range [0, 1]. The Broyden-Fletcher-Goldfarb-Shanno (BFGS) algorithm was used in the training phase of the network. For consistency with the other model combination methods used, all the data were used in the training of the neural network. The results of the model are shown in Table 24 and 25 below:

Table 24: Estimated Model Weights: Artificial Neural Network Method

	I		J		K		O	
	HSPF	SWAT	HSPF	SWAT	HSPF	SWAT	HSPF	SWAT
Daily	54.25	-181.3	-1.570	-2.080	-0.120	-14.97	-36.76	-0.014
	-1.70	0.020	-21.51	-152.1	-0.024	-29.33	3.760	-0.046
Monthly	-1.020	61.47	-9.800	-0.580	-4.880	-0.140	-41.03	-5.950
	-0.860	-94.04	1.920	-2.570	-22.58	-0.620	-48.49	-6.640
Water Quality	-246.4	-425.9	-8.590	9.120	-5.240	-2.810	-1784	-492.5
	-261.4	-271.3	-2.990	-4.170	-9.680	-11.24	295.0	-344.3

Table 25: NSE Results -Method 3: Artificial Neural Network Method

	I	J	K	O
NSE (daily)	.76	.78	.91	.77
NSE (monthly)	.92	.94	.97	.89
NSE (water quality	.91	.94	.73	.84

6.2.4 Comparative analysis

A comparison of the results of the multi-model approach and the original individual model results show an improvement in the estimates obtained with all three combination methods. Over the four catchments, overall NSE values obtained by the multi-model methods ranged from good to excellent (0.73 – 0.97). The WAM and NSE-max methods both utilized linear relationships, constraints (to unity) and averages of the two model results to estimate model weights, and as expected, generated identical weight factors for each model and the same overall results.

An examination of the results of the ANN approach showed marked improvement over individual model results and excellent agreement with the concentrations observed in the study catchments. Quantitative comparison with observed values yielded NSE values well above either the average values obtained from the original calibrations or from the two model-averaging approaches used in the study. One reason for this may stem from the methodology and structure of the ANN itself. Specifically, computer models are designed to execute of a series of algorithms and produce a numerical solution

and in general, models simply apply incorporated process equations to input data and generate estimates.

Conversely, neural networks—such as the ANN—do not begin with a pre-designed set of equations for data analysis; instead, the network processes the input data, looks for relationships in the data structure, and uses these relationships to decipher the hidden algorithms in the data patterns. The network then utilizes these algorithms to build a model. Based on this, the model formulated by an ANN is potentially more adept at mimicking actual processes in the watershed, and ultimately at predicting model estimates for the watershed processes. By combining the estimates of both watershed scale models, the ANN can utilize embedded patterns in both predictions to generate a model that contains all the processes incorporated in both model structures.

The model weights obtained by the WAM and NSE-max methods indicated that predictions obtained from HSPF were weighted more heavily than predictions obtained by SWAT for the hydrology while SWAT predictions were weighted more heavily for the water quality. However, in the case of the ANN, neither of the models was consistently weighted higher in all four of watersheds with SWAT predictions being weighted more heavily in some of the watersheds, HSPF in some and neither in others. Overall, the results obtained from the study indicate that HSPF better maps the hydrology of the watershed but only produces fair assessment of the water quality conditions while SWAT better describes the water quality. Based on this, a combination of the model forecasts as undertaken here utilizes the strengths of both models to produce estimates comprised of good hydrological and water quality predictions.

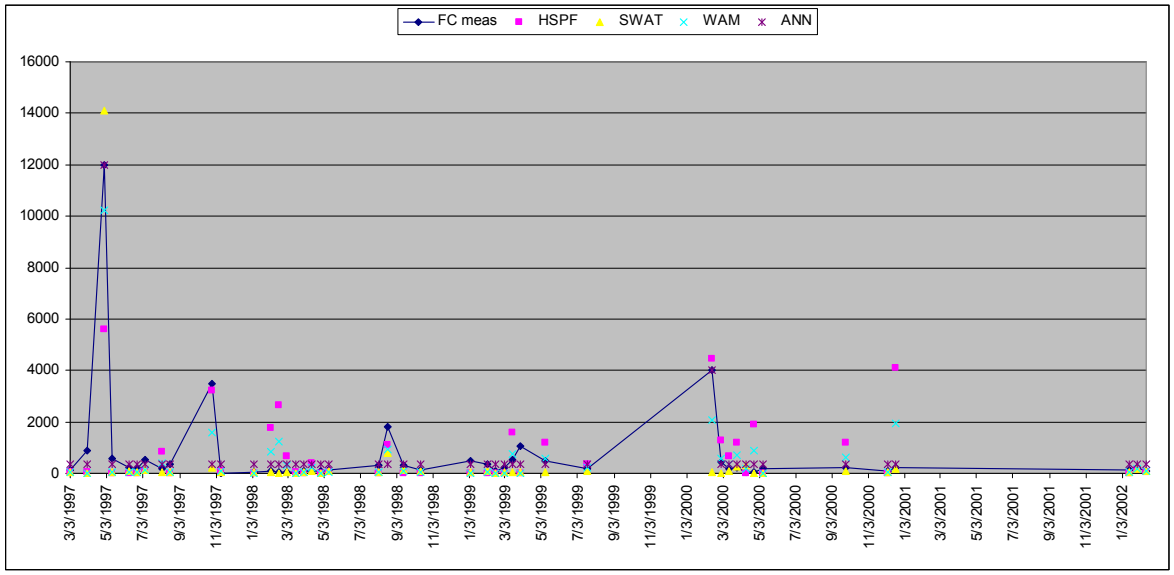

Figure 17 Comparison of model results: Water Quality – Catchment I

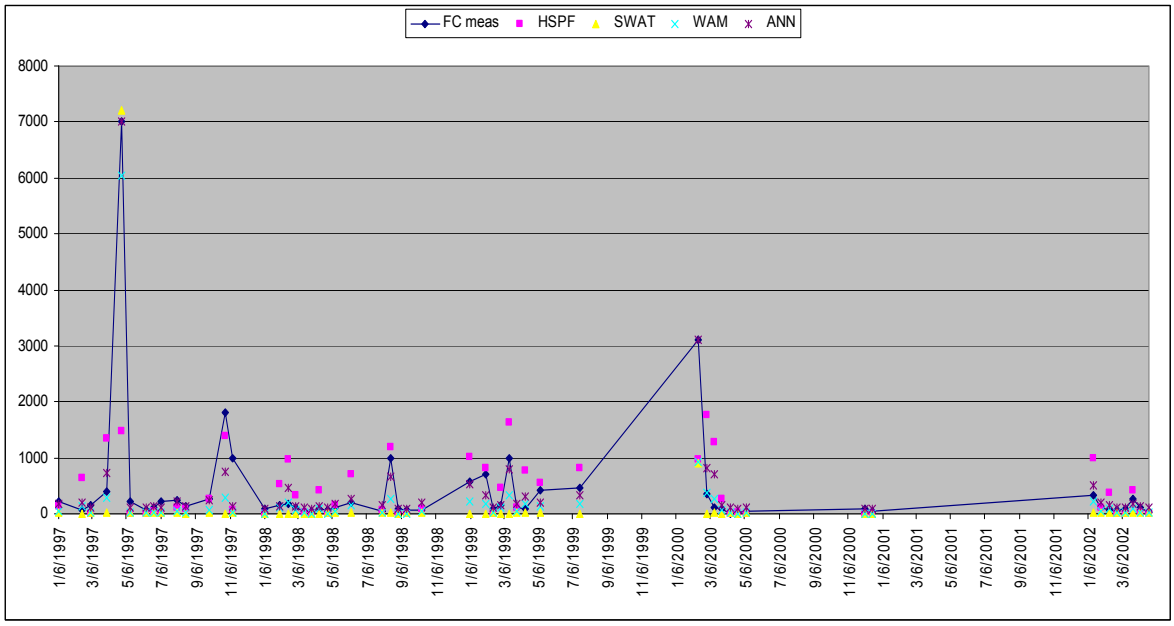

Figure 18 Comparison of model results: Water Quality – Catchment J

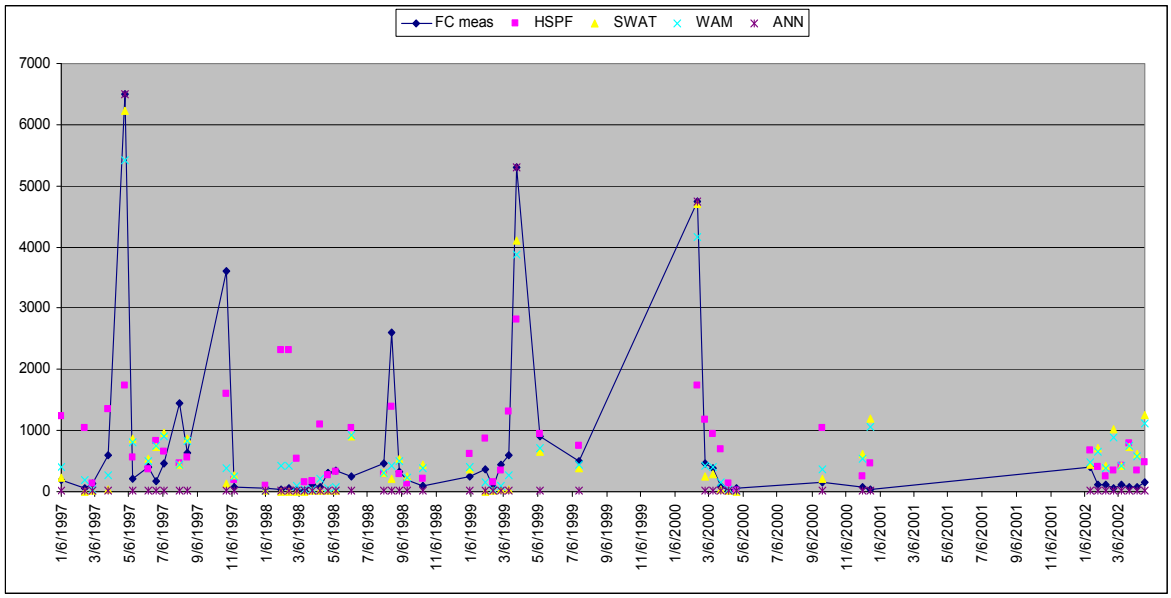

Figure 19 Comparison of model results: Water Quality – Catchment K

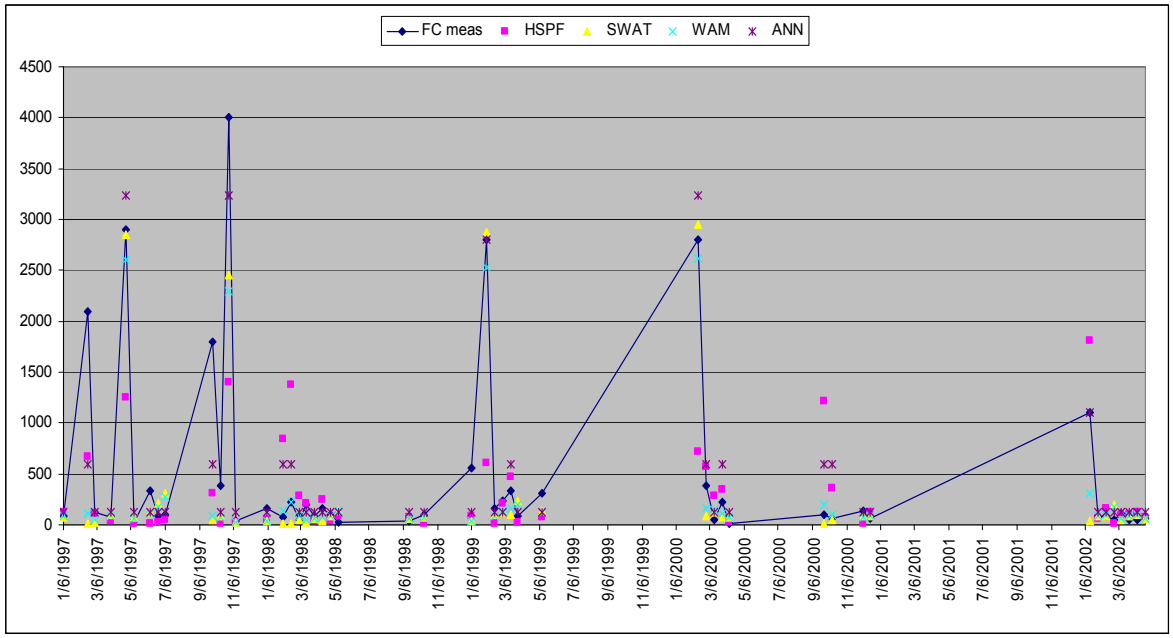

Figure 20 Comparison of model results: Water Quality – Catchment O

CHAPTER 7: DISCUSSION AND CONCLUSIONS

7.0 Summary and interpretation of major findings

This study developed and highlighted the effectiveness of combining different model estimates to improve prediction forecasts for fecal coliform contamination of streams. Both HSPF and SWAT, two watershed-scale terrestrial codes, were utilized in the analysis of four sub-catchments in the Little River Experimental Watershed (LREW) in South-Central Georgia. Observed flow measurements and fecal coliform concentrations were statistically compared with estimates from the individual models. With regard to the hydrology, the results showed that over the study period (1996 - 2002), HSPF provided a better description of the daily flows based on the Nash-Sutcliff Efficiency (NSE) coefficient values, which ranged from (0.63 to 0.88) and both models performed comparatively well in describing monthly flows (all above 0.8).

The differences in the hydrologic model performances in predicting daily flows are most likely due to the temporal resolution of the individual models. The hourly time-steps used by HSPF allows quicker model response to shorter individual storms, in contrast to the coarser daily time-step used by SWAT, which prohibits the model from accurately resolving responses to sub-daily storm events (Chin et al. 2009). Monthly flows simulated by the two models were comparable and perhaps attributable to the fact that the effect of averaging values becomes less obvious with increasing time scales.

As previously stated, the goal of this study was to use a multi-model approach to: (1) predict and quantify the dominant fate and transport processes of pathogenic indicator bacteria at the watershed scale; (2) determine the process equations that best represent the

watershed; and (3) quantify the reduction in predictive uncertainty attainable by combining predictions from two watershed-scale terrestrial fate and transport models. All three objectives were met in this study and summarized below.

With regards to objective 1, predicting and quantifying the dominant fate and transport processes of pathogenic indicator bacteria at the watershed stage, the results indicated that SWAT provided a much better description of the fecal coliform concentrations with NSE values ranging from 0.70 to 0.78 versus values of 0.24 to 0.45 obtained with HSPF. Relative performance of the models in predicting water quality results indicated that SWAT might be better suited than HSPF for predicting fecal coliform concentrations in the Little River watershed. This suggests that the process equations incorporated in SWAT may better represent the actual fate and transport processes in the LREW than those incorporated into HSPF. Separation of overland flow into surface and sub-surface components highlights the relationship between flow distribution and model accuracy. Specifically, SWAT allocated a much higher proportion of overland flow to surface runoff than HSPF and the results, as measured by the NSE, demonstrated higher correlation between the SWAT model predictions and actual measured concentration values than with the predictions generated by HSPF. The resultant finding based on model results raises the possibility that groundwater flow may not be a dominant bacteria transport mechanism in the study area.

The fecal coliform loadings determined by the models were between 10^7 and 10^{12} cfu d^{-1} for the watershed. Most of the loadings in Catchments I, J and K were due to in-stream (direct non-point) sources of bacteria in the watershed and terrestrial sources were comparatively lower and ultimately had less impact on overall watershed loading. This

finding deviated slightly from expectation since there are no discrete point sources—such as confined animal feeding operations (CFOs), landfills or wastewater treatment plants—in these watersheds. However, there is a high concentration of wildlife with direct access to the stream reaches inhabiting the riparian zones in the study areas which most likely led to the overall high in-stream fecal coliform loading.

Catchment O differed slightly from the other study catchments in that terrestrial loadings were higher than the loading from in-stream sources in this watershed. One reasonable conclusion is that while the primary sources of fecal coliform in Catchments I, J and K are most likely of wildlife origin, since Catchment O is predominantly agricultural and houses the UGA Research Dairy, there is a much greater likelihood that the majority of loading in this catchment may have stemmed from the land application of agricultural manure.

With the exception of Catchment O, the in-stream loading to the stream reaches in the study area carried much higher concentrations of bacteria than the runoff from the land applications to the receiving stream. Possible explanations include the observations that:

(a) sampling routines generally take place during periods of base flow and as a result may miss the first flush effects from surface runoff following storm events and significantly bias the cumulative distribution of the concentrations (see Baffaut, 2006) ; and/or

(b) bacteria deposited in the cooler, damper forest buffer zones may thrive better (lower die off) than those subjected to longer overland transport to stream reaches or exposed to the elements such as with the application of manure to agricultural land.

However, this assertion remains speculative while we await research on bacteria fate and transport processes that validates or refutes this claim.

The results discussed above were obtained by comparing estimates from the two most widely used codes in TMDL analysis: HSPF and SWAT. These codes have been previously compared for hydrology (van Liew et al., 2003) and bacteria fate and transport processes (Benham et al., 2006), but not to determine loading estimates or to link loading on a receiving water body with upland sources. Comparison of the model results in this study helped in identifying some of the dominant fate and transport processes and characterizing the fecal coliform loading sources in the study sub-catchments of the LREW.

The second objective was to determine the process equations that best represent the watershed. Based on the results, the single model approach indicates that the process equations embedded in HSPF are very representative of the hydrological conditions in the Little River Experimental Watershed. The NSE values of between 0.63 and 0.88 indicate good agreement with observed values in the study area. Conversely, SWAT produced better NSE values and overall agreement with observed water quality (fecal coliform) concentrations in the watershed. Though HSPF hydrological predictions were in better accord with watershed observations, the SWAT hydrology forecasts were still within acceptable fair to good NSE range (0.56 to 0.73), while the HSPF water quality predictions showed only weak correlation with observed values. Based on this, the process equation in SWAT may be a better overall alternative for watershed analysis in this basin.

The third objective of this study was to quantify the reduction in predictive uncertainty attainable by combining predictions from two watershed-scale terrestrial fate and transport models and was addressed in the second phase of the analysis. This phase of the analysis involved utilizing three different model combination approaches to predict flow and bacteria concentrations in the sub-catchments. The data were first analyzed using the Weighted Average Method (WAM) followed by Nash-Sutcliffe Efficiency Maximization Method (NSE-max method). It was demonstrated that a weighted average of the model predictions as applied by the two methods could be used to improve the accuracy (as determined by the NSE) of the individual models. However, the overall improvements were generally modest when compared with the relative performance of the models.

The third multi-model approach applied to the data was the artificial neural network method (ANN). The results obtained by the ANN showed substantial improvements in both the hydrological and water quality components of the models. The ANN uses the model predictions from both the flow and the bacteria concentrations to identify these hidden patterns in the data then utilizes these relationships to generate an algorithm that simulates the processes involved. In essence, the model generated by the ANN produces greater predictive validity in terms of its ability to mimic the fate and transport processes in the watershed more accurately than other models with built-in but general algorithms.

Presently, several studies exist that investigate the use of multi-model combination/ averaging as a reliable method to improve forecasting results (Granger, 2001; Clemens, 1989; Thompson, 1976; Newbold and Granger, 1975; Dickinson, 1973).

While this method has previously been applied to hydrological studies (Kim et al., 2006; Shamseldin et al., 1997), it has never before been extended to studies of water quality. This study attempts to fill this gap by applying a multi-model approach to reduce the significant model uncertainty (Chin, 2009) and improve model prediction estimates associated with water quality modeling. Consequently, this study constitutes a first attempt at applying these methods to water quality analysis and a potential launching pad for improving contaminant concentration estimates which constitute the foundation of TMDL analyses.

The results presented here underscore the benefits of using a multi-model approach to TMDL analyses. Amongst these benefits is a significant improvement over the usual *a priori* selection of a watershed-scale fate and transport model for use in TMDL linkage and terrestrial analysis, which may not provide the best description of both the hydrology and water quality in a study area. It also helps to identify the watershed codes that best describe the processes in the study watershed. Improving model forecast generally entails employing better alternatives to decrease the uncertainty in the parameters that degrade model performance (Kim et al., 2006). By combining model forecasts, the methodology presented here also indirectly combines process equations, which can significantly improve prediction capability by reducing model uncertainty—a fundamental weakness of current water quality modeling.

The study also identified and quantified the fate and transport processes in the watershed thereby advancing the knowledge on some of the complex relationships underpinning the link between terrestrial loading and resulting contaminant concentration in a watershed. In sum, the ideas presented here constitute a step in the right direction in

the effort to (i) identify relevant watershed processes; (ii) improve model selection methods; and (iii) build a model representative of the actual conditions under investigation, while presenting a solid foundation for the required evaluations necessary to determine strategies and develop viable TMDL implementation plans for the remediation of impaired waters.

7.2 Limitations

This study presented a new approach for improving TMDL analysis by examining methods to predict and quantify relevant processes in the environmental fate and transport of pathogens in a watershed. It highlighted the weaknesses inherent in using the normal method of *a priori* model selection and suggested methods for improving model forecasts by combining model predictions to reduce inherent structural uncertainty in watershed-scale fate and transport models. These strengths not withstanding, shortcomings derived from data and model limitations open the possibility that the resulting parameter estimates may either be over or understated.

First, though the study utilized the two most widely used watershed-scale codes, both HSPF and SWAT are deterministic. Water quality analysis involves estimating contaminant concentrations in a water-body which is both stochastic and heterogeneous in nature (Shirmohammadi et al., 2006). The concentration distribution of a contaminant (e.g. fecal coliform) in an impacted water-body is essentially a probability distribution function. Deterministic models, however, generate output estimates using fixed input points that may not fully capture the variability of the pollutant concentration within the

body of water. Though this weakness has been acknowledged in the literature (Benham et al., 2006), mention of its probable impacts should not be omitted here.

Secondly, limitations in the available data that were beyond the control of the study may have prohibited the proper characterization of bacteria sources in the watershed. Hypothetically, such data limitations can potentially introduce prediction errors into model loading estimates (Benham et al., 2006), although they are not likely to affect the environmental fate or transport of the pollutant in the watershed. Because of the paucity of data on wildlife populations, the impacts of direct in-stream loading of fecal coliform contributions from the considerable quantity of waterfowl and other water-dwelling wildlife were essentially ignored in spite of the fact that ducks and geese are generally considered the largest contributors of fecal coliform to the watershed (GA EPA, 2006). As has been the precedent in TMDL analyses (AL DEM, 2003; SC DHEC, 2004; KY DFWR, 2006; GA EPD, 2006), deer estimates were used as a proxy to account for fecal coliform contributions from wildlife inhabiting the watershed.

Thirdly, the study period encompassed a seven year-period that included both very wet and very dry water years. The overall results obtained suggest that HSPF better simulates the hydrology and SWAT the water quality in this watershed; however, since the data were not disaggregated to examine the impact of rainfall quantities on model performance, it is not possible to determine if the model performances for HSPF and SWAT would differ under different hydrologic conditions. In addition, because flow measurements are essentially used to map concentration distribution patterns during non-sampling periods, changes in flow could have a direct and distinct effect on both hydrological and water quality predictions.

Despite these limitations, this study has yielded several new insights and findings consistent with existing theory and research. Notably, the results presented here indicate that a multi-model approach has the potential to not only identify a watershed-scale fate and transport model that adequately describes the watershed under investigation, but to quantify the dominant fate and transport processes and utilize multiple model predictions to reduce predictive uncertainty in modeled contaminant loadings.

This study addressed pathogen indicator bacteria (fecal coliform), but the methods introduced here can be easily extended to examine any other target contaminant in TMDL analyses. By utilizing two well-established, scientifically rigorous and freely accessible codes, the methodology discussed here can significantly reduce watershed model development by eliminating the need to retrain personnel or purchase new software. This can prove very useful for decision-makers as they balance environmental health assessments and social impacts against the economic burden associated with implementing successful management strategies for watershed remediation.

7.3 Recommendations for future research

Given the limitations discussed above, the following suggestions are recommended to improve TMDL and watershed-scale water quality analyses:

(a) improving current watershed–scale fate and transport models by developing methods to reduce uncertainty introduced by the use of averaged point values to describe the probability distribution functions characteristic of contaminant distributions;

(b) investigating the environmental fate (survival rate) and transport processes of pathogenic indicator bacteria (such fecal coliform) deposited with wildlife manure in moist, continually shaded forested areas such as riparian zones;

(c) improving data collection on wildlife to include population estimates for other wildlife species, particularly those known to contribute significantly to fecal coliform concentrations in the watershed;

(d) investigating the impact of very wet and very dry water years on model performance and model weights.

In spite of numerous attempts to estimate fecal coliform loading for agricultural lands (Benham et al., 2006; Crowther et al., 2002; Soupir et al., 2006; Tian et al., 2002), our understanding of the mechanics underpinning microbial transport are still sketchy. In addition, bacteria die-off/ re-growth and survival rates in forested environments and from wildlife sources have not been formally investigated and consequently not well understood. As a result, more research is required to truly understand bacterial fate and transport processes, link terrestrial sources to resulting concentrations in receiving streams and assess the uncertainty associated with estimating bacteria loading in a watershed. Such improvements can go a long way towards producing dependable assessments that accurately characterize bacteria sources and generate reliable pollutant estimates necessary for developing effective TMDLs to remediate impaired waters.

In sum, this study's contribution to the field of water resources and water quality engineering is indebted to my on-going research collaboration with Dr. David Chin (see Chin, 2009; Chin, Sakura-Lemessy, Bosch and Gay, 2009a). The significance of Chin (2009) is that it represented the first study to apply a response-surface iterative approach

to watershed-scale model calibrations. The multi-model approach developed in this study builds on these efforts which attracted the attention of scientists in the forefront of water quality modeling research (see Oliver et al. 2009). In fact, the multi-model formulation technique has apparent potential for addressing a major limitation in extant models: the predictive uncertainty associated with water quality modeling. Perhaps the most fitting acknowledgement of this model's potential is the considerable interest our preliminary analysis, which appeared in Chin et al (2009a), [see also Chin (2009) and Chin et al., (2009b)] generated in a session devoted to *Bacteria, Metals and Pathogens* (Session D3) at this Summer's 5th International SWAT Conference held at the University of Colorado in Boulder. Amongst the issues highlighted by panelists (e.g. USDA scientists Drs. Claire Baffuat and Ali Sadeghi) regarding our approach were the high NSE values obtained when the study watersheds were analyzed using SWAT (see http://ssl-video.tamu.edu/august-6/d3.aspx).

Amongst the panelists, Dr. Baffaut's presentation was particularly noteworthy for pinpointing how much the single-model calibration and NSE Maximization methods we developed in our paper have to offer in terms of generating results that were not only a considerable improvement over comparative studies but highlight the significant need to revaluate the manner in which current bacteria modeling is undertaken. In fact, the calibration method used in the study is already recognized as one that will likely, under similar watershed conditions (land uses, landscape etc), produce more reliable estimates. Further, on the basis of a comparative analysis of four selected papers**,** the major difference was the significance of the parameter values presented by Chin et al (2009), which were a distinct point of departure from the values typically obtained using SWAT

models— and one of the significant points to emerge from the conference's deliberations. Specifically, the values of the calibrated parameters for the study basin (Catchment K) for absorption/extraction and decay were much lower than values obtained for those parameters in previous studies. The surprisingly low parameter values and corresponding good NSE values obtained suggest that under the existing watershed conditions almost all deposited bacteria enter the stream reach with insignificant population die-off.

This represented a shift in the understanding of the fate and transport processes associated with watershed characteristics and brought to light the fact that all the field tests used to develop the SWAT process equations focused on agricultural land uses. As such, virtually no research was done that examined the fate and transport of bacteria deposited in cooler, moister and continuously shaded forested areas such as riparian zones. As a result, the differences in bacteria decay and extraction coefficients, such as unexpected low extraction values, minimal die-off and overall higher NSE values, were unexplainable with the present level of knowledge and understanding.

Overall, the detailed nature of our analysis, calibration and multi-model formulation techniques clearly make the method and research undertaken in this dissertation a worthy and timely addition to the on-going efforts to correct for predictive uncertainty and advance knowledge on water quality modeling. I hope that the resulting insights on water quality modeling gained will make a valuable contribution to the field of water quality engineering, particularly with respect to issues surrounding whether the processes involved in the environmental fate and transport of wildlife fecal bacteria affect input parameter estimates for different land uses and landscape positions. Moreover, I am convinced that when such approaches to the analysis of bacteria fate and transport are

undertaken, our recommendations heeded, and strengths of this model fully realized and utilized—the improvement of water quality modeling and ultimately TMDL formulation and implementation would be advanced by the contributions of this dissertation.

Works Cited

Ajami, N., Q. Duean , X. Gao, and S. Sorooshian (2006). Multi-model combination techniques for hydrologic forecasting: Application to distributed model intercomparison project results. *Journal of Hydrometeorology 7(4)* pp. 755 – 768.

AL DEM (2003). Total Maximum Daily Load (TMDL) development for fecal coliform in the Dry Creek Watershed. Department of Environmental Management, Alabama.

American Society of Agricultural Engineers (ASAE) (1998). ASAE Standards, 45th edition: Standards, Engineering Practices, Data. St. Joseph, MI.

APHA (1995) Standard Methods for the Examination of Water and Wastewater 19/e. Washington, DC: American Public Health Association

Arabi, M., R. Govindaraju, and M. Hantush (2007). A probabilistic approach for analysis of uncertainty in the evaluation of watershed management practices. *Journal of Hydrology 333(2 - 4)*, pp. 459 - 471.

Armstrong, J. (1989). Combining forecasts: the end of the beginning of the end? *International Journal of Forecasting, 5*, pp. 585 - 588.

Arnold, J. and P. Allen (1996) Estimating hydrologic budgets for three Illinois watersheds. *Journal of Hydrology (176)*, pp. 55 - 77.

ASCE (American Society of Civil Engineers) (1993). Criteria for evaluation of watershed models. *Journal of Irrigation Drainage Engineering 119(3)*, pp. 429 - 442.

Bates, J. and C. Granger (1969). The combination of forecasts. *Operations Research Quarterly (20)*, pp. 451 - 468.

Benaman, J. C. Shoemaker and D. Haitt (2005). Calibration and Validation of Soil and Water Assessment Tool on an Agricultural Watershed in Upstate New York. *Journal of Hydrologic Engineering*, *DOI: 10.1061/(ASCE)1084-0699(2005)10:5(363).*

Benham, B., C. Bauffaut, R. Zeckoski, K. Mankin, Y. Pachepsky, A. Sadeghi, K. Brannan, M. Soupir and M. Habersack (2006). Modeling bacteria fate and transport in watersheds to support TMDLs. *Transactions of the ASABE 49(4)*, pp. 987 - 1002.

Beven, K., and A. Bindley (1992). The future of distributed models: Model calibration and uncertainty prediction. *Hydrological Processes 6(3)*, pp. 279 - 298.

Bicknell B., J. Imhoff , J. Kittle , T. Jobes and A. Donigan Jr. (2001). Hydrological Simulation Program-Fortran HSPF version 12 User's Manual. Aqua Terra Consultants: Mountain View, California.

Bicknell, B., J. Imhoff, J. Kittle, Jr., and A. Donigian Jr. (2001). Hydrological Simulation Program – HSPF: User's manual for release 12. Technical Report, National Exposure Research Laboratory, Office of Research and Development, US Environmental Protection Agency, Athens, Georgia, 2001.

Bosch, D., and J. Sheridan (2007). Stream discharge database, Little River Experimental Watershed, Georgia, United States. *Water Resources Research 43(9)* W09473, doi: 10.1029/2006WR005833.

Bosch, D., J. Sheridan, R. Lowrance, R. Hubbard, T. Strickland, G. Feyereisen and D. Sullivan (2007). Little River Experimental Watershed database. *Water Resources Research (43)*, doi:10.1029/2006WR005844.

Box, G., and D. Cox (1986). An analysis of transformations. *Journal of the Royal Statistical Society, Series B, 26*, pp. 211-246.

Cabelli, V., A. Dufour, L. McCabe and M. Levin (1982). Swimming-associated gastroenteritis and water quality. *American Journal of Epidemiology 115(4).* pp. 660 - 161.

Carpenter, A. (2006). Preventing non-point source pollution - Environmental Update 25 – September 2006. Hazardous Substances Research Centers: South and South west Outreach Programs, Georgia Tech Research Institute.

Chin, D. A. (2006). Water-Quality Engineering in Natural Systems. John Wiley and Sons, New York, N .Y. 2006.

Chin, D. A. (2008). Risk-based margin of safety for TMDLs in pathogen-impaired waters. Unpublished manuscript.

Chin, D. A. (2009). Predictive uncertainty in water quality modeling. *Journal of Environmental Engineering*, doi:10.1061/(ASCE)EE 1943-7870.0000101.

Chin, D., D. Sakura-Lemessy, D. Bosch and P. Gay (2009a). Watershed-scale fate and transport of bacteria. *Transactions of ASABE 52(1)*, pp. 145 – 154.

Chin, D., D. Sakura-Lemessy, D. Bosch and P. Gay (2009b). Enhanced estimation of terrestrial loadings for TMDLs – a normalization approach. *Journal of Water Resources Planning and Management.* (in press)

Claeskens, G., and N. Hjort (2008). Model Selection and Model Averaging. Cambridge, U.K: Cambridge University Press.

Clemens, R. (1989). Combining forecasts: a review and annotated bibliography. *International Journal of Forecasting (5)*, pp. 559 – 583.

Copeland, C. (1999). Clean Water Act: A summary of the law. Environmental and Natural Resources Policy Division. CRS Report for Congress: RL 30030. Http://www.ncseonline.org/NLE/CRSreports/water/h2o-32.cfm.

Copeland, C. (2005). The Clean Water Act and total maximum daily loads (TMDLs) of pollutants. Resources, Science and Industry Division, CRS Report for Congress: 97-831 ENR, January 05, 2005.

Copeland, C. (2006). Water Quality: Implementing the Clean Water Act. Resources, Science and Industry Division, CRS Issue Brief for Congress: IB 89102. February 28, 2006.

Cybenko, G. (1989) Approximation by superposition of a sigmoid function. *Mathematics of Control, Signals and Systems (2)*, pp. 303 – 314.

Davies-Colley, R., R. Bell, and A. Donnison (1994). Sunlight inactivation of enterococci and fecal coliforms within sewage effluent diluted in seawater. *Applied Environmental Microbiology (60)*, pp. 2049 - 2058.

Department of Environmental Conservation, New York State (1992). Reducing the impacts of stormwater runoff form new development: A manual for local planners, building inspectors and developers. New York State Department of Environmental Conservation: Division of Water, Bureau of Water Quality Management.

Department of Environmental Quality (1993). Non point source pollution assessment report- November 1993: State of Louisiana. Http://nonpoint.deq.state.la.us/assess31.html

Dickinson, J. (1973). Some statistical results in the combination of forecasts. *Oper. Res. Q., 24 (2)*, pp. 253 – 260.

Dickinson, J. (1975). Some comments on the combination of forecasts. *Oper. Res. Q., 26*, pp. 205 – 210.

Donaldson, R. and M. Kamstra (1997). Neural network forecasting combining with interaction effects. *Journal of the Franklin Institute (14)*, pp. 227 – 236.

Donner, B. A. (2004). Total coliform TMDL for Cypress Creek (WBID 1402). Technical Report, Florida Department of Environmental Protection, September 2004.

Draper, N. and H. Smith (1981). Applied Regression. USA: John Wiley and Sons, Inc.

Ellis, J. and Y. Wang (1995). Bacteriology of urban runoff: the combined sewer as a bacterial reactor and generator. *Water Science Technology 31(7)*, pp. 303 – 310.

Faucett, L. (1994). Fundamentals of Neural Networks: Architectures, Algorithms and Applications USA: Prentice Hall International.

Feyereisen, G., R. Lowrance, T. Strickland, J. Sheridan, R. Hubbard, and D. Bosch (2007a). Long‐term water chemistry database, Little River Experimental Watershed, Southeast Coastal Plain, United States. *Water Resources Resources 43(9)* 09474, doi:10.1029/2006WR005835.

Feyereisen, G., T. Strickland, D. Bosch, and D. Sullivan (2007b). Evaluation of SWAT manual calibration and input parameter sensitivity in the Little River watershed. *Transactions of the ASABE 50(3)*, pp. 843‐855.

Fiordaliso, A. (1998). A non linear forecast combination method based on Takagi-Sugeno fuzzy systems. *International Journal of Forecasting (14)*, pp. 367 – 379.

Field, J., A. Kato and G. Schraa (1995). Enhanced biodegradation of aromatic pollutants in cocultures of anaeorabic and aerobic bacterial consortia. *Anthonie van Leeuwenhoek (67)*, pp. 44 – 77.

Geldreich, E. (1965). Detection and significance of fecal coliform bacteria in stream pollutions studies. *Journal of Water Pollution Control Federation 37(12)*, pp. 1722 - 1726.

Georgia Department of Natural Resources (2002). Total Maximum Daily Loads (TMDLs) for fecal coliform in 303(d) listed streams in the Oconee River Basin. Technical Report, Environmental Protection Division, January 2002.

Georgia Department of Natural Resources (2003a). Total Maximum Daily Loads evaluation for twenty-eight streams segments in the Flint River Basin for fecal coliform. Technical Report, Environmental Protection Division, January 2003.

Georgia Department of Natural Resources (2003b). Total Maximum Daily Loads evaluation for seventy-nine stream segments in the Chattahoochee River Basin for fecal coliform. Technical Report, Environmental Protection Division, January 2003.

Goonetilleke, A., E. Thomas, S. Ginn, and D. Gilbert (2005) Understanding the role of land use in urban stormwater quality environment. *Journal of Environmental Management (74)*, pp. 31 - 42.

Granger, C. (2001). Invited review: Combining forecast-twenty years later. *Journal of Forecasting (8)*, pp. 167 - 173.

Granger, C., and R. Ramanathan (1984). Improved methods of combining forecasts. *Journal of Forecasting (3)*, pp. 197 – 204.

Green, W. and G. Ampt (1911) Studies on soil physics - 1: The flow of air and water through soils. *Journal of Agricultural Science (4)*, pp. 11- 24.

Hall, K. and B. Anderson (1986). The toxicity and chemical composition of urban stormwater runoff. *Canadian Journal of Civil Engineering (15)*, pp. 98 – 105.

Hartman, E., J. Keller and J. Kowalski (1990). Layered neural networks with Gaussian hidden units as universal approximations. *Neural Computing (2)*, pp. 210 – 215.

He, X. and X. Xu (2005). Combination of forecasts using self-organizing algorithms. *Journal of Forecasting (24)*, pp. 269 – 278.

Hopfield, J. (1982). Neural networks and physical systems with emergent collective computational abilities. *Proceeding of the National Academy Science (79)*, pp. 2554 – 2558.

Hydrocomp, Inc. (2008) Hydrologic Simulation Program Fortran (HSPF). Hydrocomp, Inc: Http://www.hydrocomp.com/HSPFinfo.htm. Assessed: March 20, 2008.

Im, S., K. Brannan, S. Mostaghimi and J. Cho (2004). A Comparison of SWAT and HSPF Models for simulating hydrologic and water quality responses from an urbanizing watershed. *Presentation at ASCE Meeting: ASCE Meeting Paper Number: 032175.*

KY DFWR (2006). Kentucky Department of Fish and Wildlife Resources, February 2006 in Total Maximum Daily Load for E. coli in Brush Creek. Department for Environmental Protection, Kentucky.

Khan, M., C. Chatwin and R. Young (2007). A framework for post-event timeline reconstruction using neural networks. *Digital Investigation (4)*, pp. 146 - 157.

Lin, K. (2005). Distributing responsibility for clean water: the total maximum daily load (TMDL) program. MIT., Cambridge, MA.

Lin, P. -E., D. Meeter and X .-F Niu (2000). A nonparametric procedure for listing and delisting impaired waters based on criterion exceedances. Technical Report FDEP Contract Report LAB015, Department of Statistics, Florida State University, Tallahassee, Florida.

Liptak, B. (eds.) (2006). Instrument Engineer's Handbook: Process Control and Optimization 4th Ed. Boca Raton, FL: CRC Publishers.

Lopes, T., K. Fossum, J. Phillips and J. Monical (1995). Statistical summary of selected physical, chemical, and microbial characteristics and estimates of constituent loads in urban stormwater, Maricopa County, Arizona. Water-Resources Investigations Report 94-4240. US Geological Survey, Tucson, AZ.

Mantovan, P., and E. Todini and M. Martina (2007). Reply to comment by Keith Beven, Paul Smith and Jim Freer on "Hydrological forecasting uncertainty assessment: Incoherence of the GLUE methodology". *Journal of Hydrology*, 338, 319-324.

McCulloch, M. and S. Pitts (1943). A logical calculus of the ideas immanent in nervous activity. *Bulletin of Mathematical Biophysics (5)*, pp. 115 – 133.

McFarland, A. and L. Hauck (1999). Relating agricultural land-uses to in-stream water quality. *Journal of Environmental Quality (28)*, pp. 836 - 844.

Mein, R. G. and A. G. Goyen (1988) Urban runoff. *Civil Engineering Transactions*, Institute of Engineering, Australia CE30, 225 - 238.

Minsky, M., and S. Papert (1969) Perceptrons Cambridge MA: MIT Press

Moriasi, D., J. Arnold, M. V. Liew, R. Bingner, R. Harmel, and T. Veith (2007). Model evaluation guidelines for systematic quantification of accuracy in watershed simulations. *Transactions of the ASABE 50(3)*, pp. 885 - 900.

Nash, J. and J. Sutcliffe (1970). River flow forecasting through conceptual models, Part 1: a discussion of principles. *Journal of Hydrology (10)*, pp. 282 – 290.

Natural Resources Defense Council (1999a). The causes of urban stormwater pollution. In Stormwater Strategies: Community Responses to Runoff Pollution. Http://www.nrdc.org/ pollution/storm/chap2.

Natural Resources Defense Council (1999b). The consequences of urban stormwater pollution. In Stormwater Strategies: Community Responses to Runoff Pollution. Http://www.nrdc.org/ pollution/storm/chap3.

Natural Resources Defense Council (1999). Non-point source pollution control processes and planning principles. In the Illinois Urban Manual.

Natural Resources Defense Council (1999). The consequences of urban stormwater pollution. In Stormwater Strategies: Community Responses to Runoff Pollution. Http://www. nrdc.org/pollution/storm/chap3.

Neitsch S., J. Arnold, J. Kiniry and J. Williams (2005). Soil and Water Assessment Tool: User's Manual. Grassland, Soil and Water Research Laboratory and Blackland Research Center: Temple, Texas.

Neitsch, S., J. Arnold, J. Kiniry, J. Williams and K. King (2002). Soil and Water Assessment Tool Theoretical Documentation. Version 2000, Technical Report 02-0, U.S. Department of Agriculture, Agriculture Research Service, Grassland, Soil and Water Research Laboratory, Temple, Texas.

Neitsch, S. L., J. G. Arnold, J. R. Kiniry, R. Srinivasan and J. R. Williams (2004). Soil and Water Assessment Tool Input/Output File Documentation. Version 2005, Grassland, Soil and Water Research Laboratory and Blackland Research Center: Temple, Texas.

Newbold, P., and C. Granger (1974) Experience with forecasting univariate time series and the combination of forecast. *Journal of the Royal Statistical Society A (137) Part 2*, pp. 131 – 146.

Novotny, V. amd H. Olem (1994). Water Quality: Prevention, Identification and Management of Diffuse Pollution. New York, NY: Van Nostrand-Reinhold.

Office of Water (1985). Final report on the federal/state/local nonpoint source task force and recommended national nonpoint source policy. Washington DC: US Environmental Protection Agency.

Olivieri, V., C. Kruse, K. Kawata, and J. Smith (1977). Selected pathogenic microorganisms contributed from urban watersheds. Watershed Research in Eastern North America, A Workshop to Compare Results, Volume II. Report No. NSF/RA-770255. Edgewater, Maryland: Smithsonian Institute. Chesapeake Bay Center for Environmental Studies, February 28-March 3, 1977. pp. 635 - 659.

Parker, J., K. Fossum and T. Ingersoll (2000). Chemical characteristics of urban stormwater sediments and implications for environmental management, Maricopa County, Arizona. *Environmental Management (26)*, pp. 99 – 115.

Paul, S., P. Haan, M. Matlock, S. Mukhtar and S. Pillai (2004). Analysis of the HSPF water quality parameter uncertainty in predicting peak in-steam fecal coliform concentrations. *Transactions of the American Society of Agricultural Engineers, 47(1)*, pp. 69 - 78.

Phillips, J. (1988). Nonpoint source pollution and spatial aspects of risk assessment. *Annals of the Association of American Geographers, 78 (4) (December 1988)*, pp. 611 - 623.

Pitt, R. (2002). Receiving water impacts associated with urban runoff. In Handbook of Ecotoxicology by D. Hoffman, B. Rattner, G. Burton, Jr., and J. Cairnes. Boca Raton, FL: CRC - Lewis.

Priddy, K. and P. Keller (2005). Artificial Neural Networks: An Introduction Bellingham, WA: Society for Photo-Optical Instrumentation Engineers (SPIE).

Roffolo, J. (1999). TMDLs: the revolution in water quality regulation. California Research Bureau, Sacramento California: April 1999.

Rosenbatt, F. (1958). The Perceptron: a probabilistic model for information storage and organization in the brain. *Psychological Review (65)*, pp. 386 – 408.

Sartor, J. and G. Boyd (1972). Water pollution aspects of street surface contaminants. U.S. EPA: Washington, D.C.

Shabman, L. and E. Smith (2003). Implications of applying statistically based procedures for water quality assessment. *Journal of Water Resources Planning and Management 129 (4)*, *July/August 2003,* pp. 330 – 336.

Shamseldin, A., K. O'Conner and G. Liang (1997). Methods for combining the outputs of different rainfall-runoff models. *Journal of Hydrology (197*), pp 203 - 229.

Shi, S. and B. Lui (1993) Nonlinear combination of forecast with neural networks. *Proceedings of 1993 Joint Conference on Neural Networks, Nagoya, Japan Volume 1*, pp. 959 – 962.

Shier, D., R. Lewis and J. Butler (2009). Hole's Anatomy and Physiology 12/e. New York, N.Y: McGraw- Hill.

Shirmohammadi, A., J. M. Sheridan, and L. E. Asmusssen (1986). Hydrology of alluvial stream channels in southern Coastal Plain watersheds. *Transactions of ASAE (29)*, pp. 135 - 142.

Shirmohammadi, A., I. Chaubey, R. Harmel, D. Bosch, R. Munoz-Carpena, C. Dharmasri, A. Sexton, M. Arabi, M. Wolfe, J. Frankenberger, J. (2006). Uncertainty in TMDL models. *Transactions of the ASABE 49 (4)*, pp. 1033 - 1049.

Singh, J., V. Knapp and M. Demissie (2008). Hydrologic modeling of the Iroquois River Watershed using HSPF and SWAT. Watershed Science Section, Illinois Department of Natural Resources and the Illinois State Geological Survey. Illinois State Water Survey Contract Report 2004-08.

Smith, R., G. Schwarz and R. Alexander (1997). Regional interpretation of water-quality monitoring data. *Water Resources Research, 33(12)*: 27812798, December 1997.

SC DHEC (2004). Total Maximum Daily Load (TMDL) development for fecal coliform in the Allison Creek Watershed. Department of Health and Environmental Control, South Carolina.

Stow, C., K. Reckhow, S. Qian, E. Lamon III, G. Arhonditsis, M. Borsuk, and D. Seo (2007). Approaches to evaluate Water Quality Model Parameter Uncertainty for Adaptive TMDL Implementation. *Journal of the American Water Resources Association*, *43(6)*, pp. 1499 - 1507.

Sullivan, D., H. Batten, D. Bosch, J. Sheridan and T. Strickland (2007). Little River Experimental Watershed, Tifton, Georgia, United States: A geographic database. *Water Resources Research (43) W09471*, doi:10.1029/2006WR005836.

Texas Environmental Profiles (2003). Water quality. Environmental Profiles.

Tippecanoe Environmental Lake and Watershed Foundation (2005). Dissolved oxygen. Http://www.telwf.org/watertesting/dissolvedoxygen.htm

Thompson, P. (1976). How to improve accuracy by combining independent forecasts. *Mon. Wea. Rev.,(105)*, pp. 228 – 229.

Thomann, R. and J. Meuller (1987). Principles of Surface Water Quality Modeling and Control. New York, NY: Harper Row Publishers.

Turchin, V. (1977). The Phenomenon of Science. New York, NY: Columbia University Press.

United States Code (US Code). Water quality standards and implementation plans. US Code: Title 33 Section 1313 (d) (1) (C).

US EPA (United States Environmental Protection Agency) (1996). Non-point source pollution: the nation's largest water quality problem. Pointer 1: EPA841-F-96-004A. Environmental Protection Agency, Washington, DC.

US EPA (United States Environmental Protection Agency((1997). Guidelines for preparing the comprehensive state water quality assessments. Office of Water, Washington, DC (4503F).

US EPA (United States Environmental Protection Agency) (2008). Southeast Profile. Http://www.epa.gov/region4/oepages/4profile.htm. Accessed: Sunday February 24, 2008.

US EPA (United States Environmental Protection Agency) (2001). Protocol for developing pathogen TMDLs. Office of Water, Washington, DC. EPA 841-00-002.

US EPA (United States Environmental Protection Agency) (1999). Preliminary data summary of urban storm water best management practices. EPA-821-R-99-012. Washington, DC.

US EPA (United States Environmental Protection Agency) (2000). Aquatic life criteria for dissolved oxygen (saltwater): Cape Cod to Cape Hatteras. Fact Sheet: EPA-822-R-00-012. Office of Science and Technology, Health and Ecological Criteria Division, Washington, DC.

US EPA (United States Environmental Protection Agency) (2000). Estimating hydrology and hydraulic parameters for HSPF. *BASINS Technical Note 6: EPA-823-R00-012* Washington, DC: July, 2000.

US EPA (United States Environmental Protection Agency) (2007). Better Assessment Science Integrating Point and Non-point Sources (BASINS): Basic Information. June 27, 2007.

US EPA (United States Environmental Protection Agency) (2008a). Southeast Profile. Http://www.epa.gov/region4/oepages/4profile.htm. Last modified Tuesday February 19, 2008. Accessed: Sunday February 24, 2008.

US EPA (United States Environmental Protection Agency) (2008b) National Section 303(d) List Fact Sheet. www.state.nj.us/dep/stormwater/tier_A/pdf/NJ/SWBMP_1%20print.pdf.

USGS (United States Geological Survey) (2000). Droughts in Georgia. US Geological Survey Open-file Report 00-380: October 2000.

Van Liew, M., J. Arnold, and J. Garbrecht (2003). Hydrologic simulation on agricultural watersheds: Choosing between two models. *Transactions of the ASABE 46(6)*, pp. 1539 - 1551.

Vellidis, G., R. Lowrance, P. Gay, J. Sheridan and D. Bosch (1999). Water quality of Piscola Creek Watershed. ASAE Technical Paper No. 99-2131. St. Joseph, MI: ASAE.

Vrugt, J., H. Gupta, W. Bouten, and S. Sorooshian, S. (2003). A Shuffled Complex Evolution Metropolis algorithm for optimization and uncertainty assessment of hydrologic model parameters. *Water Resources Research, 39(8)*, doi:10.1029/2002WR001642.

Werbos, P. (1974). Beyond Regression: New Tools for Prediction and Analysis in the Behavioral Sciences. Cambridge, MA: Ph.D. Thesis, Harvard University, Harvard.

Wnek, G. and G. Bowlin eds. (2008). Biomaterials and Biomedical Engineering, Vol. 1, 2/e. New York, NY: Informa Healthcare USA.

APPENDIX

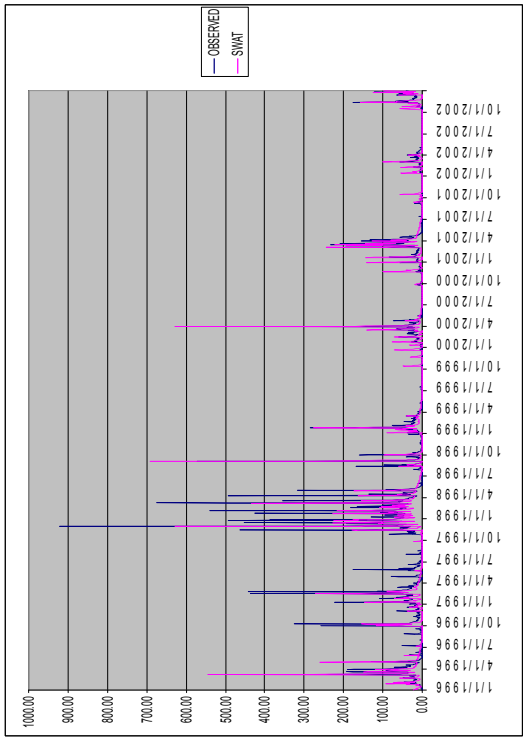

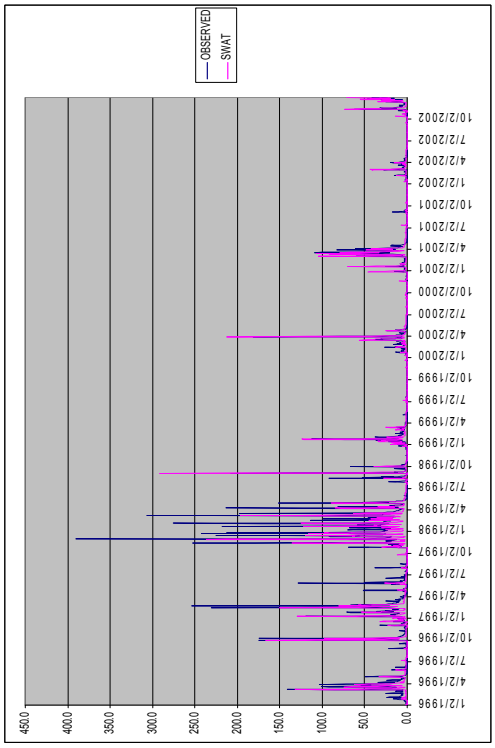

Hydrology: Daily Flows- Catchment I (SWAT and HSPF)

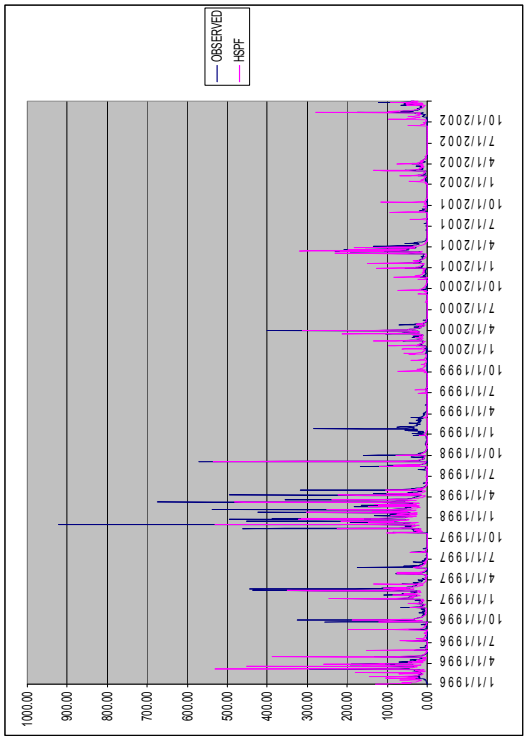

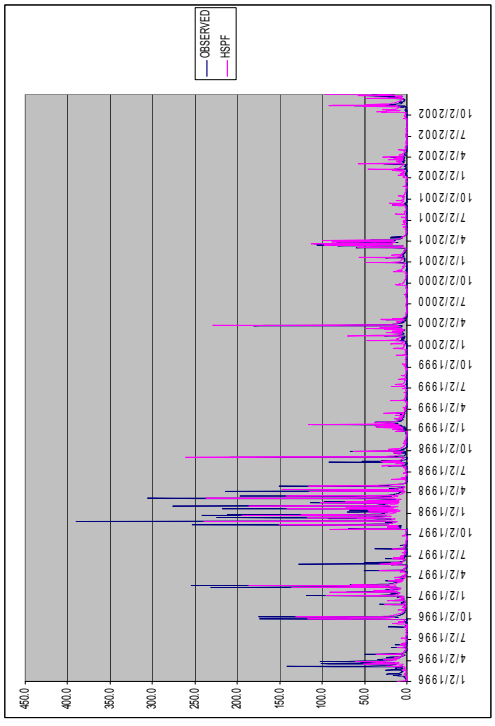

Hydrology: Daily Flows- Catchment J (SWAT and HSPF)

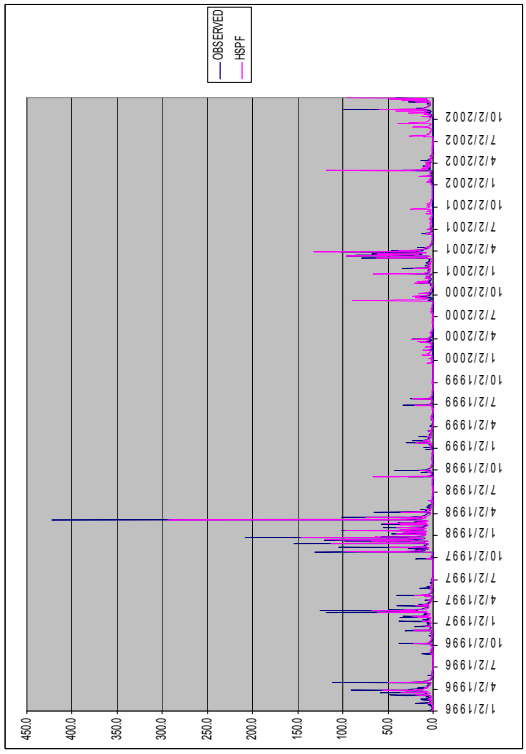

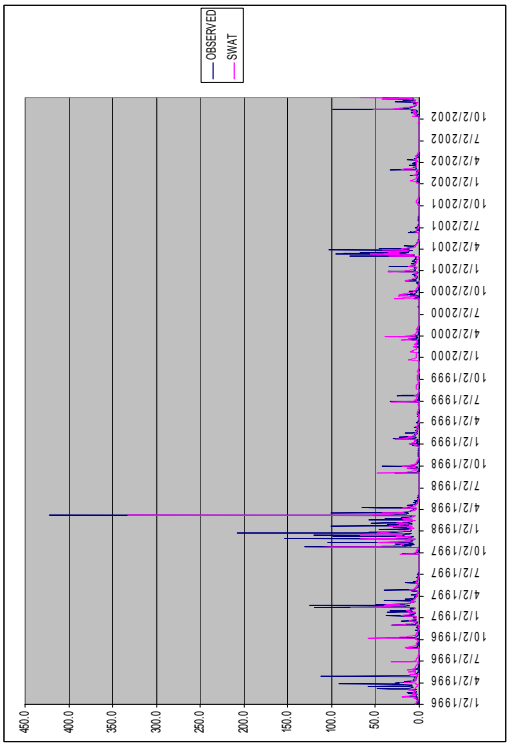

Hydrology: Daily Flows- Catchment K (SWAT and HSPF)

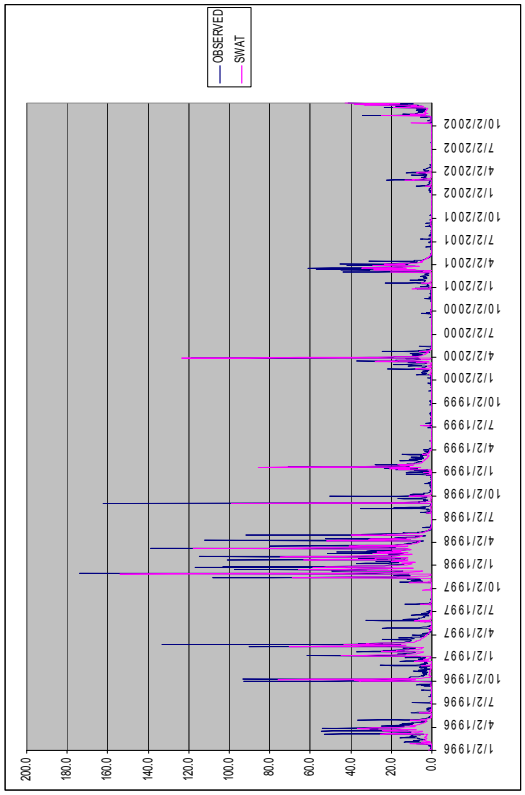

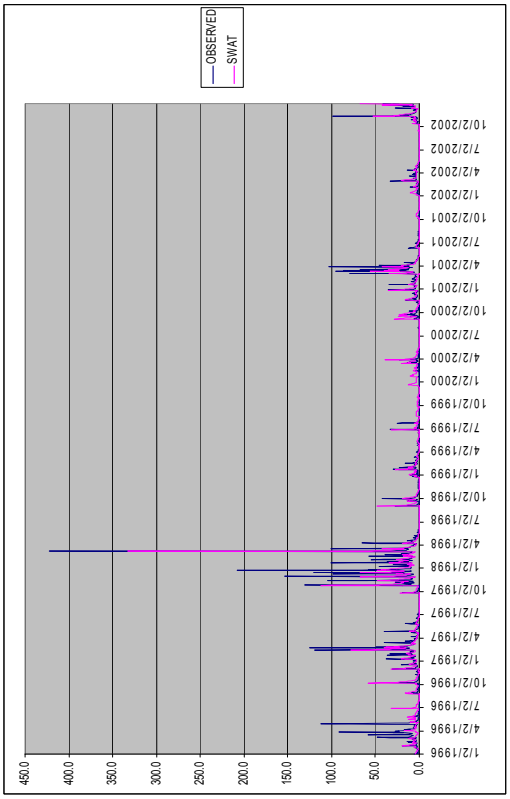

Hydrology: Daily Flows- Catchment O (SWAT and HSPF)

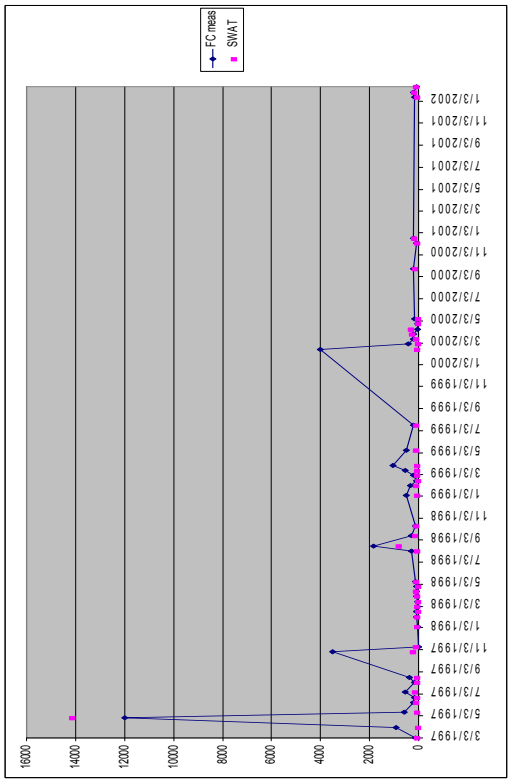

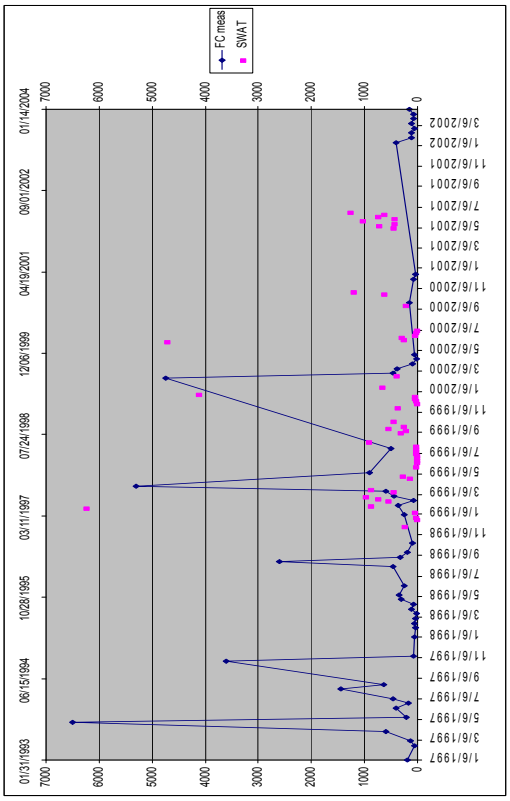

Water Quality: Fecal Coliform - Catchment I (SWAT and HSPF)

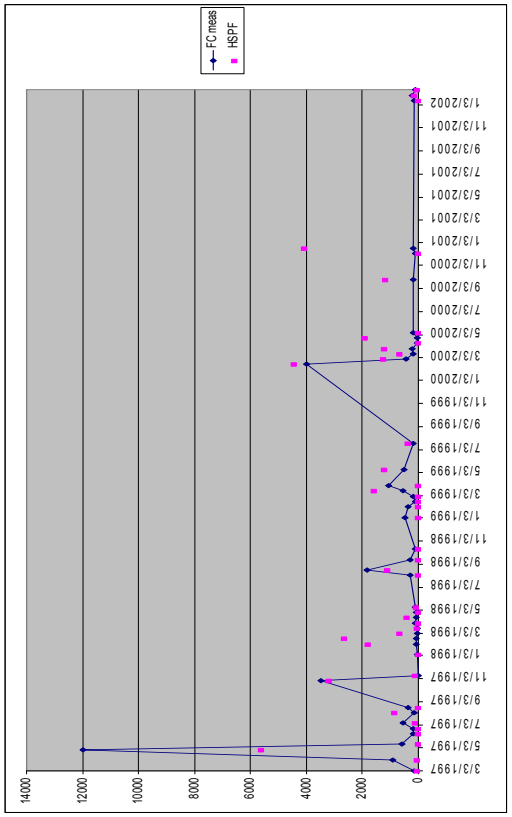

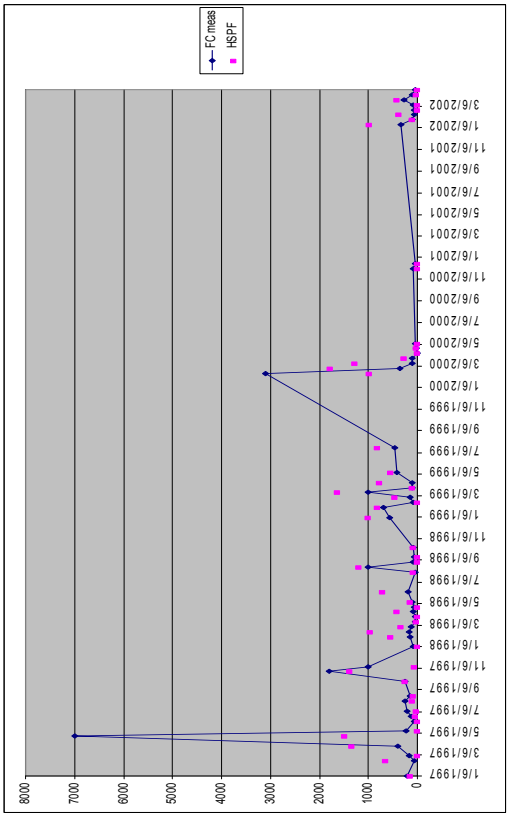

Water Quality: Fecal Coliform - Catchment J (SWAT and HSPF)

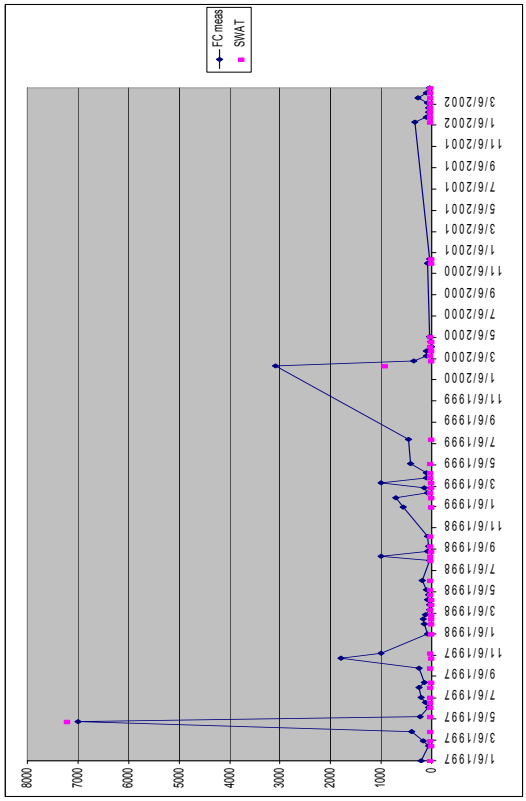

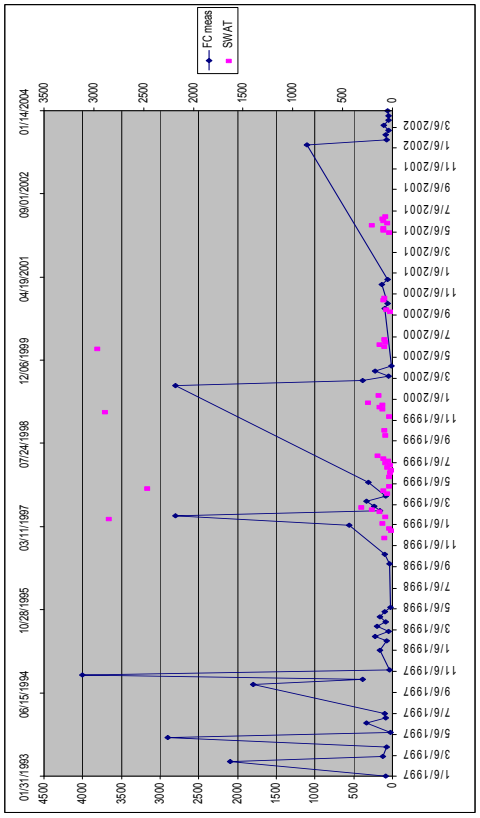

Water Quality: Fecal Coliform - Catchment K (SWAT and HSPF)

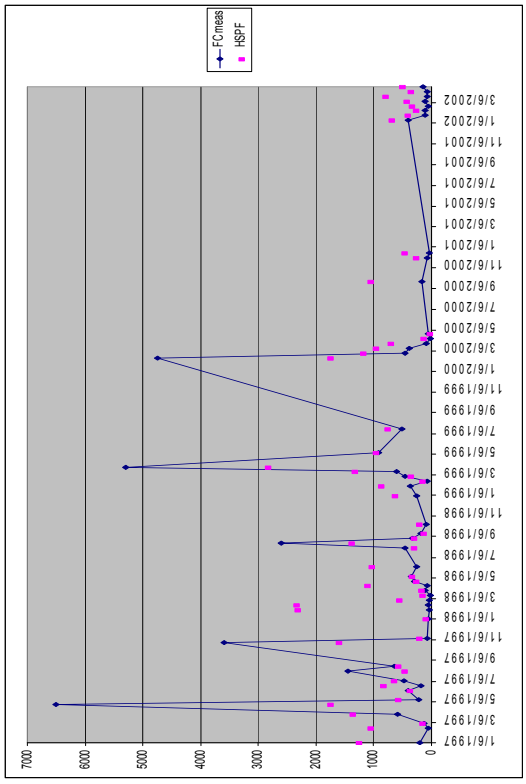

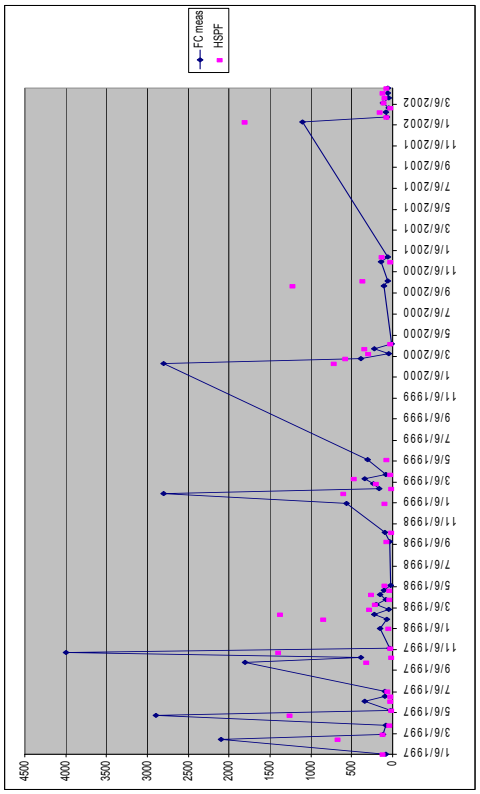

Water Quality: Fecal Coliform - Catchment O (SWAT and HSPF)

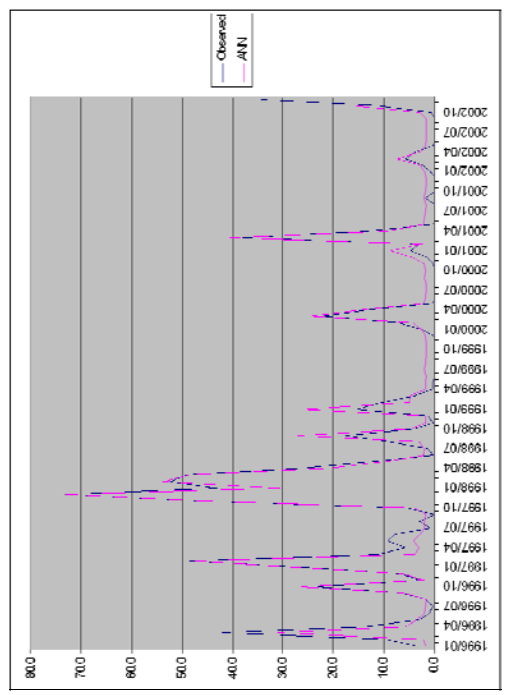

Artificial Neural Network: Hydrology Monthly Catchment I

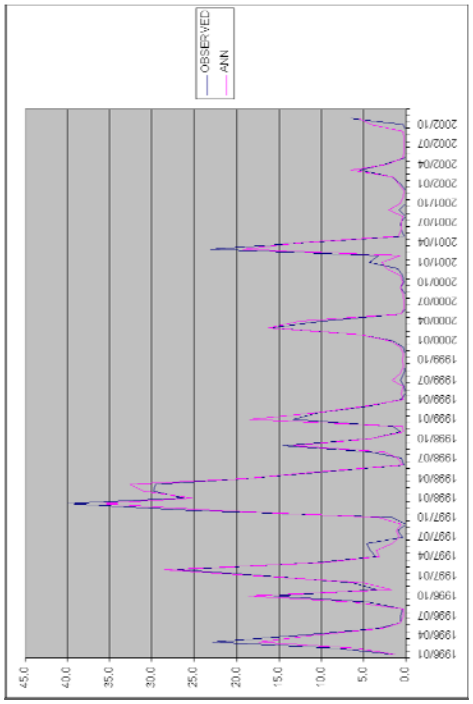

Artificial Neural Network: Hydrology Monthly Catchment O

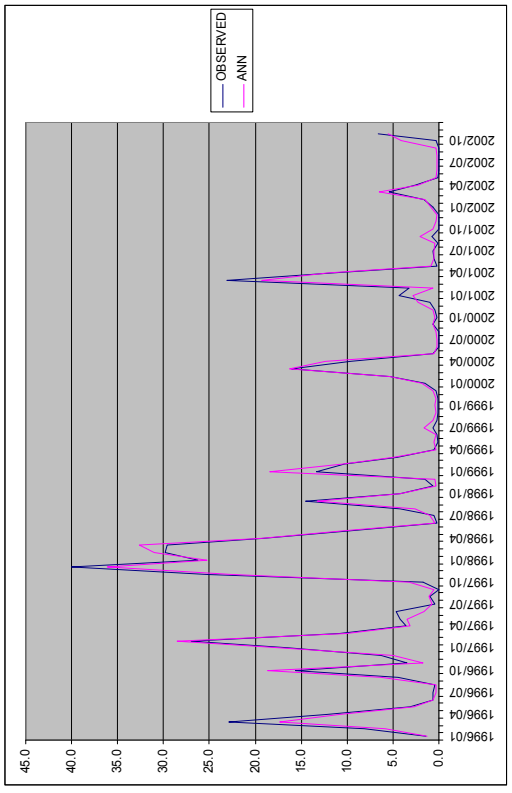

Artificial Neural Network: Hydrology Monthly Catchment I

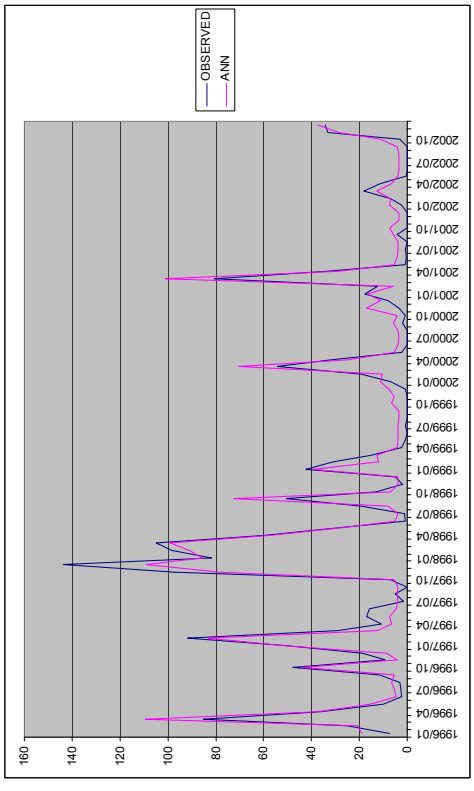

Artificial Neural Network: Hydrology Monthly Catchment K

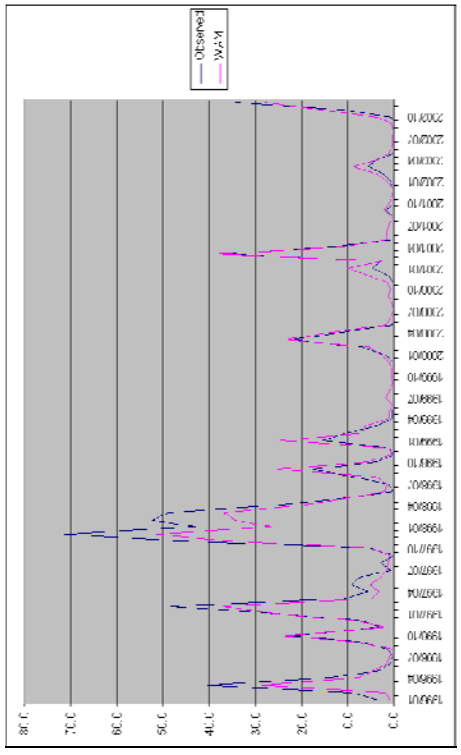

Weighted Average Method: Hydrology Monthly Catchment J

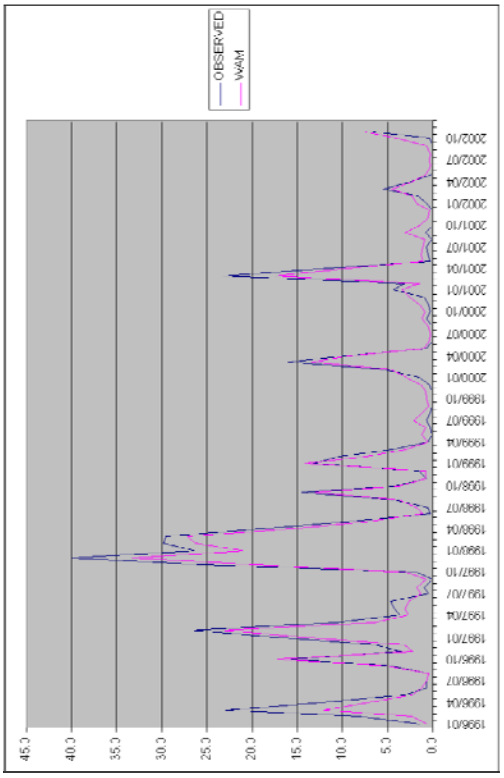

Weighted Average Method: Hydrology Monthly Catchment O

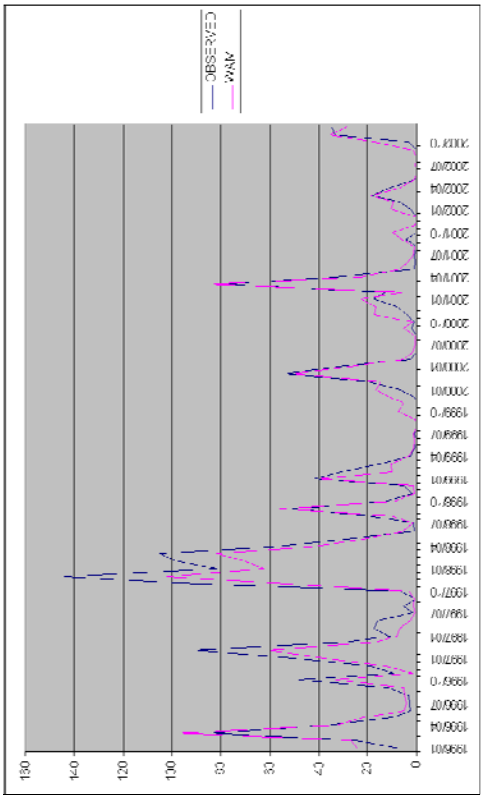

Weighted Average Method: Hydrology Monthly Catchment I

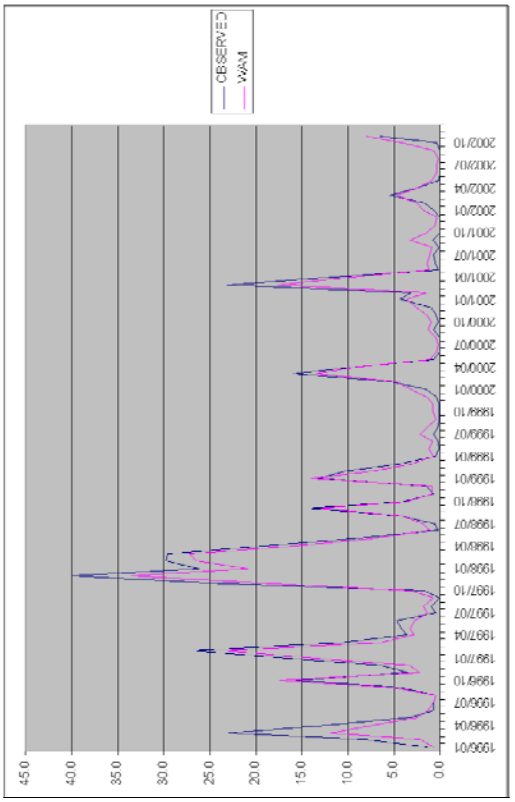

Weighted Average Method: Hydrology Monthly Catchment K

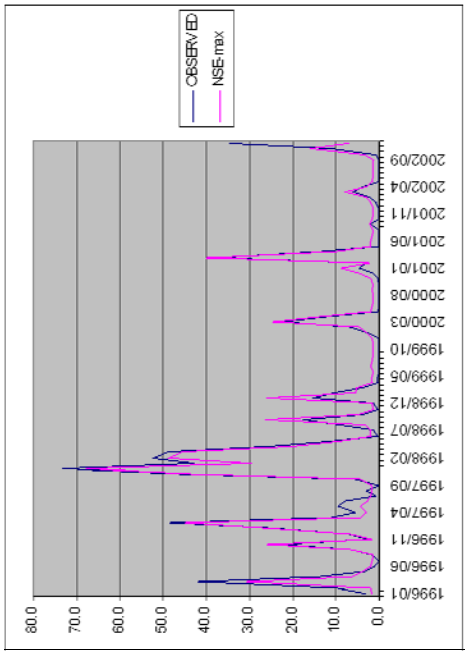

NSE-max Method: Hydrology Monthly Catchment J

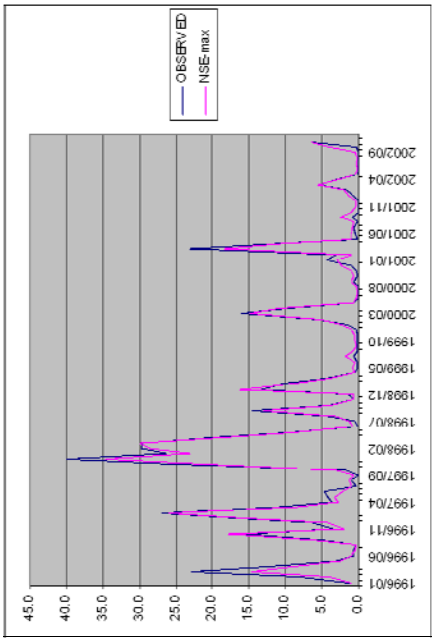

NSE-max Method: Hydrology Monthly Catchment O

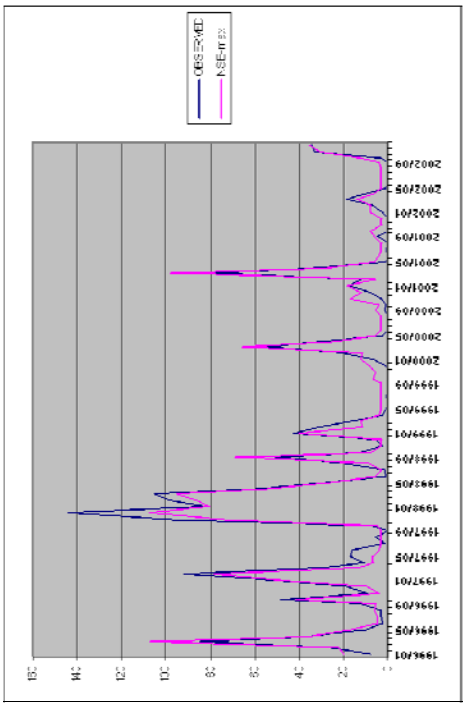

NSE-max Method: Hydrology Monthly Catchment I

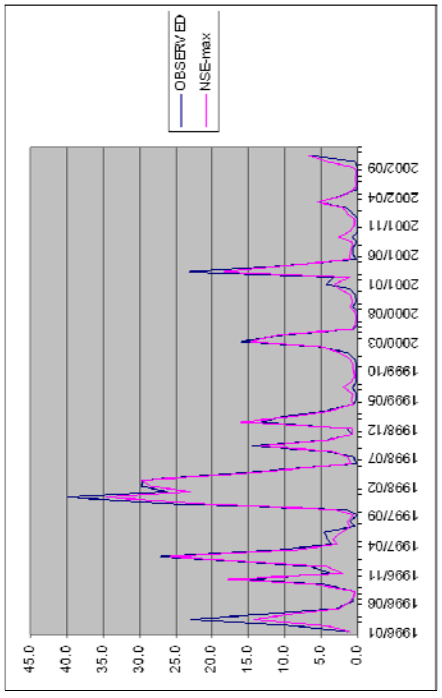

NSE-max Method: Hydrology Monthly Catchment K